ACUTE INTRACRANIAL HAEMORRHAGE:

PATHOPHYSIOLOGICAL AND MAGNETIC RESONANCE STUDIES

by

Alistair Jenkins, FRCS ©

Submitted for the degree of Doctor of Medicine

to the University of Glasgow

being the result of research conducted at the

Wellcome Surgical Institute, Glasgow

and the

Institute of Neurological Sciences, Glasgow.

Submitted March 1989

ProQuest LLC.
789 East Eisenhower Parkway
P.O. Box 1346
Ann Arbor, MI 48106 – 1346

TABLE OF CONTENTS

LIST OF TABLES

table **page**

LIST OF FIGURES

figure **page**

figure **page**

figure **page**

ACKNOWLEDGEMENTS

This work was supported by grants from the Medical Research Council, the Greater Glasgow Health Board, the Scottish Home and Health Department, The Scottish Hospital Endowment Research Trust, the University of Glasgow and the Institute of Neurological Sciences Research Trust.

To Professor GM Teasdale, my advisor, are due the credit for the submission of this thesis and my thanks for his encouragement, instruction and generosity.

The medical, scientific and technical staff of the Wellcome Surgical Institute were constantly helpful and encouraging. My thanks in particular to Dr J McCulloch for his patience and friendship, and to Mr D Mendelow for his enthusiasm.

Professor DI Graham prepared the neuropathological material and was enormously helpful at all stages.

Dr D Hadley, Dr J Patterson, Dr B Condon, Dr D Wyper and Mrs A Lawrence were my co-workers in the Magnetic Resonance Department. The MR studies reported here could not even have been started without them. Their help went far beyond the level of mere teamwork.

Dr J Patterson kindly wrote the computer program used in MR signal intensity studies.

Thank you to Jean Winning, Marion Cresswell and Pat Christie, the overworked MRI technicians.

All photographic services were provided quickly and efficiently by Linda Scott, even when presented with impossible time schedules.

SUMMARY

Summary

Previous studies have shown an extensive area of ischaemia around an acute intracerebral haematoma, and that this ischaemia contributes to patients' clinical condition and outcome. The relative contribution of tissue pressure and chemical vasoconstriction in the production of ischaemia is uncertain. If vasoconstrictors present in blood were found to play a significant rôle, and if ischaemia could be detected early, it might prove possible to improve blood flow by pharmacological manipulation of the vasoconstrictor effect.

The studies reported here used the new technique of Magnetic Resonance Imaging (MRI) to investigate intracerebral and subarachnoid haemorrhage, and associated changes in the brain parenchyma. Ischaemic change was assayed in an experimental animal model using different intracerebral space-occupying lesions, and local effects of a haematoma were observed at stages up to three months.

The first part of the study was concerned with assessing the sensitivity and specificity of MRI in acute and subacute intracranial haemorrhage (ICH). The diagnostic yield of MRI is determined by the choice of radiofrequency (RF) pulse sequences appropriate to the condition. A system was developed which used computer analysis of *in vitro* relaxation time measurements of brain, blood and cerebrospinal fluid (CSF) to predict optimum pulse sequences for imaging patients with ICH.

T1 and T2 of fresh human post-mortem grey matter and white matter, and of CSF from patients undergoing myelography, were

measured *in vitro* using a MR spectrometer. Relaxation times of blood from volunteers, and of CSF samples after the addition of blood to simulate different degrees of subarachnoid haemorrhage (SAH), were also measured daily for 15 days. T1 and T2 of blood fell sharply over the first 48 hours and gradually over the rest of the period. There was an insignificant fall in the values for bloodstained CSF. On day one, there were substantial differences between the relaxation times of all the tissues, but the fall in the relaxation times of blood led to overlap with the values for brain tissue.

A simple computer program used these measurements to calculate values for image signal intensity for all the tissues. Signal intensity values were obtained for all the pulse sequence combinations available on the Picker 0.15T imager. From these results, sequences were chosen which produced the greatest separation of the signal intensities, and hence the image contrast, of normal and haemorrhagic tissues. A Spin-echo (SE) 2200/80 sequence was chosen for clinical imaging studies as it combined good tissue contrast with good definition and a short imaging time (9.2 mins).

Clinical studies were then undertaken on patients with subarachnoid haemorrhage, intracerebral haematoma and head injury.

33 patients with a clinical diagnosis of SAH were imaged by both MRI and computed tomography (CT) between 8 hours and 6 days after the onset of symptoms, 30 being imaged preoperatively and 3 only postoperatively. Seven had both pre- and postoperative MR, and four patients had both MRI and CT performed after operation. The computer prediction of SAH signal intensity was confirmed. Although

two different CT scanners were used over the period of the study, they did not differ significantly in diagnostic yield for the features examined. MRI diagnosed SAH correctly in 25 patients, CT in 24. Intracerebral bleeds were identified by MRI in 12 patients and by CT in 10. Complications of SAH (hydrocephalus and hemisphere swelling) were diagnosed more frequently by CT when changes were small. MRI proved to be at least as good at localising the site of the bleeding lesion (16 MRI, 11 CT) and better at visualising aneurysms (14 MRI, 0 CT). Providing MRI-compatible aneurysm clips were used - the Sugita range proved suitable - less image degradation was caused by the clip on post-operative studies using MRI, enabling small haematomas to be seen more easily. Ischaemic changes were not positively identified with either method.

20 patients with intracerebral haematomas shown by CT were studied using MRI. 11 were caused by trauma, 4 by rupture of an aneurysm or arteriovenous malformation, and five were hypertensive bleeds. 17 haematomas were supratentorial and 3 infratentorial. In 13 patients, the haematoma was seen as a hypo- or isointense area surrounded by a hyperintense, oedematous area. In 6 patients it was seen as uniformly hyperintense. In one recurrent bleed, mixed intensities were seen. In most patients, the intensity of the haematoma was lower than predicted by computer analysis, suggesting that the relaxation times of haematoma *in vivo* are lower than those of blood *in vitro*.

50 patients with head injury were examined by MRI and CT within 7 days of injury. All of 20 haematomas > 1cm seen on CT were identified by MRI. MRI showed evidence of cortical contusion in 44

patients, subcortical lesions in 29, deep white matter lesions in 15, and basal ganglia lesions in 10. CT identified changes in these areas in 23, 23, 1 and 2 patients respectively, but no statistical compatison was possible because of the use of two CT scanners of differing quality. The appearance of deep brain lesions on MRI correlated with a lower level of consciousness on admission ($p < 0.001$).

In the third part of the study, a 25µl haematoma was injected stereotactically into the right caudate nucleus of two groups of anaesthetised rats, and the effects compared with similar groups injected with either mock CSF or inert silicone oil. A sham operated group was used for comparison. Intracranial pressure and blood pressure were measured. Regional and hemisphere blood flow were measured by ^{14}C iodoantipyrine auroradiography one minute after lesion placement, and neuropathological analysis was undertaken at four hours.

Increases in ICP on injection of the mass lesion were small and did not significantly alter cerebral perfusion pressure.

Ischaemia was seen in the region of the lesion in all animals receiving an injection. When blood flow in other regions (eg frontal cortex) on the ipsilateral side was compared in each group with the contralateral side, significant differences were observed in all but one of the regions measured in the blood injection group. Significant differences were not found in the other groups. Similarly, blood flow to the cerebral hemisphere as a whole, with reference to the contralateral hemisphere, was significantly reduced

in the blood group but not in the others.

Neuropathological analysis showed a small area of irreversible ischaemia around the lesion in all animals receiving an injection. In the CSF group this was no larger than in the sham operated group. In the blood or silicone oil groups, the ischaemic area was substantially larger. There was however no significant difference between the groups receiving blood and silicone oil injections, and there were no signs of ischaemia in remote areas.

The sectioned brains of animals given a similar 25μl haematoma were examined by light microscopy after sacrifice at periods from 2 hours to 3 months. Blood was seen to track around intracerebral vessels. The extent of oedema was maximum at 24-48 hours, with increasing phagocytosis of the clot between 48 hours and 14 days. Hypertrophy and proliferation of astrocytes resulted in the formation of a glial scar by 3 months.

Conclusions

1. Intracranial haemorrhage from a variety of causes was well demonstrated by Magnetic Resonance Imaging in both acute and subacute situations in three series of selected patients. To diagnose haemorrhage conclusively, care must be exercised in the selection of radiofrequency pulse sequences. Computer modelling of MRI using data from *in vitro* tissue studies proved to be a useful method of selecting appropriate sequences.

2. MRI showed extensive tissue change around small and large haematomas at an early stage, while the signal intensity of haematomas seen on MR images was lower compared to that of uninvolved brain than had been predicted by *in vitro* studies. It was thought possible that these two findings might be in part explained by early transudation of fluid from the haematoma, but it was not possible to prove this in patients or to produce an appropriate animal model for MR and tissue analysis.

3. Small animal studies showed an immediate and profound effect on the vasculature in the region of an intracerebral haematoma and at more distant sites which could not be explained solely by its space-occupying effect, as similar-sized lesions of inert fluids did not cause changes of equal extent. It is therefore possible that substances diffusing or tracking from the clot might contribute to ischaemia, but this could not be proven experimentally, although blood was seen to track along the perivascular spaces for some distance from the clot. In the experimental situation widespread ischaemia was transient; local ischaemic change increased to a peak by 48 hours, and reduced progressively thereafter with concomitant phagocytosis and absorption of the clot to leave a small glial scar.

Chapter 1

INTRODUCTION 1:

Intracranial Haemorrhage

INTRACRANIAL HAEMORRHAGE

Preface

One day in 1880, Gustave Flaubert, author of *Madame Bovary*, awoke as usual and ran himself a hot bath. While lying soaking, he had a sudden blinding headache; he managed to stagger to the living room and collapsed, still dripping, onto the sofa. The doctor was called. There was little he could do; he merely put the patient to bed, summoned the few remaining relatives, and prepared the death certificate: cerebral apoplexy.

One hundred years on, Flaubert would be rushed to hospital. A CT scan - or perhaps MRI - would confirm the diagnosis. His episodic epilepsy since the age of 27 would be noted: has he perhaps been harbouring an arteriovenous malformation all these years? The consultant would be called, the patient transferred to a specialist unit. There surgery would be considered; if thought inappropriate - a fairly arbitrary decision, as we shall see - a variety of intensive "conservative" therapies would be offered.

One hundred years on, poor Gustave Flaubert might be no better off. Although the overall management of patients with intracranial haemorrhage has improved, few fundamental advances have been made in the treatment of the condition itself. Such advances can only be made on the basis of a thorough knowledge of the pathophysiology of the condition, and this is at present controversial and poorly understood.

Both intracerebral and subarachnoid haemorrhage are characterised in a number of patients by neurological dysfunction and eventual disability which are out of proportion to the magnitude of the original bleed, and which are caused by immediate or delayed ischaemic processes, both focal and global. In subarachnoid haemorrhage without a secondary space-occupying lesion, particularly when subarachnoid clot is extensive, it is accepted that ischaemia is due to the action on small or large blood vessels of vasoactive substances liberated at the time of bleeding or as the haematoma is metabolised. The cause of ischaemia in intracerebral haematoma, however, is contentious. Current theories, based largely on experimental work, favour an initial mechanical vasoconstriction by local pressure from the mass causing swelling, which causes further and more widespread ischaemia (Mizukami 1983). The possible contribution of chemically mediated vasoconstriction in this situation (Sussman 1974) is largely ignored.

The work reported in this thesis examined specific aspects of intracerebral and subarachnoid haemorrhage in the clinical and laboratory settings. The new technique of Magnetic Resonance Imaging was investigated for its potential to demonstrate intracranial bleeding and to reveal early oedema or ischaemia. Using a small animal model of intracerebral haemorrhage, studies of blood flow and pathology in the region of a haematoma were conducted in an attempt to clarify the mechanisms concerned in the production of changes seen in MRI patient studies.

In the pre- CT scanning era, cerebral angiography delineated haematomas by their space-occupying effect, but diagnostic specificity was poor. CT scanning enabled precise diagnosis of the presence and extent of intracranial haemorrhage. Ischaemia, however, cannot be distinguished reliably from oedematous change, and can rarely be identified early after a bleed.

The technique of Proton Magnetic Resonance Imaging (MRI) has proved its ability to demonstrate tissue changes in cerebral ischaemia at a much earlier stage than Computed Tomography (Sipponen et al 1983). MRI is highly sensitive to minor alterations in tissue water content or its chemical binding. This raises the question of its potential in demonstrating oedema or reduced blood flow in the region of a bleed at a stage where treatment, if available, could be started before permanent neurological deficit occurs. The installation in 1984 of a MRI unit in Glasgow, together with a facility for *in vitro* MR analysis of tissues, enabled studies to be carried out into the ability of MRI to demonstrate intracranial bleeding and to examine changes in the brain in the region of a bleed.

The development of a small animal model of intracerebral haematoma at the Wellcome Institute, Glasgow (Bullock et al 1984; Nath et al 1986), gave the controlled conditions necessary for neuropathological analysis and autoradiographic studies of blood flow. These were used to analyse oedema and ischaemia, and to examine the comparative influence of local pressure rises and vasoactive substances in their production.

In the subsequent chapters, an examination of the background to current practice in the treatment of intracerebral and subarachnoid haemorrhage will be followed by a review of the theory and practice of Magnetic Resonance Imaging with special regard to intracranial haemorrhage. The results of the experimental and clinical studies will then be given and discussed.

Pathophysiology

1. Intracerebral haematoma

Spontaneous intracerebral haematoma is more common in men than women, and has its highest incidence in the 50-60 year age group (Cuatico et al 1965). In one series (Arseni et al 1967) it accounted for 2% of the inpatient diagnosis of an intracranial space-occupying lesion. It is most commonly secondary to hypertensive vascular disease (Kase 1986): although not all cases have definitive investigation or post-mortem, this is the presumed cause in 70-96% (Kase 1986; Mohr et al 1978; Leussenhop et al 1967). Degeneration of the media (lipohyalinosis), with or without the formation of fusiform micro-aneurysms, occurs in the perforating or small sub-cortical arteries as a result of hypertension (Fisher 1971). Together with fluctuations in systemic blood pressure, this predisposes to rupture. The site of the haemorrhage is in the basal ganglia in 35%, the subcortical white matter in 25%, the thalamus in 20%, the cerebellum in 10% and the pons in 5% (Mohr et al 1983).

Up to 30% of spontaneous bleeds are due to other causes, particularly when occurring in the frontal, temporal or occipital lobes. Small vascular malformations, amyloid angiopathy, bleeding into primary or secondary tumours, oral anticoagulation and sympathomimetic drugs account for most of the remainder of cases (Kase 1986; Little et al 1979; Vinters et al 1983).

Pasqualin et al (1986) found evidence on CT scan of intracerebral haemorrhage in 34% of patients presenting with cerebral aneurysm rupture; 79% of these were found at the initial presentation and 29% after rebleed. 55% arose from aneurysms of the

middle cerebral artery.

Traumatic intracerebral haemorrhage may result from injury to the arteries and veins of the cortex and subcortical white matter, when it is often accompanied by subdural haemorrhage and contusion and laceration of the brain (Bostrom & Helander 1980; Teasdale & Galbraith 1981). A discrete haematoma may arise in a few days from confluence of "salt & pepper" contusions (Bostrom & Helander 1980) or may be present at initial investigation. If situated deeply in the region of the basal ganglia, the prognosis is poorer than for haematomas situated peripherally (MacPherson et al 1986). Microscopic haematomas and gliding contusions seen post-mortem in cases of severe, diffuse head injury (Oppenheimer 1968; Adams et al 1982; Adams et al 1986) are seldom seen on CT scans during life.

24-48 hours after experimental intracerebral haemorrhage, a thin rim of proteinaceous fluid is seen by microscopy at the haematoma-brain interface, surrounded by a small area of cerebral oedema (Enzmann et al 1981). This is accompanied by mild adventitial inflammation of small vessels in the region. A gradual loss of haemoglobin from the clot is seen between 4 and 8 days, during which time oedema reaches its peak and new vessels are to be seen forming. These begin to be bridged by collagen at around eight days to form a capsule. Early infiltration of the edge of the haematoma by mononuclear cells gives way to an increase in macrophages and fibroblasts, which progressively remove the haematoma and form a collaginous capsule and matrix. Patency of vessels adjacent to the haematoma has not been examined and would be difficult to assess on fixed specimens.

In the patient, spontaneous haemorrhage has a variety of clinical manifestations. Usually the onset is sudden with headache and a variable loss of consciousness; death may supervene. Bleeding is usually complete within a few hours (Arana-Inguez et al 1976). Particularly where there is a bleeding diathesis, the course may be slower and bleeding may continue over days. Depending on the site of the haemorrhage, there will be temporary or permanent neurological deficits. Prognosis depends on a number of factors (Cuatico et al 1965). A more sudden onset, and the presence of focal deficits or a reduced conscious level, carry a poor prognosis, but age does not affect the morbidity or mortality of the stroke itself. Intracranial pressure may be normal in spite of potentially life-threatening intracranial shifts (Mitsuno et al 1966); marked systemic hypertension, however, has a poor prognosis. Anatomical site is the most important element in prognosis (Cuatico et al 1965, Paillas & Aillez 1973). Cuatico states that the size of the haematoma does not equate well with the eventual outcome; most authors have found that patients with haematomas more than about 80ml in volume have a very low rate of survival (Volpin et al 1984; Bolander et al 1983). The poor prognosis of intraventricular extension may be much improved by ventricular drainage (Chan & Mann 1988). Overall survival rates vary considerably between series; contemporary values range from 8% (Duff et al 1981) to 51% (Arana-Inguez et al 1976).

Cuatico also states that variations in conscious level in the acute phase are a reflection of increased space-occupying effect, and equates this with increasing oedema; it is known that the rebleed rate of non-aneurysmal hypertensive haemorrhage is low (Arana-Inguez

et al 1976; Ojemann & Mohr 1975). Mitsuno (1966) suggested that midline shift and tissue pressures produced locally by a haematoma may be responsible for the extension of an ischaemic zone around it, in the manner postulated by Langfitt et al (1964) and refined by Mizukami and Tazawa (1983). According to this theory, "squeezing of the microcirculation" in the parenchyma adjacent to a haematoma causes local ischaemia and oedema. This oedema causes the compromise of further small vessels, more ischaemia, more oedema and so on - the "onion-skin" effect.

There is no evidence to back up or refute the possible rôle of chemically induced vasospasm in the ischaemia associated with intracerebral haematoma. Arseni et al (1967) stated that blood in haematomas can infiltrate the parenchyma of the brain; Arana-Inguez (1976) stated just as firmly that it cannot. Experimental studies (Tsubokawa et al 1983), using Evans' blue dye diffusion and gravimetric studies, have only gone a short way towards answering this question.

Current clinical imaging techniques, while excellent at localising the haematoma and monitoring possible reaccumulation after operation, give little insight into the pathophysiological mechanisms surrounding it. Low density is seen on CT scans only when ischaemia or oedema is well established, and neither early or late CT changes equate well with function.

2. Ischaemia in subarachnoid haemorrhage

After rupture of a cerebral aneurysm, blood escapes at arterial pressure into the subarachnoid space or brain parenchyma. Frequently

this continues until intracranial pressure and blood pressure equilibrate, at which point there is acute global ischaemia and loss of consciousness; thus 20-25% of patients die before admission to hospital. In those who survive, the aneurysm seals itself with a fibrin plug and the intracranial pressure usually reverts to physiological levels. Perfusion pressure is restored, although there may be a variable degree of residual neuronal death and neurological deficit consequent upon this acute ischaemia. There would appear to be little that can be done to alter this chain of events.

The process of delayed cerebral ischaemia, however, does not generally start before the 3rd or 4th day after the bleed; its frequency is greatest during the second week and the risk is minimal after 3 weeks (Mizukami et al 1982).

The risk of delayed ischaemia has been shown to correlate with the amount of blood in the subarachnoid space as seen on CT scans (Fujita 1985; Mohsen et al 1984); a reasonable conclusion would be that it is a result of liberation into the subarachnoid space of vasoactive substances present in this blood, or synthesized by the cerebral vessels after rupture (Gaetani et al 1986).

Almost 30 naturally-occurring substances have been identified as potential culprits (White et al 1983; Gaetani et al 1986). These include serotonin, catecholamines, haemoglobin, deoxyhaemoglobin, fibrin degradation products and free radicals. Experimental models and clinical work have focussed on many of these in the past few years. Most recently attention has been drawn to the action of arachidonate metabolites on the disulphide bonds of the arterial wall (Sasaki et al 1984; Gaetani et al 1986): prostaglandins and their

analogues are well demonstrated spasmogens, while the levels of prostacyclin, an important vasdilator, are reduced in the CSF of patients with subarachnoid haemorrhage.

Ischaemia is the major cause of brain damage after subarachnoid haemorrhage (Asano & Sano 1977, Crompton 1964); pathological study of fatal cases shows focal or generalised swelling with ischaemic cell death in the arterial territories affected. Studies, however, show that cerebral blood flow does not necessarily correlate with measureable vasospasm on angiograms (Zingesser et al 1968); as in intracerebral haemorrhage, CT scan changes do not equate with ischaemia or infarction.

Treatment

1. Intracerebral haematoma

Treatment options include surgical removal of the haematoma, or a number of conservative measures of varying aggressiveness. In traumatic extradural and subdural haematoma, the benefits of early surgery are now clearly established (Mendelow et al 1979; Seelig et al 1981; Teasdale et al 1982). In intracerebral haematoma, however, the case is more difficult to make. Since the successful removal by Bagley (1932) of a white-matter haematoma, much attention has been directed at surgery. A wave of pessimism, however, followed the publication by McKissock et al in 1961 of the results of the first prospective comparison of surgery and conservative treatment: the overall mortality was 51%, and the mortality in the surgical group 65%; taking all factors into account, no statistical difference was found between the outcomes of the two groups, but a trend was seen

favouring non-surgical management.

A review of results obtained since 1961 shows three things: a general improvement in management mortality, both medical and surgical; claims by the proponents of both treatments as to their superiority; and above all, a lack of properly controlled trials (highlighted by Duff et al in 1981).

Leussenhop et al (1967) reported 64 patients, in all of whom surgery was considered; it was performed in 37. There was an overall mortality of 37% and a surgical mortality of 32%. They commented that about 50% of patients were suitable for surgery, and that the most important surgical complication was clot reaccumulation. Scott & Werthan (1970) considered unoperated patients and found a 50% mortality; Paillas & Aillez (1973) operated on all their patients with a 35.6% mortality. These results seemed to show that the balance was falling in favour of surgery; they were echoed in 1976 by Arana-Inguez et al who had an overall mortality of 51% (the same as McKissock) and an operative mortality of 34%. They went so far as to recommend guidelines for surgery: it should be performed in patients not critically ill from the outset if the condition deteriorates to any degree, or fails to improve in the case of large lobar haematomas; and also to reduce sequelae in the latter if focal signs are present. Surgery should not be performed if the haematoma is small and/or deep, if the patient is in coma, or if there is an improvement with medical treatment (hypertonic solutions and steroids).

This was followed in 1977 (Kaneko et al) by a startling series of patients undergoing early operation in whom the mortality was

only 8%; however only four years later Duff et al (1981) produced a small series, treated conservatively, all of whom survived. Their conservative management consisted of the administration of hypertonic solutions according to elevation of measured intracranial pressure.

Bolander et al (1983) had a 13% surgical and a 20% conservative mortality in 74 patients. The results of others were reviewed and this conclusion reached: "clearly, surgical series have a lower mortality than conservatively treated patients". They measured haematoma volume by computed tomography and found that 9 out of 10 patients whose clot measured more than 80ml died, irrespective of treatment. This relationship to volume was confirmed by Volpin et al (1984) who further concluded that surgery should only be considered in patients whose haematomas are in the 26-85ml range. Early reports of stereotactic evacuation appear promising (Backlund et al 1978; Bosch et al 1985).

These results are examined at some length to emphasize the continuing uncertainty as to the treatment of haematoma. The high mortality rate in surgery is ascribed partly to the poor initial condition ofthe patient, and partly to vasomotor instability following the bleed, while the comparable rates in unoperated patients are ascribed to continuing space-occupying effect and consequent ischaemia. Experimental results confirm the presence of ischaemia acutely (Bullock et al 1984, Nath et al 1986); uncertainty as to the benefits of removal of a mass lesion has also been shown experimentally (Kingman et al 1987).

2. Ischaemia in subarachnoid haemorrhage

Attempts at prevention or reversal of immediate or delayed ischaemia have mostly been directed at drug treatment. In a review in 1980, Wilkins found 184 references to clinical drug trials; far more, of course, would be found for animal studies. The literature on the subject is characterised by reports of successful treatment with a wide variety of drug régimes, the success of which could rarely be replicated in other institutions. Some drugs used in SAH have actually exacerbated the problem; the antifibrinolytic drug tranexamic acid was the subject of a multicentre trial which showed that its benefits in preventing rebleeding were equalled by its predisposition to delayed ischaemia (Vermuelen et al 1984). Few of the drugs tried have stood the test of time. Those which have are the least specific, aimed at improving cerebral perfusion pressure by induced systemic hypertension (Brown et al 1978; Muizelaar & Becker 1986). More specific drugs currently under investigation are the calcium antagonists, in particular Nimodipine, and prostacyclin analogues (see above).

In general, however, the current treatment of delayed ischaemia involves promoting cerebral perfusion and avoiding detrimental factors. Prevention is a more attractive prospect than cure; as well as the pharmacological approaches studied, evidence has been accumulating to the effect that removal of blood from the subarachnoid spaces can help to prevent ischaemia. In a CT study, Mohsen et al (1984) showed that delayed ischaemia and its oucome varied directly with the amount of blood seen in the basal and insular cisterns. Fujita (1985) correlated blood concentration to

Hounsfield number. When blood was adequately sucked and washed away at operation, the Hounsfield numbers fell and there was no delayed ischaemia in these patients. Limits for measured values were proposed. This supported the work of Mizukami (1982) who found no delayed neureological deficit where subarachnoid blood was adequately removed. This apparently attractive solution has two main drawbacks: firstly, it is technically difficult to achieve adequate clearance of blood, and impossible in some situations (Mizukami 1982), and secondly, operation must be performed acutely, preferably within 24-48 hours.

Aims of this study

As ischaemia is the main cause of morbidity in both operated and unoperated patients with intracerebral haematoma, and in subarachnoid haemorrhage, perhaps the greatest hope of effective treatment lies in the pre-emptive treatment of this complication. There are many obstacles in the way of this goal; the studies here are an attempt to define and answer specific questions.

The Magnetic Resonance studies examine these questions:

1. Can Magnetic Resonance Imaging display intracranial haemorrhage reliably in the acute and subacute clinical situation?
2. Does MRI show changes in the region of a bleed which might suggest ischaemia or oedema, and can it help in the understanding of the early pathophysiological events following haemorrhage?

The studies of experimental haematoma are intended to complement the MRI studies by looking at these questions:

3. What is the sequence of pathological events following a small intracerebral haemorrhage?
4. Is the local and global ischaemia consequent upon an intracerebral haemorrhage solely due to its space-occupying effect, or does the nature or content of blood itself play a part?

A brief description and review of Magnetic Resonance Imaging and its potential in studies of acute haemorrhage will be given in the next chaper. The model of intracerebral haemorrhage has been

described previously (Bullock et al 1984; Nath et al 1986) and will be discussed further in chapter 5.

Chapter 2

INTRODUCTION: 2

Magnetic Resonance Imaging

History

The evolution of Magnetic Resonance Imaging (MRI) appears as one of the the swiftest technological revolutions in medicine. Only seven years separate the triumphant publication of an image of the brain in which "the two hemispheres are clearly separated" (Hutchison et al 1980) and the visualisation on images of the cochlear and vestibular portions of the eighth cranial nerve, and it is easy to forget the years of constant development of ideas and techniques which made such a revolution possible.

In 1946 the first descriptions of the phenomenon of nuclear magnetic resonance (NMR) were published independently by Bloch et al at Stanford and Purcell et al at Harvard; they received jointly the Nobel prize in 1952. They showed that atoms whose nuclei contained an uneven number of nucleons (protons and neutrons), in this case hydrogen (^1H), could be made to absorb and re-emit energy of a characteristic frequency, and produced signals from the hydrogen nuclei of water molecules. In the succeeding years NMR was used mainly to increase knowledge about the structure and behaviour of simple molecules, and the principle of chemical shift was developed which enabled the identification and analysis of organic molecules. Chemical shift NMR makes use of the slight differences in resonant frequency of a particular nuclear species bound in different molecules to identify and quantify these molecules within a sample. Its rôle in ^{31}Phosphorus studies in biological systems is under investigation.

In the 1950s Shaw et al (1956) turned their attention to the biological possibilities of NMR, in the estimation of the water

content of foods. NMR is still used in the food industry to determine optimum freezing conditions. At this time Odeblad et al (1955) started a series of experiments on biological systems, including red blood cells, to test biological hypotheses. Their investigations of cyclic changes in cervical mucus laid the foundation for work on oral contraception. At this time early work was also emerging on the quantification of blood flow by NMR. Singer et al (1959) related signal amplitude on a ^{1}H system to blood flow, and actually produced measurements on a living human subject. Nearly 20 years on (Singer & Crooks 1983), this method is being used in imaging studies to produce accurate blood flow measurements.

The first realisation that the proton relaxation properties of water differed according to molecular and physiological environment, which is the basis of contrast on MR imaging, came in the mid-1960s with studies by Bratton et al (1965) on frog muscle at rest and undergoing contraction. Results of spectroscopy and of T1 and T2 measurements differed according to the state of contraction; since the absolute amount of water could not be changing, the assumption had to be that there were changes in the binding of water in the region of macromolecules.

In the late 1960s and early '70s biological Magnetic Resonance studies pursued two rather separate directions: many groups investigated the potential of nuclei other than ^{1}H (^{31}P, ^{13}C, ^{23}Na, ^{39}K, ^{17}O) to give new information about living systems, while others turned their attention to the exciting possibilities of studying living organisms in part or as a whole. It was the latter approach, of course, which led to the concept of imaging, and which deserves

attention here.

In 1971 R Damadian, working in New York, showed that NMR could distinguish *in vitro* neoplastic tissue from non-neoplastic tissue on the basis of T1 relaxation time differences. The following year Weisman et al (1972) published data on time-related changes in MR signals from a tumour implanted in the tail of a living rat. Damadian expanded on the idea of taking measurements of relaxation times of a body or limb moved through a static magnetic field (field focusing nuclear magnetic resonance or FONAR) to the formation of images based on the intensity of signal from each part of the subject. The first image of a live animal was produced by this method in 1976 and showed a tumour in a rat.

Meanwhile P Lauterbur and co-workers were working on another method of spatial localisation. By refining the method of Gabillard (1951), in which a linear magnetic field gradient was superimposed on the static magnetic field to produce a diffraction effect, Lauterbur (1973) showed that multiple projections taken during the application of a gradient rotating in the X and Y planes (or a rotating subject) could produce a two-dimensional image after reconstruction of the resulting signals using back-projection. Later a third, slice-select gradient, was added (Lai and Lauterbur 1981).

By this projection-reconstruction method, an image of a recently killed mouse was produced by Hutchison et al in Aberdeen in 1974 which showed acute oedema at the site of its fractured neck. The Aberdeen group went on to set up one of the first low-field MR imagers in clinical use, a 0.04T resistive system which had the static field orientated perpendicular to the patient and used a unique

"spin-warp" imaging technique; the production version of this imager was adopted by other units.

In 1977 Damadian et al succeeded in obtaining an image of the human thorax, proving that although signal-to-noise ratio decreased as magnet size increased, it was possible to build a magnet large enough to image any part of the human body. From then on it has been a matter of improvements in hardware and software together with clinical trials in many centres leading to the incredible improvement in image quality and diagnostic yield seen over the past few years.

How it works

Just as it is not essential to have an in-depth knowledge of the mechanics of the internal combustion engine to ride on the number 59 bus, so magnetic resonance images can be assessed without a degree in physics. However, just as it is useful to know the language and the currency to obtain the correct fare and destination, so a basic understanding of MR principles will help both in the direction of appropriate imaging strategies and in the interpretation of images. For a full explanation and discussion of the principles and applications of MRI the reader is directed to the constantly growing literature on the subject; what will be given here is a brief and simplified outline.

At the heart of the understanding of MRI is the concept of angular magnetic moment. This is the property possessed by atoms with an uneven number of nucleons - protons and neutrons. Such atoms spin about an axis, like the earth; and like the earth, they thus generate a magnetic field, the magnetic vector of which is perpendicular to the rotational axis. They can thus be regarded as being like tiny magnets, with a "north" and a "south" pole.

Under normal circumstances, the nuclei spin in random orientations, but when subjected to an external magnetic field they align so that the magnetisation vectors point either parallel or antiparallel to the field direction - in effect, the atoms point either towards or away from the "north pole" of the external magnet. There is a slight excess of nuclei which point in the parallel direction (about 1 in 10^{6}). This gives the tissue a net magnetisation, and is responsible for the nuclear magnetic resonance signal. The

energy level of antiparallel nuclei is slightly greater than that of parallel nuclei, by an amount which varies with the strength of the external field. Under these conditions the nuclei also "wobble" or precess around the field direction in the same way as a spinning top precesses if tipped slightly. The precessions of the nuclei are not aligned with each other - they are out of phase. The frequency of this precession (ω) is characteristic of each nuclear type and is called the Larmor frequency. It is related to the strength of the applied field (B) by the formula

$$\omega = \gamma B$$

where γ is a constant, the magnetogyric ratio, unique to each nuclear species. Magnetic field strength is measured in Gauss (G) or Tesla (T); 10^4G = 1T.

The Larmor frequency is of the same order as electromagnetic radiation in the radiofrequency (RF) range. If a radiofrequency signal of precisely the right frequency is applied to the tissue, the small excess of parallel orientated nuclei will absorb energy from it. They will be tipped towards the higher energy antiparallel direction by an angle which depends on the amplitude and length of the pulse. The precession of the nuclei also becomes aligned (in phase). When the radiofrequency signal is terminated, the nuclei will realign with the magnetic field and will once again precess randomly. As they do this, the energy originally absorbed is released as a radio signal, again of the same frequency, which can be picked up by a receiver for processing.

This process is responsible for the three parameters of MR measurements, which are in turn responsible for the appearances on

images of different tissues. The amplitude of the emitted signal reflects the amount of the nuclear species present in the area of the sample being analysed - in ^{1}H MR this is the Proton Density (PD). The time taken for the nuclei to realign themselves after being tipped through 180° is the longitudinal relaxation time or T1. This is also known as the spin-lattice relaxation time - the time taken for the nuclei to transfer their energy to their surroundings, the "lattice", by collision and thermal interaction. The time taken for the phased precessions of the nuclei to become unphased is the transverse relaxation time or T2. This is also known as the spin-spin relaxation time, and is the result of interaction between neighbouring spinning nuclei and of differences in precessional angular velocity caused by inhomogeneities in the external magnetic field. It is always equal to or shorter than T1.

The relaxation times of tissues differ according to the molecular environment of the water molecules whose protons are responsible for the MR signal. Where water is tightly bound in a lattice structure, such as in bone, relaxation times are short, while in liquids such as cerebrospinal fluid (CSF) they are much longer. Soft tissues such as brain have intermediate values, with variable tissue-to-tissue differences.

Proton density, T1 and T2 all contribute to the total MR signal from a tissue. However, by manipulation of the external radiofrequency signal sequence it is possible to achieve two effects: the accentuation or "weighting" of any of the three parameters, and the spatial localisation of the signal from different parts of the tissue.

Proton density can be measured by a Saturation-recovery pulse sequence, where the nuclei are rotated through 90° and then allowed to relax back to their original configuration. The amplitude of the emitted signal, as stated above, is a measure of the concentration of the nuclei. Multiple excitatory RF pulses are applied in sequence and the resulting signals averaged to give a more accurate measurement; it must be ensured that the time between pulses - the repetition time (TR) - is sufficiently long to ensure complete relaxation each time.

T1 is usually assessed by an inversion-recovery technique, in which a 180° pulse is used to "invert" the nuclei, and the time taken for total relaxation ("recovery") is measured. In practice, an additional 90° pulse is applied in MR imaging at an interval τ because the receiving RF coil cannot measure vectors moving in its own axis. Actual measurement of T1 can be obtained by following the 180° pulse by a 90° pulse at varying time intervals; where a maximal signal is recorded after the 90° pulse, complete relaxation is assumed to have occurred. Once again the sequence of pulses is repeated at a certain repetition time; again a particular tissue will only give its maximal signal if the repetition time is long enough to ensure complete relaxation. If τ is changed or the repetition time shortened, the signal from a particular tissue can be altered; in this way its appearance on an image and its contrast with other tissues can be manipulated. For this reason the choice of RF pulse sequences is very important in MRI; different sequences will highlight different tissues, and the choice of sequence can mean the difference between identification or otherwise of a pathological tissue.

T2 is usually assessed by a refinement of the Spin-echo technique. An initial 90° RF pulse is followed after an interval τ by a 180° pulse. After the 90° pulse the nuclei initially precess in phase; however they gradually lose coherence, with some losing speed and "lagging behind" the others. The 180° pulse causes a further 180° rotation; those nuclei which were moving faster and had moved ahead are now further behind the slower moving nuclei. The faster moving nuclei continue to move faster, and will now catch up with the slower-moving nuclei at a point (2τ) before overtaking them. The amplitude of the emitted signal at 2τ is related to both proton density and T2; by varying τ it is possible to calculate T2. Again, manipulation of τ and of the repetition time in imaging studies will produce signal changes and differences in image appearances.

In imaging, as opposed to *in vitro* tissue investigations, it is more difficult to achieve results which reflect only T1, T2 or proton density. Images or RF pulse sequences are therefore referred to as T1, T2 or PD weighted. This means that manipulation of the RF sequence has resulted in an image which reflects mainly one or other of the parameters. This is important because if all three parameters are allowed to contribute, they can negate each other's effect on the total signal intensity: intensity is increased with greater proton density and longer T2, but reduced with a longer T1. The proton density of most soft tissues is around 70-85%, and increases due to disease processes are of the order of 10% (Bydder et al 1984). Changes in T1 and T2, however, can be several hundred per cent. This means that proton-density weighted images are used less in clinical imaging than the others, and also that the influence of PD in T1 and

T2 weighted images can often be largely ignored. In general, commonly-used saturation-recovery, inversion-recovery, and spin-echo sequences reflect proton-density, T1 and T2 respectively. This is far from absolute, however; with spin-echo sequences, for instance, a long echo time (2τ) and a long repetition time will result in T2 weighting, a short echo time and a long repetition time will result in PD weighting, and a short echo time with a short repetition time will result in T1 weighting.

The second effect of manipulation of the external RF signals is the achievement of spatial localisation of MR signals emitted from a sample or subject. The technique relies on the fact that the resonant frequency of the hydrogen atoms is dependent on the external magnetic field strength: the higher the field, the higher the frequency. When the subject is in the static magnetic field of the imager, the resonant frequencies of all the atoms are virtually identical. If a current is applied to large coils within the magnet, this field can be manipulated so that it is stronger at one end of the subject than at the other. This is known as a magnetic field gradient. The protons will then resonate at differing frequencies, depending on their position within this gradient field: those at one end will have a higher frequency from those at the other, with a continuous spectrum between. The applied RF pulse can then "tune in" to a particular frequency, exciting only nuclei in one particular plane or "slice". A second gradient applied along one axis of the plane so defined divides the slice further into rows with differing frequencies, which are localised in the same way. The final step of

localising a point in the row is accomplished by applying a gradient in the third plane. This third gradient is applied in an incremental fashion so that it produces increasing differences in the orientation or phase of the precessing nuclei. Spatial localisation is thus obtained by the application of two gradients at right angles, one of which selects the slice and the other of which encodes frequency, and a third which encodes phase of the spinning nuclei. Thus each point in the tissue has a unique set of characteristics, like a co-ordinate in three dimensions. Depending on the sequence of application of the gradients, images may be produced through any body plane. The translation of frequency and phase into spatial information for eventual display is achieved by computer application of a mathematical technique, 2-dimensional Fourier transformation.

In this way fairly large volumes (eg the head) can be examined in a single investigation and several contiguous "slices" displayed sequentially (Crooks et al 1982). Slice thickness depends on the size of the small range of frequencies of the RF emitted following frequency encoding by the magnetic gradient. The narrower this range, or bandwidth, or the stronger the field gradient, the narrower will be the slice examined. Resolution within the slice is better with higher field strengths, because of an improved signal-to-noise ratio and better field uniformity. It is also improved by closer coupling of the transmit/receive coils to the region examined, hence the introduction of surface coil imaging (Axel 1984) where receiver coils are tailored to provide optimal signal by close application to the appropriate area.

Hazards of MRI

The possibility of health hazards to both patients and staff has been extensively examined for many field strengths. These hazards can be divided into five main groups and will be considered briefly here.

1. The effects of static magnetic fields. Although high static fields induce T-wave changes in the electrocardiogram at levels above ≃ 0.3T, this is a purely electrical effect caused by the flow of blood (a weak conductor) through the field. It is not reflected in a physiological effect (Beischer & Knepton 1964). There are no effects on enzymatic reactions up to 20T (Ravinovitch et al, 1967) and no measureable effects on nerve conduction in a field of 2T after 4 hours (Schwartz. 1978, Gaffney & Tenforde 1980). It is estimated that a field strength of >24T would be required to alter nerve conduction by 10% (Wilkswo & Barach 1980). Budinger (1979) therefore concludes that there is no positive scientific evidence for detrimental effects on humans from static magnetic fields.

2. The effects of rapidly varying magnetic fields caused by gradient application. Time-varying magnetic fields generate electric currents by the Faraday induction phenomenon:

$$e(\text{volts}) = -10^{8}(dB/dt)\pi r^{2}$$

where **e** is the induced emf, dB/dt is the rate of change of the field, and **r** is the radius of the loop in which the EMF is produced. This yields a value of ≃1μA/cm^{2} for a very high field change of 1T/s. For comparison, a nerve action potential is 3000μA/cm, heart fibrillation is induced at 300-1000μA/cm^{2}, and magnetic phosphenes (a visual impression of flashing lights caused by retinal stimulation) at

$17\mu A/cm^2$ (Budinger, 1968).

3. The effects of radiofrequency radiation. The frequencies used in MRI are in the low RF range and would therefore be expected to induce local heat by the same mechanism as a microwave oven. Energy is absorbed principally at the surface of the body, and the maximum heat rise for an absorbed energy of 4W/kg at 10 min would be $\simeq$ 0.7°C. In the presence of intact heat-losing mechanisms the actual temperature rise would be negligible, and discomfort from this source has not been a problem (Budinger 1981). Similar results were found in a patient study by Kido et al (1987) where measurement of several physiological parameters showed no significant effects other than a $\leq$ 0.5°C rise in axillary temperature.

4. Specific effects on surgical implants. RF Heating effects on large and small metallic implants are again negligible (Davis et al 1981). A more real threat is in the dislodgement or movement of ferromagnetic implants due to static and gradient fields (New et al 1983). Field strengths are not sufficient to cause movement in orthopaedic prostheses, and in most other situations (vascular clips etc) fibrotic reaction is sufficient to hold the implant in place. In the brain, however, the movement of recently applied vascular clips is more than a theoretical possibility. Such clips applied to the subpial surface of the brain post-mortem have been shown to dissect through the cortex (R Grant, personal communication). Experiments to assess torque and movement of these clips in a 0.15T field will be described later.

Demand cardiac pacemakers are usually equipped with a reed switch which is designed to be triggered by an external magnetic

source for periodic patient checks. Such equipment is obviously subject to disruption by MRI and patients must be screened for the presence of pacemakers prior to imaging (Pavlicek et al 1983).

5. Access to the patient within an imager for monitoring or support is limited. Equipment designed to overcome this problem will be described.

Health hazards from MRI have so far proved to be theoretical or avoidable, so long as stringent screening proceedures are adhered to. If this is the case, the advantages of the lack of ionising radiation outweigh the potential disadvantages.

Advantages of MRI in CNS examination

Since the first published description of cerebral abnormalities by Hawkes et al in 1980, the brain has been one of the principal areas of research in MRI and the field in which routine clinical imaging has most quickly become established. MRI has several advantages over other imaging techniques in central nervous system (CNS) investigation:

1. The potential for tissue contrast is better than that of CT. Whereas CT is based on projections of electron density alone, the MRI signal has four contributing elements: the density of the nuclear species, T1, T2, and motion or flow (SW Young, 1984). This results in superb grey-white matter contrast, particularly on inversion-recovery images; high levels of sensitivity to tissue abnormality; and good vascular definition.

Where tissue contrast is lacking, as has been found in some tumours with respect to either nervous tissue or surrounding oedema, studies show that paramagnetic contrast agents may enhance contrast. These agents consist of heavy metals - iron and gadolinium have both been used with success (Carr et al 1984) - bound to chelating agents such as DTPA. These increase the local field experienced by protons by dipole-dipole coupling, and thus affect relaxation times in areas where they have access to tissues due to vascular permeability upset.

The information yield of MRI may be made still greater when phosphorus and carbon can be imaged, although it is likely that these images will be superimposed on ^{1}H images as the signal from these nuclei is otherwise poor.

2. The lack of artefact from bone means that structures in the

posterior fossa and directly beneath the skull vault can be clearly seen (Young et al 1981). Bone produces no signal on images because its rigid matrix structure leads to an extreme shortening of relaxation times, so that its signal has long decayed before sampling takes place.

3. ^{1}H MRI is by its nature very sensitive to changes in tissue water (G M Bydder, 1984). Most pathology in the CNS leads to local or general oedematous processes or changes in the binding of water, and MRI can almost certainly detect these earlier.

4. Because flow can be visualised on MR images, there is potential for imaging vessels and aneurysms (Singer & Crooks 1983; Bryant et al 1984; Doyle et al 1981).

5. There are no known harmful effects, and so the investigation can be repeated frequently in follow-up.

Disadvantages are few but important; they include the following:

1. Although the sensitivity of MRI to oedema is great, there is often poor differentiation between tumour and oedema (GM Bydder, 1984). This may be improved by the use of paramagnetic contrast media (Carr et al 1984).

2. The time taken for the acquisition of images is longer than that of CT. Unlike CT, where imaging time has fallen steadily since its inception, the relaxation and repetition times in MR form a fundamental barrier. Access to the patient during this long imaging time is further reduced by the configuration of the imager, and specialised support and monitoring apparatus is necessary (Hadley et al 1985).

3. MRI is very sensitive to movement, although perhaps slightly less so than CT; however, because image acquisition time is longer, the problem is potentially greater.

4. Metallic implants such as aneurysm clips can degrade images to such an extent that they are worthless. Moreover, there is a potential hazard in that the magnetic field may cause movement of the implant (New et al, 1983). Other hazards have been discussed above.

MRI has proved sensitive to pathological change in a wide variety of neurological diseases. Some, hitherto diagnoses of exclusion, can now be directly diagnosed with reference to MR studies; in others, the sensitivity of the method is evident while its specificity is still in doubt. Bradley et al (1984) compared MRI and CT prospectively in 400 patients with suspected brain or spinal cord disease; they concluded that the two studies should be considered complementary, with MRI performing better than CT in multiple sclerosis, syringomyelia and in the posterior fossa, while CT could separate tumour from oedema and was better in detecting meningiomas. Brant-Zawadski et al (1984) concluded that a multislice SE study with a long repetition time is the optimal MR screening technique and that it is more sensitive than CT for routine imaging. It should be noted that neither intracranial haemorrhage nor trauma was included in the study. Franken et al (1986) used a survey of referring physicians' opinions to study the impact of MRI on diagnosis and management. In 84% of cases, pre-examination and post-examination diagnoses were identical, with the diagnosis being changed in 8.5% and narrowed or

refined in 7.4%. However over half of the referring physicians considered that MRI yielded diagnostic information not available from studies performed previously on the patients, with an overall 39% increased confidence in the original diagnosis.

The use of MRI in intracranial haemorrhage will be considered in some detail, with consideration first being given to some associated conditions.

Head injury

Because of the difficulties in investigating restless, ill subjects by a method where stability and co-operation are at a premium, few studies have been performed to date on head-injured patients. In a preliminary report, Gandy et al (1984) examined three patients with moderately severe head injury and concluded that MRI identified small extracerebral collections more easily than CT and that several more areas of abnormality could be identified in the brain parenchyma using MRI. They surmised that the appearances might correlate with post-traumatic psychoses. This possibility was taken up by Levin et al (1985) who examined neurobehavioural sequelae (rather exhaustively, and in only one patient) and correlated them with focal lesions seen on initial and subsequent MR images. On the basis of the MR appearances in severe, 'diffuse' brain injury, they conjectured that a better terminology might be 'multifocal' brain injury.

Han et al (1984) compared MRI and CT in 25 patients at varying time intervals after head injury (up to 10 years!). No unconscious,

unstable or ventilated patients were included. MRI proved to be better in the demonstration of extracerebral lesions and their extent, partly because of the lack of bone artefact and partly because of the availability of direct coronal section imaging. Like Sipponen et al (1983, 1984) and Moon et al (1984), they found that MRI could demonstrate subacute and chronic subdural haematomas (SDH) where difficulty might be experienced with CT due to isodensity; even where MR contrast between brain and SDH was poor, the displacement of superficial cortical veins and other surface structures made diagnosis easy. Intracerebral haematomas were seen (at 0.3T) as an area of medium to low signal with a surrounding area of hyperintensity. Primary brain injury was not discussed. They concluded that "despite the limitations imposed by long imaging time... there is considerable diagnostic potential for this modality". Snow et al (1986) were more pessimistic. In 35 patients imaged 1 day to 10 years after trauma, they identified 2 patients with acute subarachnoid clot and one with intracerebral haemorrhage seen on CT but not MRI. Again extracerebral collections were equally well seen. There were 5 cases where contusional change was demonstrated with MRI but not with CT. They concluded that "because of the potential failure of MRI to diagnose acute subarachnoid or acute intraparenchymal haemorrhage, CT remains the procedure of choice in diagnosing head injury less than 72 hours old". Jenkins et al (1986) concentrated mainly on the demonstration by MRI of lesions indicative of primary brain injury in patients with all degrees of severity of injury, finding abnormalities in 88% of patients - twice as many as with CT. The number and site of these lesions corresponded well with

conscious level changes. Both extracerebral and intracerebral haemorrhage were consistently demonstrated with the pulse sequences used. Similar results were reported by Wilberger et al (1987) who examined 24 patients with GCS ≤ 7 and normal CT scans and ICP, showing MR abnormalities in all cases. These were seen principally in the white matter and brain stem; no neurological improvement was seen in 19 patients with widespread parenchymal abnormalities. They concluded that "MRI may aid our understanding of the substrate for and natural history of traumatically induced coma.".

Cerebrovascular disease

Compared with CT, MRI shows a larger area of abnormality in patients with established infarction (Sipponen et al 1983). Serial studies show that MRI abnormalities occur before there is any sign of CT change. The appearances are again of a non-specific rise in tissue relaxation time; clinical correlation is required for definitive diagnosis. An intriguing possibility is that very early MR changes may precede irreversible neurological deterioration; this raises the question of pre-emptive treatment in stroke and in the delayed ischaemia of subarachnoid haemorrhage. In cases of transient ischaemic attacks without pre-existing deficit, signal changes in appropriate anatomical sites have been identified in the Glasgow unit.

Aneurysms and arteriovenous malformations can be seen in many cases (vide infra). Although the resolution of the method is not yet sufficient to remove the need for angiography, this may improve; together with judicious use of oblique planar imaging, a viable and less dangerous alternative to angiography may be reached. MR can also

be of assistance in determining the aneurysm responsible for the bleed in cases of multiple aneurysms (Hackney et al 1986).

Intracranial haemorrhage

Questions have surrounded the imaging of intracranial haemorrhage since clinical trials began. Zimmerman et al (1985), giving preliminary results, suggested that the evaluation of intracerebral haemorrhage by MRI had lagged behind that of other disease processes because of the instability and lack of co-operation of patients with this condition.

Difficulties arise because it has been known since before the advent of imaging (Brooks et al 1975) that the magnetic resonance properties of blood change with field strength and with time. This was confirmed in imaging studies initially in subacute and chronic subdural haemorrhage (Sipponen et al 1984), but, as stated above, the opportunities for misdiagnosis in this condition are few. Initial studies in the Glasgow unit confirmed this; attention was then concentrated on the more controversial questions of intracerebral and subarachnoid haemorrhage.

The situation is summed up thus by Swensen et al (1985): "the literature conveys some confusion and seeming contradiction regarding T1 and T2 relaxation times of haemorrhage at various stages in its evolution."; this has led to uncertainties as to the ability of MR to display haemorrhage reliably, particularly in the acute phase. Initial reports (Bailes et al 1982, Bydder et al 1982) suggested that haemorrhage - both subarachnoid and intracerebral - was characterised by hyperintensity on T1-weighted images due to T1

shortening. This was assumed to be due to the paramagnetic effect of iron in haemoglobin. These reports were on patients several days after a bleed; as patients were imaged earlier, it seemed that haemorrhage of either type became more difficult to identify.

In 1983 Sipponen et al, again using T1-weighted sequences, had the unexpected finding of a long T1 in patients with acute haemorrhage. This was found to shorten as the same patients were re-examined over several days. They rightly suggested that this appearance had not been noticed before because other studies had not imaged patients so acutely. They also observed that manipulation of pulse sequences could lead to different intensities of the haemorrhage with respect to brain and oedema. No explanation was proposed.

DeLaPaz et al (1984) measured the T1 and T2 of haematoma, SAH and brain on T1 and T2 weighted images, and found acute haematoma and SAH to have relaxation times approximating to those of white matter. T1 was found to shorten and T2 to lengthen with time. They concluded that the specific identification of acute haemorrhage is a problem. SAH was shown as an area of hyperintensity on one T2-weighted image; they suggest that T2-weighted images with a repetition time of ≃1s might be useful in this condition. One problem with these results is in accepting the accuracy of imager-derived measurements of relaxation times.

Sipponen et al (1985) again looked at the problem of the changing appearances of intracranial haematomas, this time with imagers operating at 0.17 and 0.02T. They concluded that low-field systems have advantages in the diagnosis of acute haematomas because

T1 differentiation is greater at low field strengths. T2-weighted images showed similar intensities at both field strengths, with acute haemorrhage shown as approximately isointense with brain tissue.

Dependency of image contrast in haematoma was also shown by Gomori et al (1985). They imaged 20 patients between 1 day and 1 year after the bleed. At 1.5T, acute haematomas exhibited a central hypointensity, interpreted as being the haematoma itself, and a peripheral hyperintensity due to parenchymal oedema. Subacute haematomas exhibited an additional rim of hypointensity outside the hyperintense region, interpreted as being due to the paramagnetic effects of haemosiderin in macrophages at the margins of the haematoma; chronic haematomas showed hyperintensity throughout. At low field strengths (<0.5T), however, neither the central hypointensity nor the extra parenchymal rim of hypointensity were seen: acute haematomas were isointense with the surrounding brain, while subacute and chronic haematomas were hyperintense. The appearance of deoxyhaemoglobin within the haematoma is proposed as being responsible for the central hypointensity of acute haemorrhage. Methaemoglobin was not found in a sample aspirated from one acute intracerebral haematoma. The clinical imaging findings were confirmed for extracranial haematomas by the same group (Rubin et al 1986).

Zimmerman et al (1985) examined 5 patients within 72 hours of a bleed and found isointensity of haematoma and surrounding brain in all 5. All of 7 patients imaged between 7 and 32 days showed hyperintensity of the haematoma. No new conclusions were drawn.

Swensen et al (1985) highlighted the differences in findings

and opinions regarding the apparent T1 and T2 of intracranial haemorrhage. They reported the findings at 0.15T of human intracerebral haematoma studies, where T1 and T2 were both found to decrease with time, and of experimental haematoma in the thigh of dogs. In the latter, a high signal was observed on the first day on a SE2100/80 sequence; T1 and T2 were calculated and found to fall progressively as the haematoma aged. Haematomas were easily differentiated from surrounding tissues at all stages. Sequential changes in T1 and T2 were related theoretically to changes in pH, osmolality, haemoglobin and methaemoglobin concentration. T1 and T2 are proportional to pH; pH is acidic in the inflammatory environment of extravascular blood in a state of catabolism. T1 and T2 are inversely proportional to haemoglobin and methaemoglobin concentration; although the haemoglobin concentration falls with time, the effect is outweighed by the appearance of the much more paramagnetic methaemoglobin. As water is absorbed from the clot, so increased osmolality will lead to further relaxation time shortening.

In a study on subarachnoid haemorrhage, Bradley & Schmidt (1985) investigated in detail the possible causes of the observed changes in the relaxation times of CSF after haemorrhage. Changes are not due to cell lysis and the liberation of haemoglobin; water molecules have ready access across the red cell membrane, and no signal differences were observed *in vitro* when lysed and unlysed samples were compared. They proposed that "changes in proton relaxation enhancement effects may be attributed directly to changes in the interactions between the CSF water protons and the haem iron that occur as a result of the oxidative denaturation of haemoglobin.".

They examined the effects on relaxation times *in vitro* of changes in concentrations of haemoglobin, deoxyhaemoglobin and methaemoglobin. T2 of haemoglobin, deoxyhaemoglobin and methaemoglobin were similar. T1 of haemoglobin and deoxyhaemoglobin were similar, while that of methaemoglobin was significantly lower. They conclude that the gradual appearance of methaemoglobin is responsible for the reduced T1 of bloodstained CSF seen on clinical images, and that MRI performed within the first week after haemorrhage is likely to be non-diagnostic. It is worth noting that changes in relaxation times with the addition of blood to CSF were related to CSF measurements of T1 = 2s, T2 = 1s; as will be seen, these measurements are erroneous and lead to a fundamental flaw in the interpretation of the results.

Chakeres & Bryan (1986) performed an *in vitro* MRI and CT imaging experiment, with MR sample analyser correlation, using different concentrations of blood in CSF. T1 and T2 were found to fall with increasing blood concentration. They concluded that MRI might be more sensitive than CT in demonstrating mild SAH, but that isointensity with brain would occur at high blood concentrations. CT, although not able to demonstrate low concentrations of blood in CSF, could show solid clot more easily.

The present study

The literature on MRI in intracerebral and subarachnoid haemorrhage is thus seen to be confusing, both in the results of studies and in the explanations proposed for these results. In order to investigate the ability of MRI to shed light on the pathological processes surrounding intracranial haemorrhage, it was necessary first to find whether MRI could show haemorrhage at all stages and to try to develop methods of selecting the pulse sequences most appropriate for its demonstration.

With the almost infinite variety of pulse sequences available in MRI, it is important to choose one which is appropriate for the specific condition under investigation. In chronic or stable diseases, selection based upon trial and error may be adequate, but an approach based upon a guiding framework would clearly be preferable in most acute neurosurgical conditions. Published relaxation times of tissues in health and disease provide some basis for predicting appropriate sequences, but vary according to the field strength of the equipment and have proved to be inaccurate in several instances. Variations in sequence construction also make comparisons between images difficult. It was felt that one of the principal reasons for the lack of coherence in results mentioned above might well be in the selection, implementation and comparison of inappropriate imaging techniques.

Intracranial haemorrhage, whether spontaneous or traumatic, is essentially the intrusion of blood into previously normal brain or CSF. This study presents a rationale for pulse sequence selection in both intracerebral and subarachnoid haemorrhage using data from *in*

vitro measurements of the relaxation times of these tissues. The data were analysed by a simple computer program which calculated the relative signal intensities of the tissues for the spectrum of pulse sequences available on the imager used. The results were used to select appropriate sequences, and patient studies using these sequences are presented.

The patients studied were in three categories: subarachnoid haemorrhage, intracerebral haematoma, and head injury. These categories are not mutually exclusive, and indeed the purpose of including the head injured patients in this series was to study the ability of MRI to show local effects around the micro-haematomas seen post-mortem in the brain parenchyma of these patients, especially in diffuse axonal imjury. The results were separated into these categories for the purpose of analysis.

In chapter 3 will be found a description of the equipment used for *in vitro* and imaging studies, followed by the method and results of the *in vitro* experiments. Chapter 4 deals with possible approaches to clinical imaging, while the results of *in vivo* and patient studies are reported in chapter 5.

Chapter 3

METHODS AND RESULTS: 1

Magnetic Resonance:

description of equipment

in vitro studies

EQUIPMENT

1. *in vitro* analysis

A Brüker Minispec MR analyser was chosen for the measurement of relaxation times of all tissue samples. Because the MR characteristics of tissues depend both *in vivo* and *in vitro* on the magnetic field strength, it was important that the tissue analysis equipment should match the imaging equipment as closely as was practicable, in order that results obtained *in vitro* could be processed to give useful data for patient studies. The analyser was tuned to operate at 6MHz; the imager operates at 6.3MHz. This is equivalent to a magnetic field strength of approximately 0.15T, generated in the analyser by a permanent magnet with resistive shims.

This equipment is principally used by the oil and food industries as a quality control device, and required the following operational modifications to enable its use in human biological studies.

1. Between 35 and 40°C, MR relaxation times change by about 1-2% per degree. The magnet core temperature was measured at 39°C; this was regulated to 37°C (± 0.5°C) by constant water cooling of the probe head by a peristaltic pump.

2. The volume of tissue which gave the most reproducible results was found to be 0.3ml, and wherever possible this quantity was used in all studies. Quantities as small as 0.1ml yielded reproducible results but with a higher standard deviation from the mean of the measurements. This meant that it was possible to measure relaxation times of needle biopsy samples from living patients.

3. The number of averages, ie the number of measurements performed

and averaged by the machine during each of its iterative processes, could be varied by the user. The higher the number of averages, the more accurate the measurement; similarly, the smaller the sample, the larger the number of averages required for an accurate measurement. With the 0.3ml sample size, it was found that increasing the number of averages beyond nine did not alter the accuracy; nine averages were therefore measured unless the sample size was less than 0.2ml when sixteen averages were measured. Where the total bulk of the tissue sample permitted, at least two adjacent pieces were analysed and the mean obtained. T1 was measured using an inversion recovery sequence and T2 was measured using the Carr-Purcell-Meiboom-Gill pulse sequence. The repetition time (TR) used was greater than the T1 by a factor of five.

4. The reproducibility of the measurements was checked both with copper sulphate standards and with tissue samples. While the relaxation times of the standards were constant and showed a variation of less than 5%, in many cases there was a progressive decrease in T1 and T2 of small biological samples with time.

To attempt to reduce this effect, thought to be due to time-related effects of temperature, evaporation, and tissue metabolism, a protocol was developed for tissue excision, transport, handling and measurement. This involved the swift transfer of cleanly excised tissue to a sealed capsule for immediate analysis. Numerous types of small sealable container were tried; the most satisfactory, from the points of view of size and convenience, proved to be empty gelatin drug capsules supplied by the hospital Pharmacy department. These produced no MR signal provided that the tissue sample was first

wrapped in transparent polythene. This process proved easy and effective.

The equipment required is:

Scalpel blade

Nickel spatula

Blunt forceps

2.5cm polythene discs

Gelatin drug capsules ED 6.2mm ID 5.4mm

Aluminium tube ED 4.8mm ID 3.1mm with fitted rubber plunger - 'injector'

Standard NMR sample tubes ED 7.6mm ID 6.6mm (Brüker GMBH)

The aluminium 'injector' was made to specification in the workshop; all other equipment is standard.

The protocol for the analysis of tissue excised at operation is as follows. With reference to the MR images, an appropriate area for sampling is selected. Using dry rongeurs, the surgeon excises a 0.3-0.5cc sample which is transferred directly onto a glass slide. The researcher responsible for sample handling cuts the tissue cleanly to a size of 0.2-0.3cc. This is loaded into the 'injector', the tip of which is then wrapped in polythene and inserted into the capsule. The tissue is extruded into the capsule, surrounded by the polythene, and the 'injector' withdrawn. The capsule top is applied and the capsule is then loaded into a standard glass NMR tube. The process is illustrated in fig. 1.

fig. 1

(a) injector and capsule; tissue sample on polythene disc.

(b) the sample is aspirated into the injector, and pushed into the capsule protected by the polythene.

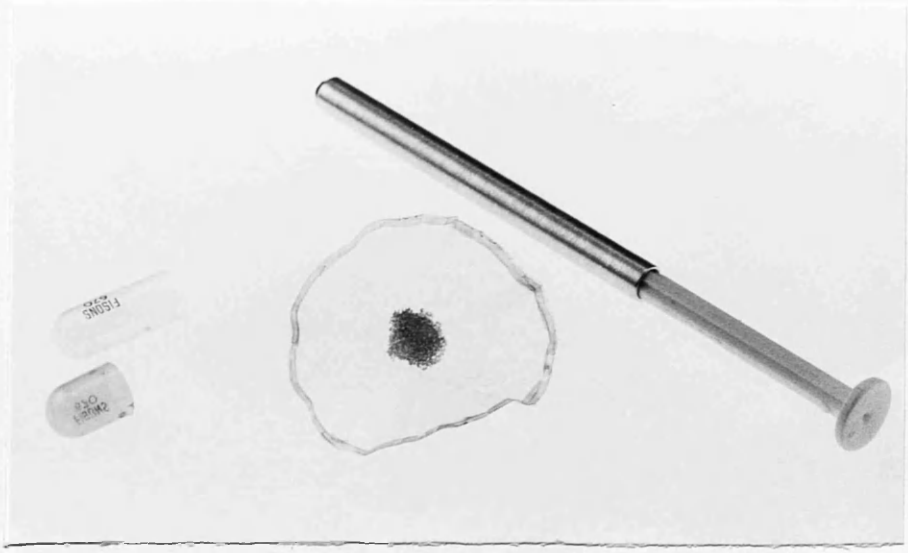

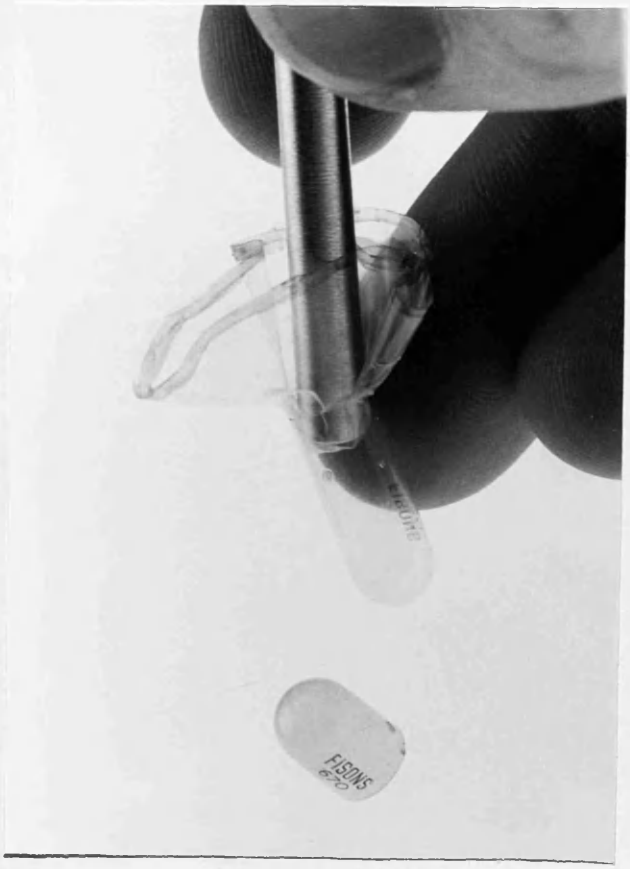

fig. 1

(c) the sample is extruded and the injector then withdrawn.

(d) sealed capsule with tissue sample.

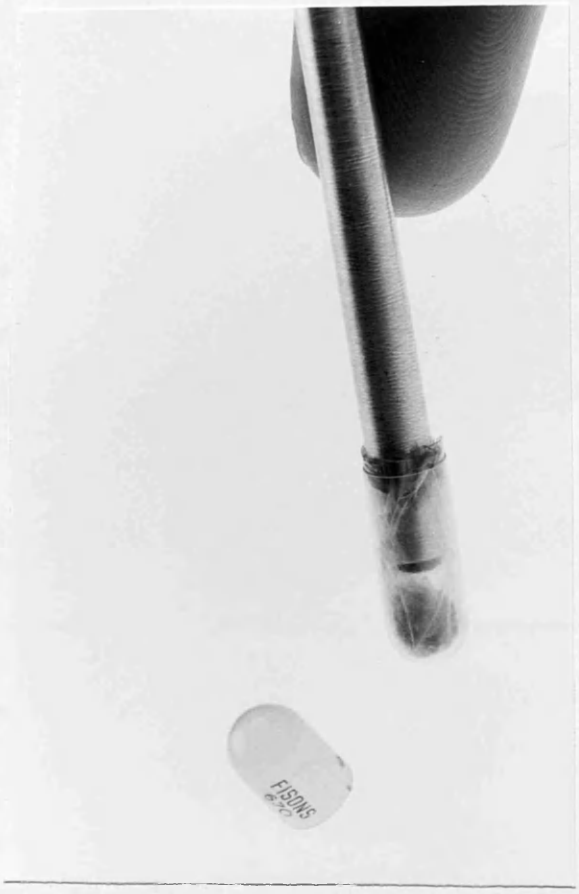

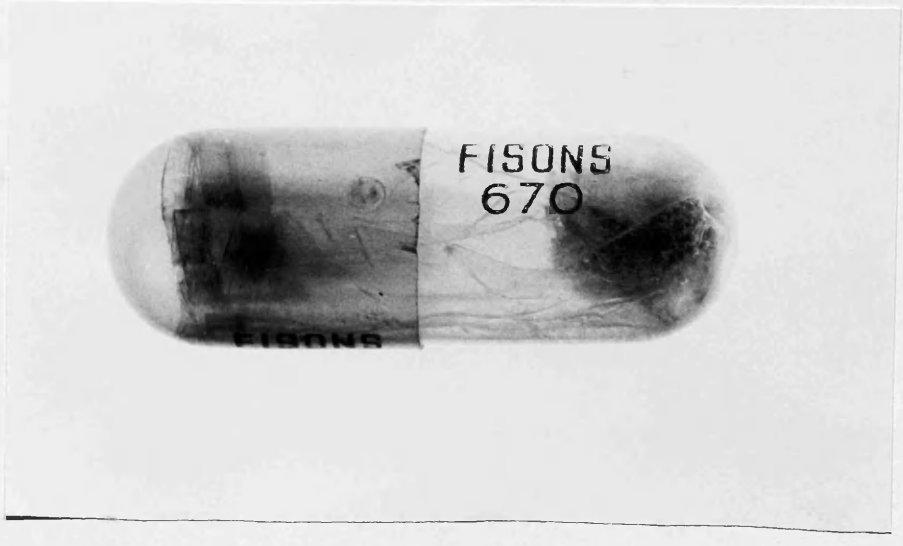

The sample is then transferred to the MR facility, which is situated within 50m of the operating rooms. Immediate mesurements are undertaken. Samples are kept in a water bath at 37°C between measurements.

The validity of the method was assessed by measuring the T1 of a copper sulphate solution with and without encapsulation. The capsule and polythene together produce no MR signal. To assess stability over time, tissue samples had T1 and T2 measurements performed immediately and after encapsulation for 2hrs. Measurements of unencapsulated brain (dog, grey-white matter homogenate)were also performed.

Sample	**n**	**0hr**		**2hr**	
		T1	**T2**	**T1**	**T2**
capsule alone	2	-	no signal	-	
$CuSO_4$	2	390±4	328±6	-	-
$CuSO_4$ (caps.)	2	389±6	326±7	-	-
Brain 0.3cc	3	323±49	162±10	279±48	161±19
Brain 0.3cc (caps.)	3	257±20	142±5	243±20	147±12
Human glioma (caps)	2	868±38	265±12	869±28	266±8

table 1

variation with encapsulation time of relaxation times (ms, ± SD of four readings) of solutions and tissues

Magnetic Resonance Imaging

Imaging was performed on a Picker 0.15T resistive imager operating at 6.3MHz. This is a low to medium power MR system in which the magnetic field is generated by a water-cooled resistive magnet; it was thus possible to house the equipment close to the neurosurgical wards and theatres, without the elaborate safety precautions attendant on high field superconductor imagers. The limitations of a low field system in terms of slice thickness and resolution are not a problem in patient studies, but make animal studies difficult. At the time of these studies software developments were not available to enable the measurement of T1 and T2 on images with any degree of accuracy, and there was no facility for proton-density imaging. This made easy correlation with *in vitro* tissue studies impossible.

All patient studies were carried out with the informed consent of the patient or relatives as appropriate. All research protocols were submitted to the Hospital Ethics Committee for approval. The MR investigations were performed using the guidelines proposed by the National Radiological Protection Board (January 1985)

To enable patients to be imaged safely, it was vital to develop MR compatible monitoring and support apparatus. Much of the equipment in routine use is sensitive to magnetic fields, or would lead to disruption of the image by conduction of stray radiofrequency to the shielded interior of the imager; in addition, access to a patient within the bore of an MR imager for observation and treatment is very limited.

Routine observation of patients who had been stable up to the

time of imaging involved ECG monitoring through a fibre optic coupling system. The ECG signal was carried by short leads from the patient to equipment still within the bore of the imager which converted the electric signal to a light signal. This was carried to the exterior via a fibre optic lead and finally reconverted to an electrical signal for display on an oscilloscope. This eliminated the problem of RF conduction from outside; however, the RF gradient currents occurring during imaging swamped the ECG signal and prevented an ECG being obtained during image acquisition. Blood pressure was measured at one minute intervals by a Dinamap monitor, while respiration was observed from outside the imager by a member of nursing staff always in attendance. The electric MR couch transport system could be overridden in case of emergency, and direct access to the patient obtained within seconds.

Ventilated patients were transferred from the ward using a portable ventilator. Unless the patient required the administration of anaesthetic gases, this ventilator was used during imaging with no effect on MR signal. Anaesthetic gases were given from Boyle's apparatus via a Penlon ventilator. Long anaesthetic tubing was employed, the problem of dead space being eliminated by the one-way flow of the gases. End tidal CO_2 was monitored in all ventilated patients. The proximity of the anaesthetic equipment to the imager necessitated re-tuning of the gradients, but there was no consequent image degradation.

The safety of imaging patients following operation to clip an intracranial aneurysm was investigated. Each of the types of

aneurysm clip in current use in the Institute was examined for evidence of torque or deflection in the magnetic field of the imager. Alignment of the axis of the clip with the field due to eddy current induction was considered acceptable because of the minimal forces involved, but clips were rejected if magnetic attraction was greater than gravitational forces. In addition, each clip was suspended in a beaker of water doped with $CuSO_4$ which was then imaged to assess the extent of signal artefact and spatial distortion caused by eddy current magnetic induction (fig. 2).

Patients were only imaged postoperatively if an acceptable clip had been used. The Sugita range of clips did not move detectably in the static or gradient fields and produced a minimal signal artefact; postoperative studies were therefore restricted to patients treated using this type of clip.

fig. 2

MR image of (a) Scovill clip and (b) Sugita clip

suspended in $CuSO_4$ solution

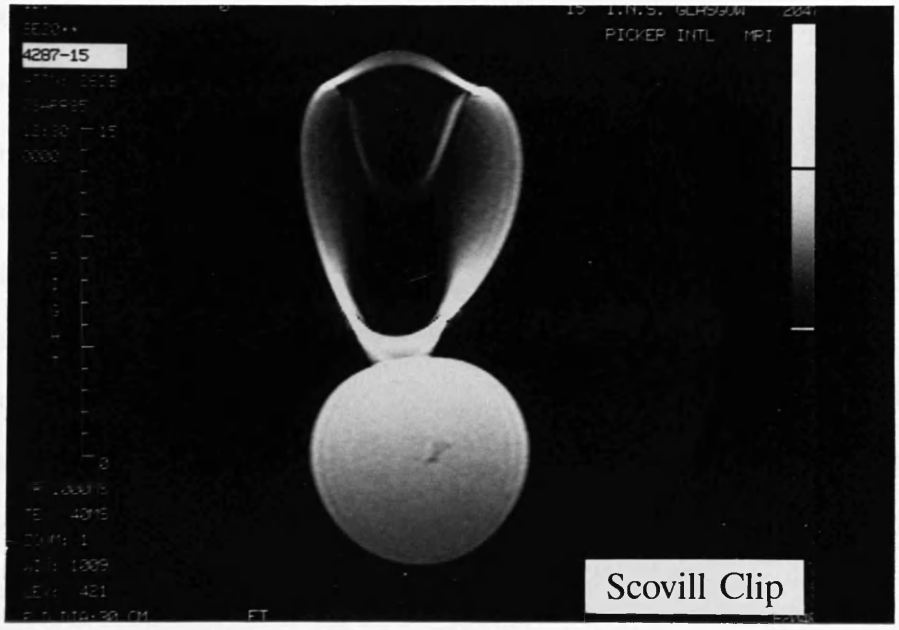

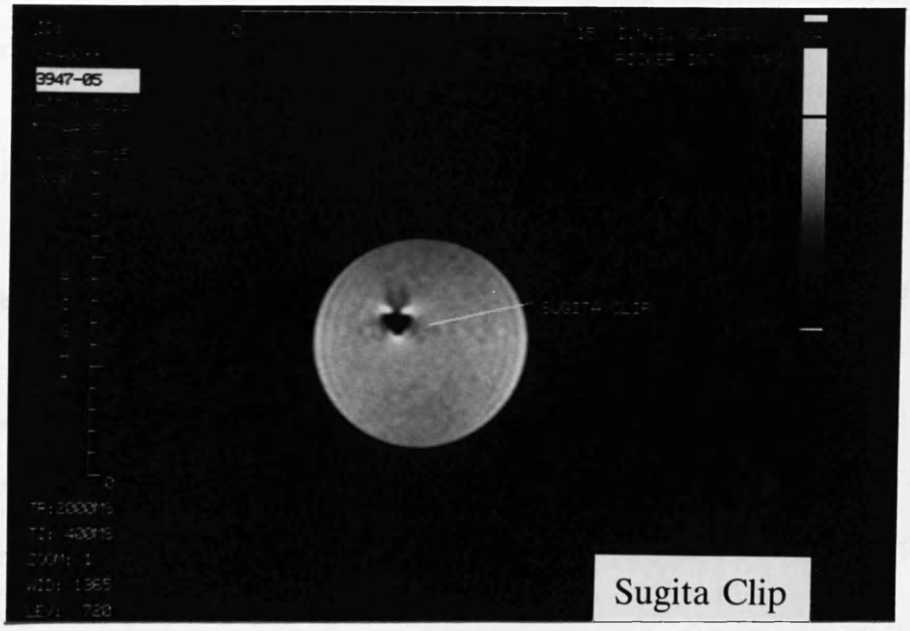

STUDIES

The intention of the *in vitro* studies was to formulate a strategy for the choice of optimal pulse sequences for the imaging of intracranial haemorrhage, having ascertained from an initial imaging study that (a) haemorrhage can be shown by MR and (b) some commonly-used pulse sequences do not show it at certain stages. The relaxation times of blood, brain, CSF and bloodstained CSF were measured *in vitro* and the measurements used to calculate the relative signal intensities of these tissues on images made using different RF pulse sequences. Sequences which maximised contrast between haemorrhage and normal tissue were selected for patient trials.

in vitro Imaging

An initial study was carried out using a model of intracerebral haemorrhage to assess the difficulty or otherwise of imaging haemorrhage and to discover whether there were changes in its MR characteristics with time. An adult dog which had been sacrificed at the termination of an unrelated, extracranial experiment had an injection of 3ml of fresh human blood into the parenchyma of the right frontal lobe via a burrhole. The head was imaged at 0, 4, and 24 hours, and at 3 and 7 days. A variety of pulse sequences were applied and the images assessed.

Fig. 3 shows SE and IR images of the head of the dog in the coronal plane.

The haematoma is in a satisfactory position in the parenchyma of the brain. At the time these images were obtained, there was a constant central artefact in the phase-encode direction on all images from the picker imager. It is seen overlying the haematoma in fig. 3 (b) and (c) but does not interfere with signal immediately adjacent. It can be seen that the intensity of the haematoma changes with respect to that of the brain over the 7 days of the experiment. The T1 and T2 of the brain were measured at the beginning and end of the experiment and were found to change by less than 5%; values were similar to those of human brain. It therefore seemed likely that difficulty would be experienced in imaging patients with haematomas at certain times after the bleed, as there is likely to be a period where blood and brain are isointense. The remainder of the project was devoted to reducing these difficulties by using studies of the tissues involved in intracerebral and subarachnoid haemorrhage - blood, brain and CSF - to help in the development of a strategy for imaging patients with these conditions.

fig. 3

Intracerebral Haematoma produced *in vitro* in the dog.

SE2000/80 images at (a), 1hr; (b), 3 days;

and (c), 7 days after lesion production

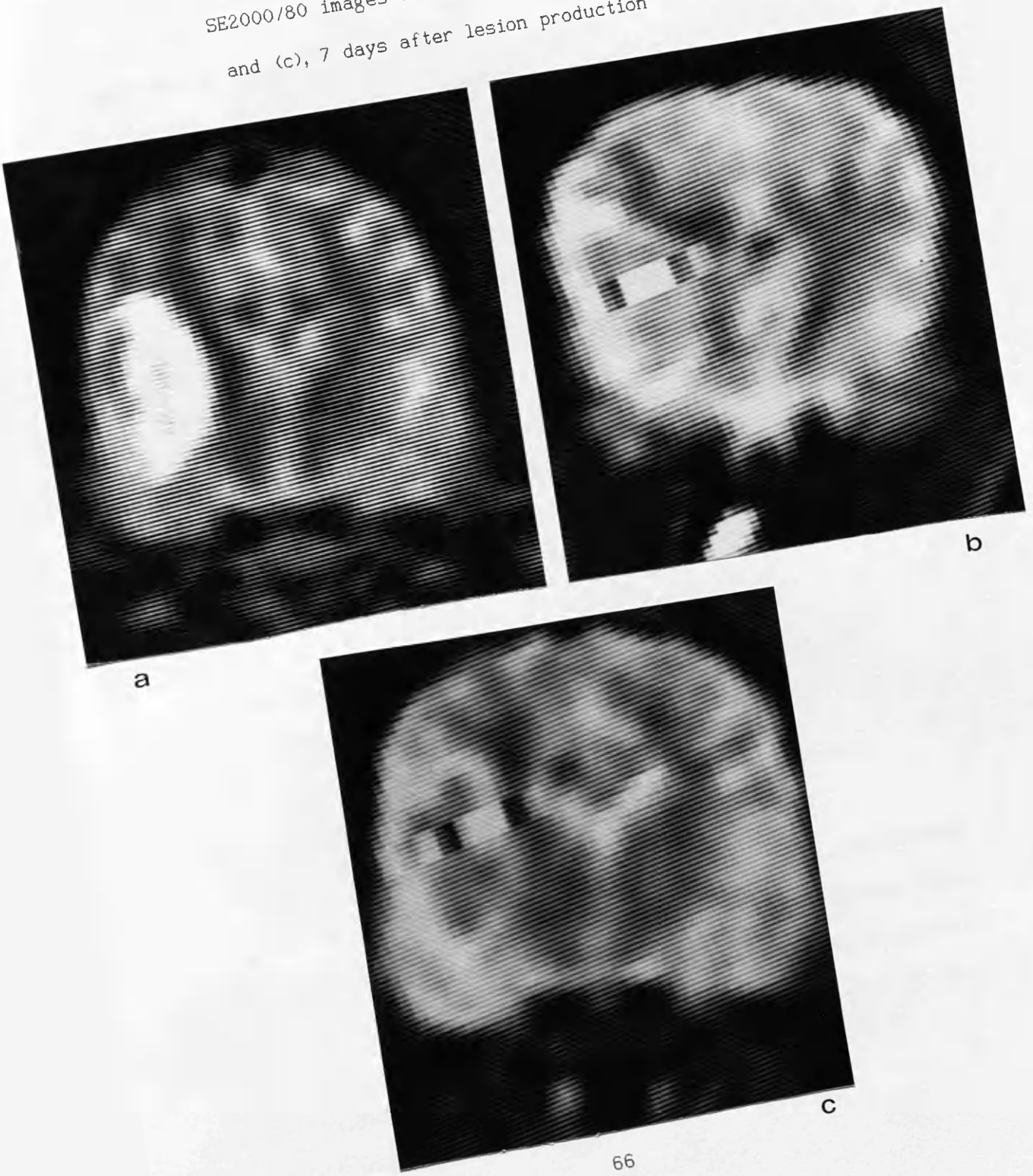

In vitro T1 and T2 measurements

Tumours

Measurements were made initially on a variety of tissues, both normal and pathological, using the technique already described. Prior to embarking on studies on haematoma, it was necessary to examine most of the common intracranial tumours to discover whether similarity of relaxation times could cause diagnostic confusion.

Acoustic neuromas, meningiomas, astrocytomas and pituitary tumours were all examined. The relaxation times obtained are shown in table 2.

Tumour	n	T1	T2
Acoustic Neuroma	4	536±60	140±33
Meningioma	3	581±75	147±20
Astrocytoma	5	666±101	234±76
Pituitary Macroadenoma	4	378±113	121±7

table 2

relaxation times (ms ± SD) of intracranial tumours

It can be seen from these results that T1 and T2 are variable within each tumour type, and furthermore that the relaxation times are not tumour-specific. Confusion with acute haematoma is possible in terms of relaxation times alone; morphology may however provide sufficient distinction.

Normal brain, blood and CSF were then examined, as was CSF doped with blood to simulate subarachnoid haemorrhage.

Brain

Human grey and white matter were obtained at post-mortem from patients who had died of extracranial disease within the preceding eight hours. Large blocks of tissue were excised from the frontal and occipital lobes and sealed in a jar immediately after removal of the brain. Within 15 minutes separate 0.3ml samples of white or cortical grey matter were taken by sharp dissection and encapsulated and analysed by the method described.

Relaxation times for human grey matter, white matter, blood and CSF are shown in table 3.

Tissue	**n**	**T1 (ms)**	**T2 (ms)** (mean ± SD)
Grey matter	6	513±57	118±8
White matter	6	242±14	86±10
Blood (immed.)	10	656±30	275±27
CSF	10	3444±170	2269±128

table 3

relaxation times of cerebral grey and white matter,

fresh whole blood and cerebrospinal fluid

Blood

0.3ml aliquots of fresh venous blood taken from volunteers were placed in sealed NMR sample tubes and analysed sequentially in two batches. The first was allowed to clot normally, while in the

second the blood was defibrinated mechanically by agitating the tubes. This second set was studied because in intracranial haemorrhage blood often does not clot fully, due to the defibrinating action of brain pulsation. T1 and T2 were measured immediately, at 4, 8, and 24 hours, and at daily intervals to 15 days.

The results of serial measurements of T1 and T2 on clotted and unclotted blood are shown in table 4.

Time from sampling		clotted		unclotted	
	n	T1	T2	T1	T2
immediate				656±30	275±27
2hr	10	701±18	307±42	601±70	257±16
4hr	10	683±34	347±22	660±55	283±16
24hr	10	633±32	332±31	624±58	276±22
2 days	10	536±71	262±31	620±32	255±14
3 days	10	376±109	184±43	504±53	191±33
4 days	10	321±91	162±29	443±62	182±21
6 days	10	287±79	146±19	371±73	172±16
7 days	10	260±59	136±13	344±64	164±17
8 days	10	238±45	130±12	306±52	153±20
9 days	10	210±29	123±16	271±53	137±21
10 days	10	193±20	112±10	260±55	130±20
14 days	10	173±19	101±12	203±47	108±20
15 days	10	167±21	102±10	188±42	104±16

T1 and T2 in ms, ± SD

table 4

relaxation times of clotted and defibrinated whole blood

measured over a 15 day period

T1 and T2 of clotted and defibrinated blood differed significantly, but both fell progressively after the first 24 hours. The relaxation parameters of brain did not change during this time if kept in a sterile environment. The fall in mean T1 and T2 is expressed graphically in fig. 4.

fig 4.

Mean values for T1 and T2 of clotted (---) and defibrinated (——) blood measured over 15 days

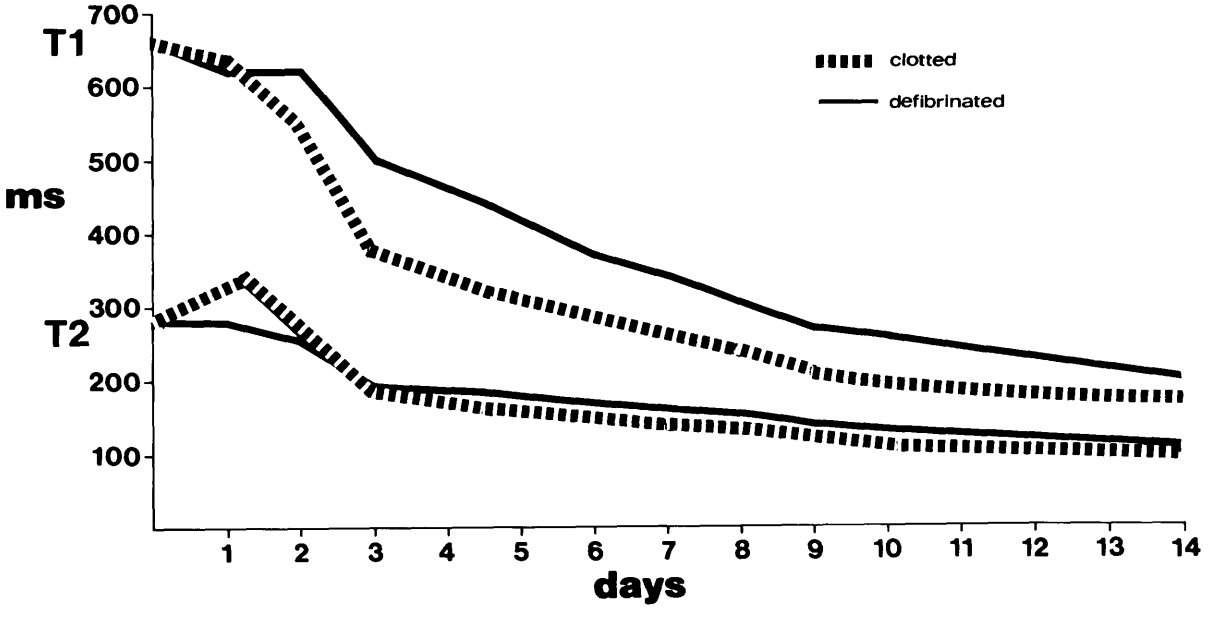

CSF

Biochemically normal CSF was taken from patients undergoing myelography for degenerative spinal disease. 0.3ml aliquots were analysed. In addition, 3 separate series of samples were prepared to simulate CSF in subarachnoid haemorrhage: fresh venous blood was added in concentrations of 40, 80 and 160 ml blood per litre of CSF (approx. 16, 32 and 64 x 10^3 red cells per mm^3, all less than 10% red blood cell solutions). All four batches were analysed daily for 15 days.

The relaxation times of CSF and bloodstained CSF are shown in table 5

Test substance	n	T1	T2
CSF	15	3444±170	2269±128
+0.04ml blood/ml	8	2940±104	1943±273
+0.08ml blood/ml	8	2583±90	1633±134
+0.16ml blood/ml	8	1590±380	928±158

T1 and T2 in ms; mean ± SD

table 5

relaxation times of CSF and bloodstained CSF

0.04ml of blood/ml CSF contains approximately 15000 rbc/mm^3, and renders the CSF sample pink but translucent. The addition of even this small amount of blood to CSF altered the T1 and T2 by 15%. A four fold increase in the blood concentration halved the CSF relaxation times. Serial measurements of these samples over 15 days showed this differentiation to be maintained; T1 and T2 of the

bloodstained samples fell, quickly at first and then more slowly, while the values for clear CSF rose gradually and proportionately less. These time-related changes are summarised in fig. 5 for the first 10 days, values for all days being given for clear CSF and 160ml blood /l CSF: for the sake of clarity intermediate values are omitted for the 40ml /l and 80ml /l samples.

fig. 5

Mean T1 (closed) and T2 (open symbols), measured over 10 days, of clear CSF (●○) and of CSF with blood added in quantities of 40ml/l (◆◇), 80ml/l (■□), and 160ml/l (▲△)

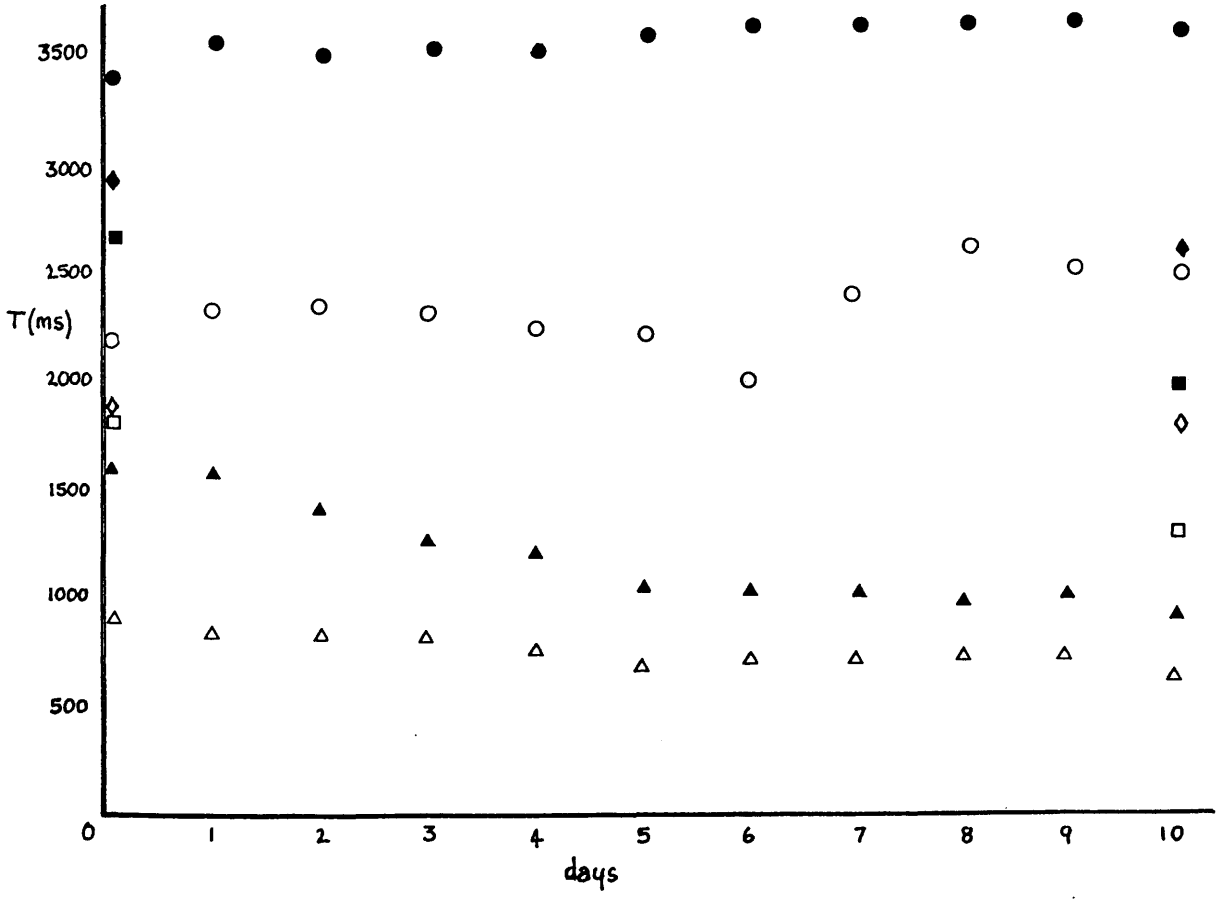

Results of analyses carried out recently in the Glasgow MR unit (Grant et al 1987) show that CSF, which is known to have a low oxygen tension *in vivo*, shows a drop in relaxation times as it equilibrates with air. For this reason the measurements were repeated under anaerobic conditions to approximate closer to the *in vivo* situation and to ensure the validity of the use of the results in the prediction of pulse sequences for use in patients.

CSF was collected anaerobically via lumbar puncture from patients undergoing myelography for degenerative spinal disease. Biochemical and bacteriological analysis was normal. The samples were transferred to stoppered glass vials, care being taken to exclude air bubbles. Relaxation times were measured and are given below.

Arterial blood was then added in three concentrations as before: 40, 80 and 160 ml per litre of CSF. Microscopy of one of the latter samples showed it to contain 64 x 10^3 red cells per mm^3. T1 and T2 were measured as before (table 6).

Test substance	n	T1	T2
CSF	4	4423±110	3076±14
+0.04ml blood/ml	4	3330±154	2223±162
+0.08ml blood/ml	4	3313±20	2065±55
+0.16ml blood/ml	4	2513±86	1880±14

T1 and T2 in ms, ± SD

table 6

relaxation times of CSF and bloodstained CSF

measured under anaerobic conditions

The relaxation times of CSF measured under anaerobic conditions are seen to be substantially higher than those of CSF allowed to equilibrate with air. When blood is added, even in small quantities, there is a similar but even more marked drop in relaxation times which is again proportional to the amount of blood added.

To assess whether the fall in relaxation times with the addition of blood is due to the breakdown products of haemoglobin (Bradley & Schmidt 1985) or to the effect of protein, measurements of relaxation time were repeated on the clear, cell-free supernatant fluid of the samples. This was aspirated at 24 hours after gravitational precipitation of the cellular element.

Protein concentration was measured at 7.5g/l on the supernatant of the 0.16ml blood/ml sample. Plasma protein solution was added to fresh CSF in quantities of 6g/l and 12g/l and T1 and T2

measured. The results of these experiments are summarised in table 7.

Test substance	n	T1	T2
CSF (24hr)	2	4196±116	2096±355
+0.04ml blood/ml	2	2806±71	3135±173
+0.16ml blood/ml	2	2351±25	2201±240
+6g PPS/l	2	3433±125	2145±21
+12g PPS/l	2	1775±43	1681±206

T1 and T2 in ms; mean ± SD

table 7

relaxation times of supernatant fluid after mock SAH, and of plasma protein/CSF solutions

The decrease in relaxation times after separation of the cellular, haemoglobin containing fraction is of the same order as that of the unseparated samples. Plasma protein solution added to CSF in concentrations approximating to those found in experimental subarachnoid haemorrhage leads to a similar drop in relaxation times. These results suggest that protein in CSF after subarachnoid haemorrhage can cause a fall in its relaxation times. Equipment to separate the haemoglobin-containing fraction from the samples was not available, and so the relative contribution of haemoglobin breakdown products to these findings could not be assessed.

SUMMARY

Initial imaging studies using sequential imaging of haemorrhage in animal brain *in vitro* showed that the MR characteristics of haemorrhage change with time. Particularly with inversion-recovery sequences, instances arose where haemorrhage was found to be isointense with brain, thus causing potential diagnostic difficulties.

A single-frequency (6MHz) MR spectrometer was used to measure the relaxation times of brain grey and white matter, and of CSF. The T1 and T2 of grey matter were 513±57ms and 118±8ms respectively, of white matter 242±14ms and 86±10ms, and of CSF 3444±170ms and 2269±128ms. Serial measurements were performed daily to 15 days on both clotted and defibrinated blood. The results confirmed the imaging findings: as clotted blood aged, its T1 and T2 fell progressively from initial values of 656±30ms and 275±27ms to 536±71ms and 262±31ms at 2 days and 167±21ms and 102±110ms at 15 days. Values for unclotted blood were similar.

Subarachnoid haemorrhage was simulated *in vitro* by adding blood to CSF in quantities of 40, 80 and 160 ml/l. The addition of increasing amounts of blood reduced the T1 and T2 of CSF progressively: 40ml/l reduced T1 and T2 to 2940±104ms and 1943±273ms respectively, 40ml/l to 2583±90ms and 16333±134ms, and 160ml/l to 1590±380ms and 928±158ms.

The next chapter describes the use of these values to develop optimum RF pulse sequences for use in the MR imaging of intracranial haemorrhage.

Chapter 4

METHODS AND RESULTS: 2

Magnetic Resonance:

Approaches to Clinical Imaging

RF Pulse Sequence Selection

Approaches to Clinical Imaging

In the spin-echo and inversion-recovery sequences available on a clinical Magnetic Resonance Imager, the T1, T2 and proton density of a tissue all contribute towards the intensity of signal it produces on an image. Different pulse sequences will highlight these parameters in different proportions, and it should thus be possible to mask or highlight contrast between tissues imaged provided that they differ in one or more of the parameters. In practice, proton density varies little in living soft tissues, and T1 and T2 are the major determinants (Beall et al 1984).

To be clinically useful in studies on patients with intracranial haematoma or subarachnoid haemorrhage, it should be possible to distinguish on images normal from abnormal tissue - in this case, blood or bloodstained CSF from brain or normal CSF - easily and predictably on images without the need for further measurements or manipulation, and without the risk of isointense signals masking the diagnosis. The aim was to develop pulse sequences which separated the intensity of the signal from the abnormal tissue from that of the normal tissue sufficiently to enable immediate diagnosis, while maintaining recogniseable anatomy.

There is an almost infinite number of pulse sequences available on a production MR imager, and it would be impossible to try all the available combinations in the clinical situation. It was therefore necessary to develop a method of finding sequences with optimum contrast without the use of patients. An attempt was made to set up an *in vitro* model which could be used to obtain images at a range of echo and repeat times; sequences with good tissue

contrast could be selected and further refined. The failure of this approach led to the use of a computer-based system which used the previously obtained relaxation values to predict appropriate sequences. Both approaches will be discussed.

Phantom Imaging

The intention of this approach was to set up a phantom filled with materials whose relaxation times approximated to those of grey and white matter. Samples of blood or CSF could be incorporated into the phantom in separate containers and the whole phantom imaged . The necessary "artificial brain" was obtained by mixing agarose gel with water doped with gadolinium.

Agarose dissolved in water and allowed to solidify lowers both T1 and T2 of the water, but lowers T1 to a greater extent. Gadolinium, a paramagnetic substance, lowers T2 to a greater extent than T1. A 2g/l solution of gadolinium-DTPA was made, aliquots of which were added to varying concentrations of agarose solution before solidification. T1 and T2 were measured on the *in vitro* spectrometer in the standard manner.

It did not prove possible to mimic the relaxation values of brain precisely. A solution of 7g/l of agarose with the addition of 90ml of gadolinium solution yielded T1 = 453, T2 = 107ms. This compares to brain grey matter mean measurements of 513 and 118ms respectively. 7g/l of agarose with 195ml gadolinium solution gave T1 = 227, T2 = 90ms, compared to white matter means of 242 and 86ms.

These values were deemed acceptable for the purposes of the project, but although reproducible relaxation times were obtainable while working with small amounts of the materials, the slower solidification of the large amounts needed for phantom construction led to gross differences between the areas solidifying at different times. It proved impossible to construct a reproducible, homogeneous phantom, and another method of predicting tissue contrast was sought.

Computer Modelling

The purpose of this approach was to develop a method of predicting, for each available pulse sequence, the signal intensity of a given tissue on the basis of its relaxation times as measured *in vitro*, and to find sequences which separated the calculated signal intensities of tissues sufficiently for contrast to be detected on MR images.

A computer program derived signal intensity (S) for each tissue at all available echo (TE) and repetition (TR) times according to the formulae:

$$S^{IRSE} = k\rho(e^{-TE/T2})(1-2e^{-(TI/T1)}+2e^{-(TR-TE/2)/T1}-e^{-TR/T1})$$

$$S^{SE} = k\rho(e^{-TE/T2})(1-2e^{-(TR-TE/2)/T1}+e^{-TR/T1})$$

where TI = delay between 180° and 90° pulses

TE/2 = time between 90° and rephase 180° pulse

ρ = proton density of tissue

e $\cong$ 2.718, the natural logarithmic base

k was taken as 1

The relaxation times of the tissues already analysed *in vitro* were processed by computer according to these formulae. The Brüker analyser does not give a direct reading of proton density (PD or ρ). However, as has been stated earlier, PD varies little between non-osseous body tissues and fluids, varying between around 80% for muscle to 100% for water. Examination of the above formulae shows that within this range of values, PD variation has a maximum effect of 20% on signal intensity. T1 or T2 differences, and changes in TR, TE and TI have each a proportionately much greater effect. PD was therefore estimated for all tissues from their water content (Beall

et al 1984), the values used being: CSF = 99%, blood = 90%, grey matter = 85%, white matter = 80% (68-77% water but also 18% fat).

The results gave the signal intensity value for all available pulse timing combinations. For the IR sequences, inversion times (**TI**) were varied stepwise in 100 ms increments from 200 to 700ms, while in the SE sequences the echo times (**TE**) varied from 24 to 160ms. The repeat time (**TR**) was varied against each of the **TI** or **TE** values in 500ms increments from 500 tO 3000ms. Thus, for each tissue a range of pulse sequence dependent signal intensities was derived. This made it possible to optimise tissue contrast by choosing sequences which maximised the difference in intensity between two or more tissues.

In practice this was most easily accomplished by plotting graphically signal intensity (**SI**) against **TR** for each increment of **TI** (in the inversion recovery sequences) or **TE** (in the spin-echo sequences).

In deriving clinically useful sequences, of course, other factors must be considered. The image must give recogniseable anatomical information, and should be able to screen for other pathology. Similarly, the condition of many patients with intracranial haemorrhage may be unstable, and it is necessary to limit total imaging time. A compromise between maximum tissue contrast, image quality and imaging time was therefore sought. Pulse sequences suggested by this method were then used to image patients and experimental animals.

1. Subarachnoid Haemorrhage.

Signal intensity values of grey matter, white matter, bloodstained and normal anaerobic CSF were plotted, and curves derived for the interpolation of intermediate values. Results are shown in fig 6.

fig. 6

Signal intensity values of grey matter (—), white matter (—·—) blood (▰▰), CSF (▭▭), and bloodstained CSF: 40ml/l (◆), 80ml/l (◆) for available echo (TE) and repeat (TR) times.

(a) Spin-echo sequences.

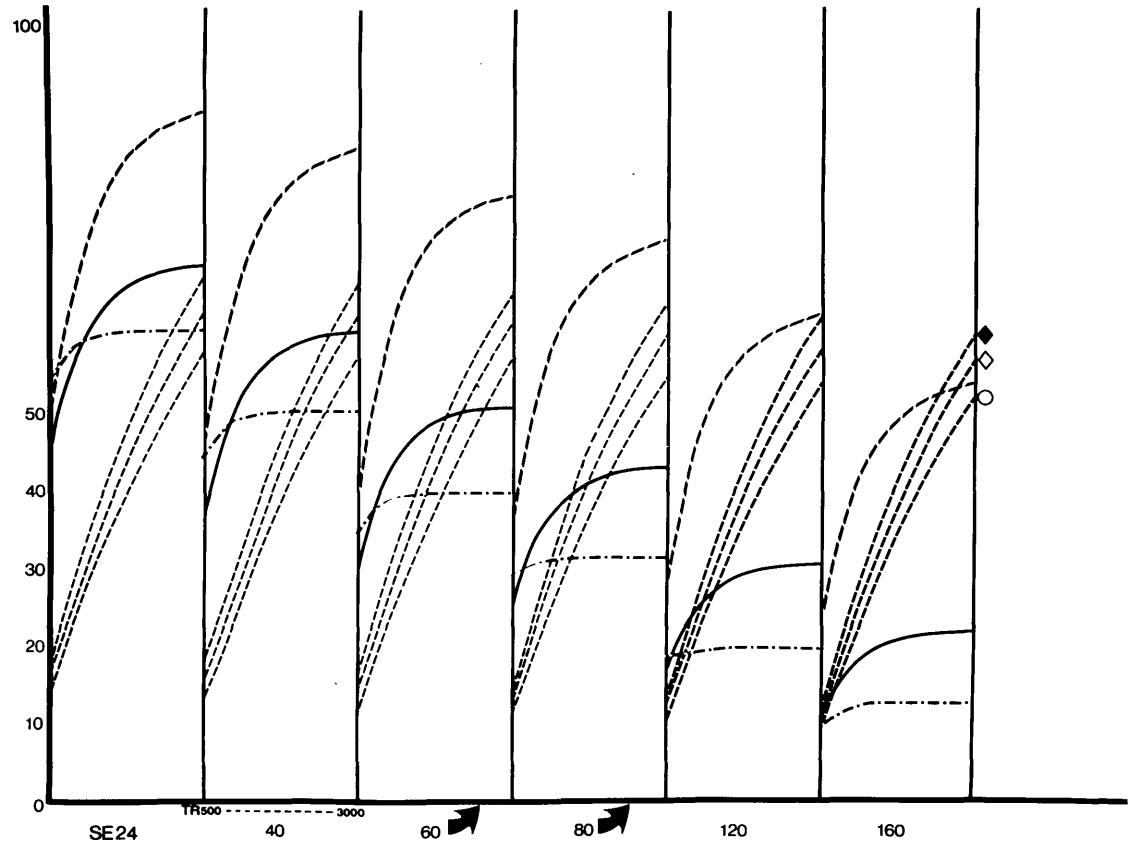

fig. 6

(b) Inversion-recovery sequences

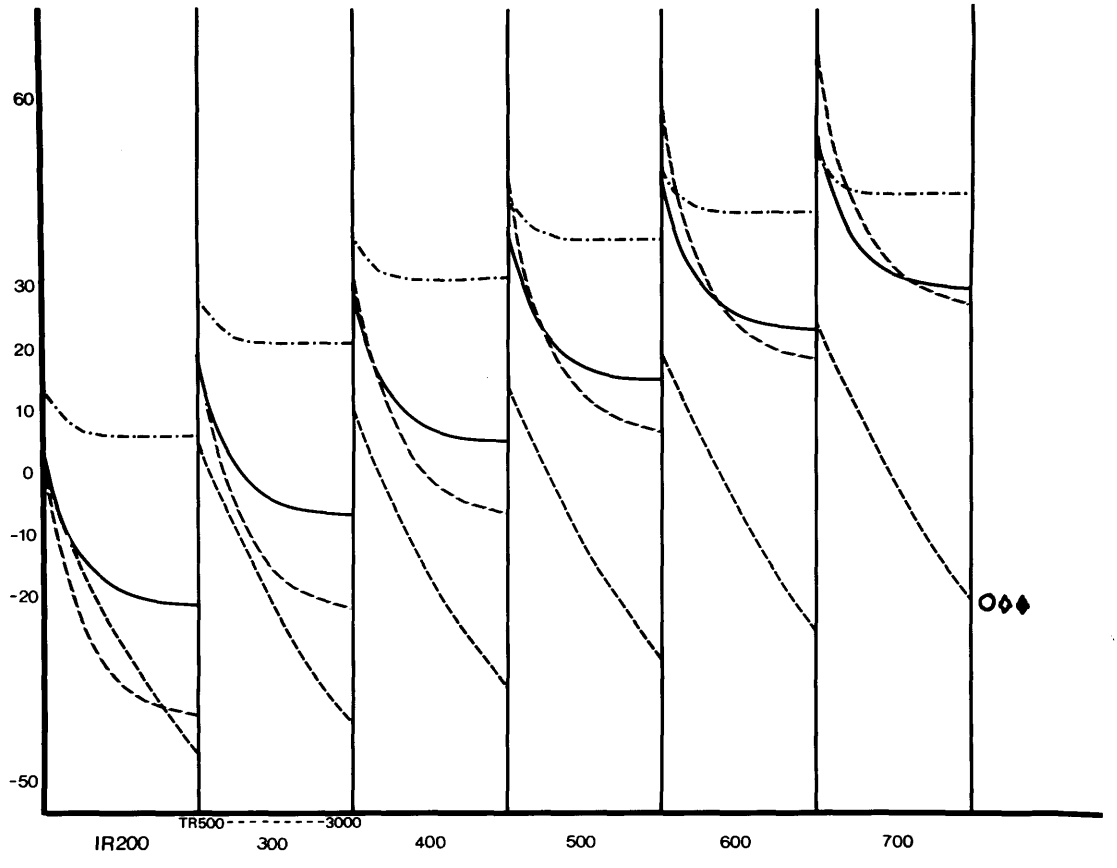

The following criteria were considered in choosing a pulse sequence to differentiate normal and bloodstained CSF for use in suspected subarachnoid haemorrhage.

1. Normal CSF should give a signal which is as close as possible to that of normal brain

2. Addition of even a small amount of blood should increase the CSF signal dramatically.

3. The sequence should provide reasonable anatomical information, and should be capable of being performed on a practicable time scale.

Fig 6 (a) demonstrates that Spin-echo sequences in general separate the signals from brain and CSF much less effectively than do Inversion-recovery sequences. The arrows show two sequences in which the signal intensity of brain and CSF is similar, but where the addition of even a small amount of blood makes an appreciable difference: the SE2500/60 and the SE2200/80. The SE2200/80 sequence was chosen for the imaging studies because a 16 slice study, including pilot scan, could be performed in 9.2 mins as against 11.5 mins for the SE2500/60.

Fig 6 (b) shows that Inversion-recovery sequences fail to fulfil these criteria. The signal from CSF is always vastly different from that of brain; the addition of blood did not change the signal enough to show a difference on the scale of this graph.

Fig. 7 shows signal intensities for CSF, bloodstained CSF and blood using the SE2200/80 sequence, together with the values for grey and white matter.

fig. 7

Signal intensities of CSF, bloodstained CSF and blood using the SE2200/80 sequence. The values for grey and white matter are also marked

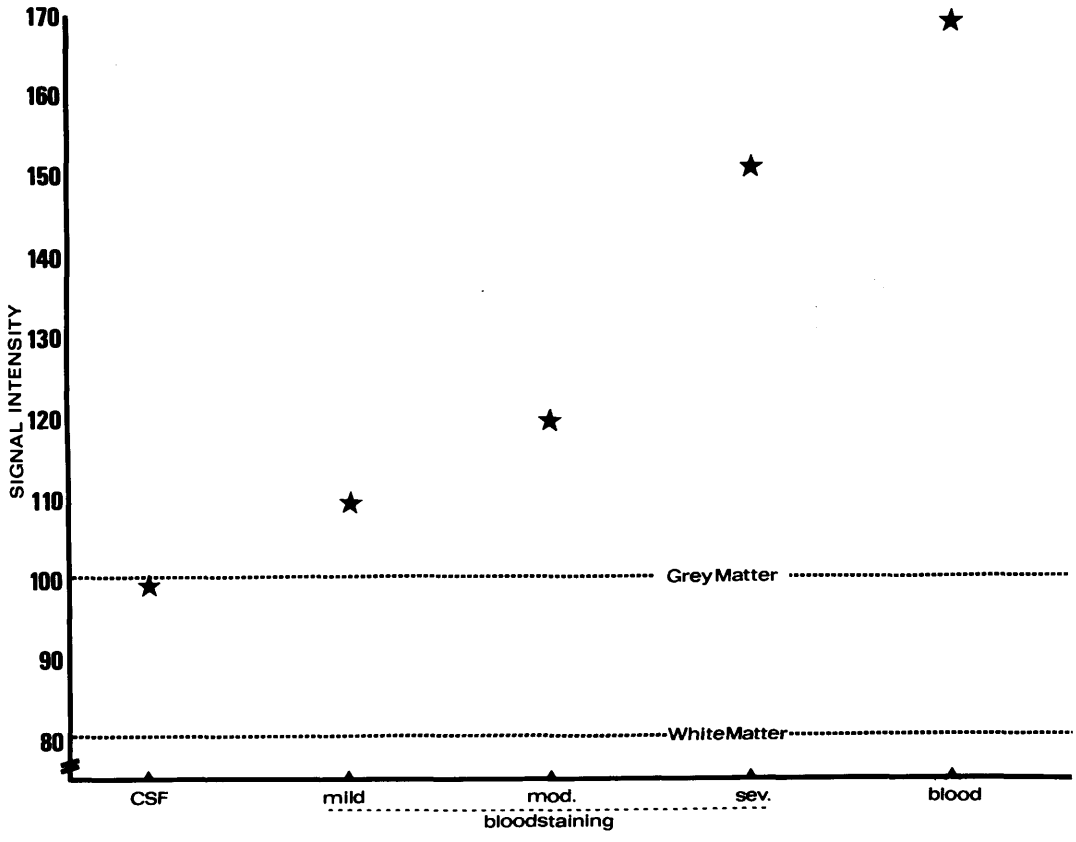

2. **Haematoma.**

Signal intensities of grey and white matter, CSF and blood 0, 4, 7 and 10 days after sampling were plotted, and curves drawn for interpolation of intermediate values. (fig 8)

fig. 8

Signal intensity values of grey matter (—), white matter (—·—) and CSF (– – –); and of blood immediately (▬), 24hr (·◆), 4 days (·●) and 10 days (·▲) after sampling.

(Spin-echo sequences)

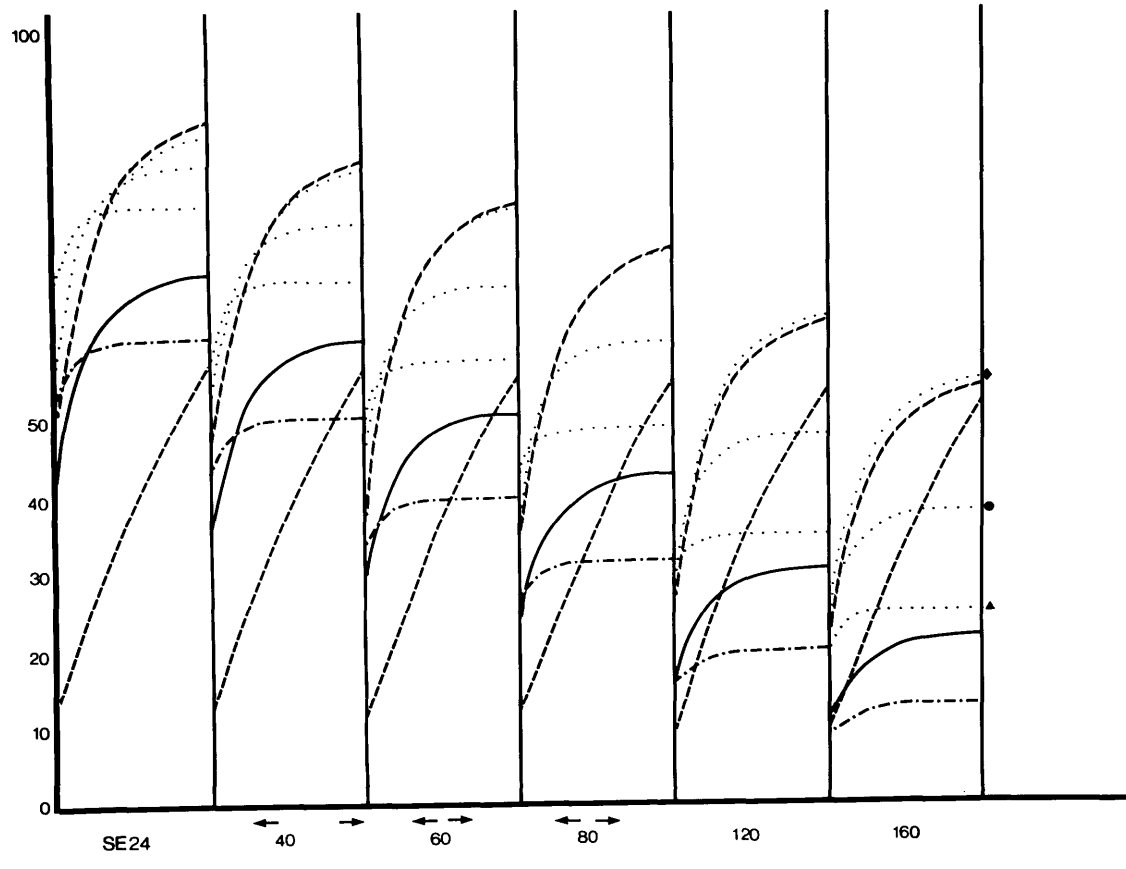

It proved easy to separate different ages of blood at long repeat times. This is not often important in clinical practice, although it confirms the early finding that subacute and chronic collections of blood have greatly differing signal intensities from fresh haematomas. More important practically are sequences which separate bleeding of any age from the surrounding brain, and which are able to be performed within the time constraints imposed by the clinical condition of patients with a haematoma. Again, Inversion-recovery sequences proved unhelpful (fig 6b), while several spin-echo sequences offered potentially useful predictions. The sequences denoted by arrows in fig. 8 all differentiate blood from brain and CSF; differences between them are in terms of imaging time - this will be greater in sequences with a long repeat time (TR).

SUMMARY

The purpose of this part of the study was to resolve the problem of selecting appropriate RF pulse sequences for the reliable imaging of intracranial haemorrhage at all stages after onset.

Setting up a phantom for the imaging of haemorrhage proved impossible due to the difficulty of reproducing substances which had similar relaxation times to brain grey and white matter.

A method was then developed in which the relaxation times of blood, brain, CSF and bloody CSF measured *in vitro* and reported in chapter 3 were processed by computer to generate comparative values of tissue signal intensity for the spectrum of pulse sequences available on the MR imager used. This method obviated the need for

repetitive trial-and-error patient or phantom studies.

Most inversion-recovery sequences and many spin-echo sequences were found to be unsuitable. Sequences were selected which fulfilled the criteria of maximising contrast and minimising imaging time, and a Spin-echo 2200/80 sequence was adopted as standard. This sequence is a standard in many MR units, including the Glasgow unit, for screening examinations. It was reassuring to find that not only should it be expected to reveal intracranial haemorrhage reliably, it was also one of the best sequences found for doing so.

The use of the selected sequences in clinical imaging is reported in chapter 5.

Chapter 5

METHODS AND RESULTS: 3

Magnetic Resonance:

In vivo and Patient Studies

In vivo and Patient Studies

Introduction

Results of Magnetic Resonance studies on patients with subarachnoid haemorrhage, intracerebral haematoma and head injury are presented. Patients with subarachnoid haemorrhage and head injury were selected prospectively on the basis of history alone; patients with haematomas measuring more than 1.5cm in diameter were selected from retrospective analysis of consecutive MR studies. Although there is some overlap between groups, they will be analysed separately. Studies were performed using a variety of RF pulse sequences according to the condition of the patient; one of the computer-predicted sequences was always included.

1. Subarachnoid haemorrhage

Thirty-three patients with a history and clinical findings suggestive of subarachnoid haemorrhage were imaged by MRI between eight hours and six days after the onset of symptoms, twenty-four of the investigations being within 48 hours. Of these, three were only imaged after an operation for intracranial aneurysm, and seven were imaged both pre- and postoperatively. Ages ranged from 15 to 69 years (mean 46.6) with a female : male ratio of 2.7 : 1. Patients in coma were excluded, but all other grades were represented; patients were selected randomly but not consecutively as the MR imager operated only on a Monday-to-Friday basis. Conscious level and the presence or absence of focal neurological signs were recorded. All patients had an unenhanced CT scan performed preoperatively, 23 on an

EMI 1010 scanner and 10 on a Philips Tomoscan. It was performed in all cases within 3 days of the ictus and within 48 hours before or after MRI. Four of these also had postoperative CT scans and MRI. Lumbar puncture was carried out at the hospital referring the patient if there was doubt as to the clinical diagnosis. It was also performed in patients whose CT scan showed no evidence of haemorrhage. If clinically indicated, each patient subsequently underwent 4-vessel catheter angiography; 30 of 33 patients were studied. In three patients the clinician responsible felt that angiography was inappropiate: one patient had a negative lumbar puncture and normal CT scan, and was asymptomatic within 24 hours, and two patients were unfit for treatment by operation.

Thirty patients therefore had both CT and MRI before consideration of angiography or operation. The diagnostic success of the investigations carried out in these patients is summarised in table 8, and the final diagnoses reached are summarised in table 9.

Investigation	+ve	-ve	not done, or technically inadequate
Lumbar puncture	16	2	12
CT	24	6	-
MRI	25	4	1 non-diagnostic
Angiography	25	2	3

table 8

SAH: summary of investigations performed preoperatively

Diagnosis	n
SAH, aneurysm or AVM	25
SAH, no aneurysm found	1
SAH, not investigated further	2
SAH excluded	2

table 9

SAH: final diagnosis

Two patients who deteriorated after angiography had been performed did not undergo operation; in the remainder, the angiographic findings were confirmed at operation. Ten patients were also imaged postoperatively by MRI; however it was not feasible to obtain CT scans of all of these, and only four had both CT and MRI.

On the basis of the computer analysis of the *in vitro* studies, a T2 weighted spin-echo (SE) 2200/80 axial sequence was chosen, using 2 averages and a 128 x 256 matrix (reconstructed to 256^2 for display) and was used in all patients. This took 8.6 minutes for the acquisition of 16 contiguous 8mm slices. Other sequences and orientations were used in selected patients. A sagittal SE 900/40 sequence (4 averages, 256 x 256 matrix) proved useful for vascular imaging and the demonstration of aneurysms, while brain anatomy was best seen using a T1 weighted Inversion-Recovery (IR) 2000/600/40 sequence.

Acceptability and safety of MRI

No patient refused MRI, and the only complaints were of mild claustrophobia and an uncomfortable couch. None of the patients deteriorated while undergoing imaging. One investigation had to be discontinued due to restlessness on the part of the patient and diagnostic images were not obtained.

MR Imaging appearances in SAH

Subarachnoid blood was seen in 25 out of 30 patients (25 of 28 patients in whom SAH was conclusively proven) using the T2 weighted SE2200/80 sequence, which showed bloodstained CSF to have a high signal compared to brain or normal CSF. The high signal was particularly prominent in the prepontine and interpeduncular cisterns, but high signal was also identified in the sylvian fissures and ventricles of some patients. The appearances of cisternal and intraventricular SAH are shown in fig 9.

Haematomas were easily identified, and will be discussed later. Areas of high signal suggestive of ischaemia or oedema were seen in one patient who deteriorated after surgery (fig. 10), but none of the patients in this series developed cerebral infarction.

Both midline and parasagittal aneurysms were well shown by a SE900/40 sequence in the sagittal plane (fig. 11,12), and at least one was seen in 14 patients. In one patient an arteriovenous malformation was seen.

Sugita clips were used in all patients imaged postoperatively. The metallic artefact on all post-operative studies was limited to an area of signal void no greater than $1cm^2$ with a thin rim of

hyperintensity (fig. 13). This was noted on both T1 and T2 weighted sequences. The only other consistent finding was of an area of focal increase in signal in the T2 weighted images and of hypointensity in the T1 weighted images at the operative site.

a

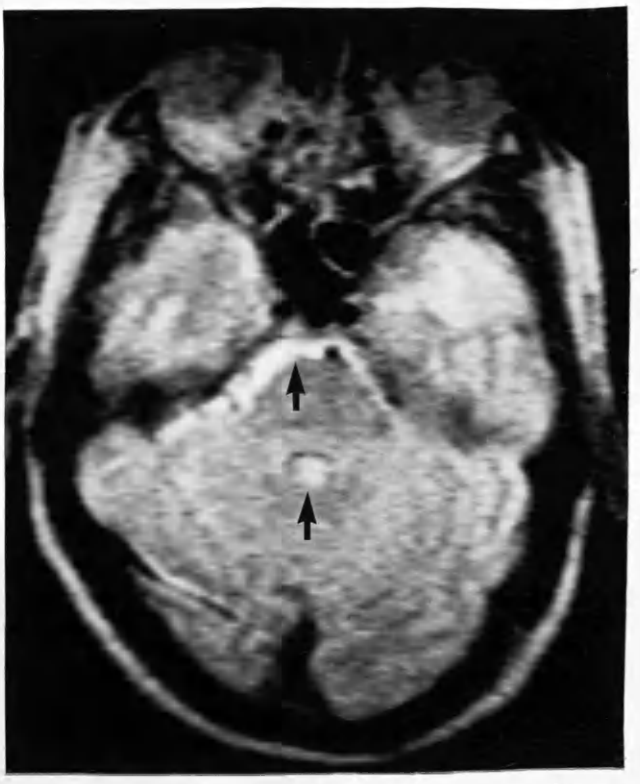

b

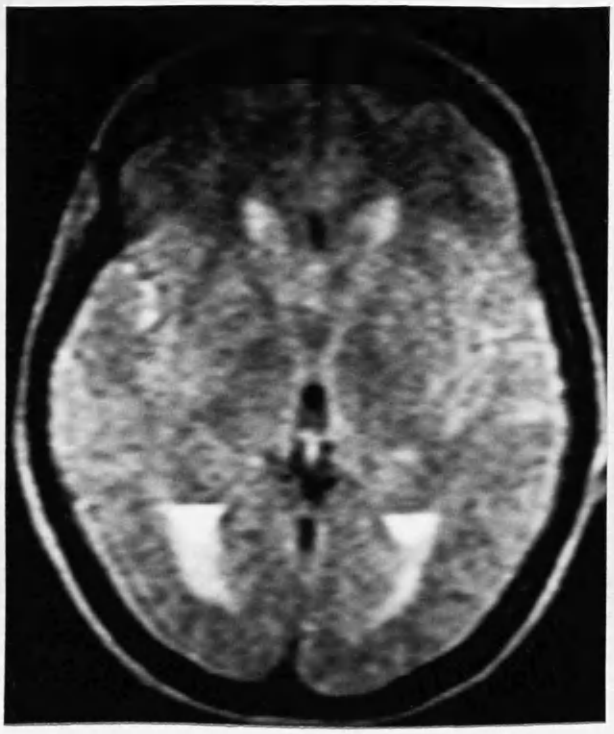

c

fig. 9

Axial SE2200/80 images showing (a) normal appearance, (b) patient with SAH evidenced by high signal in basal cisterns and IV ventricle, and (c) patient with fluid levels of blood in the lateral ventricles

fig. 10

postoperative study showing area of unusually high signal adjacent to operation site

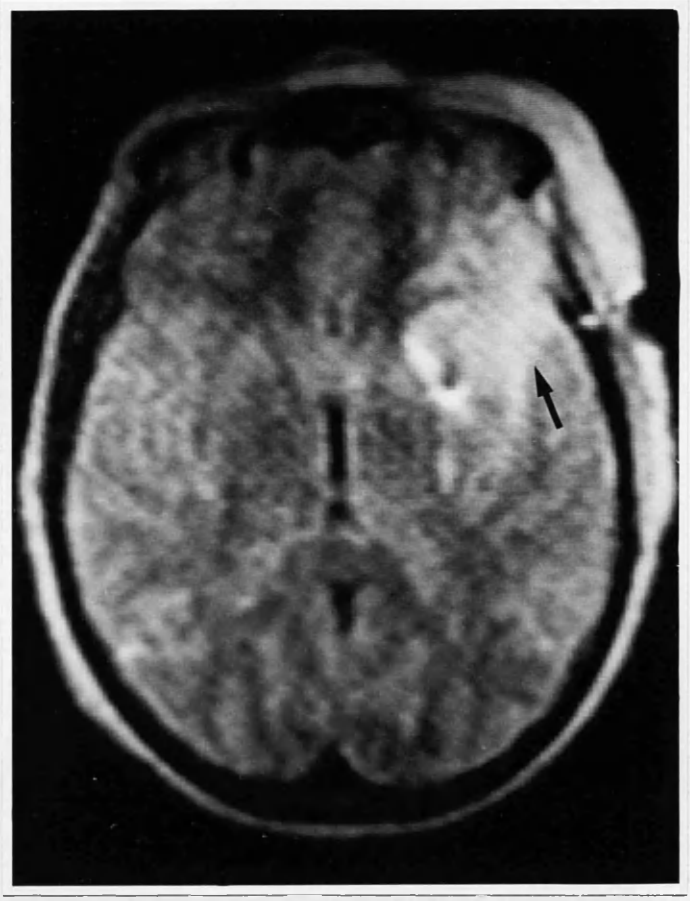

a

b

fig. 11

(a) angiogram and (b) parasagittal MRI both showing right posterior communicating artery aneurysm

fig. 12

(a) angiogram showing right middle cerebral and anterior communicating artery aneurysms. (b) axial MRI, same patient, showing bilateral MCA aneurysms and ACA aneurysm with surrounding haematoma confirming rupture

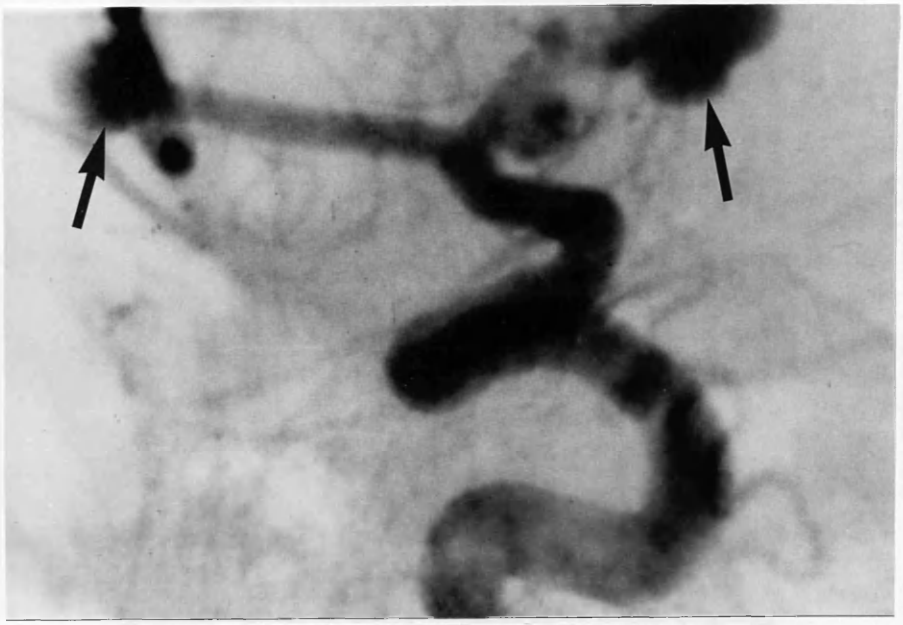

a

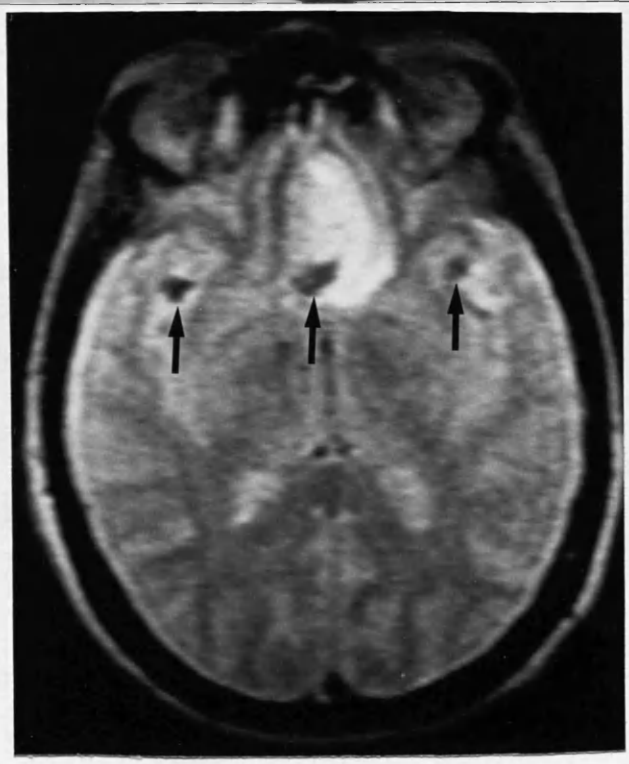

b

a

b

fig. 13

(a) CT scan and (b) MRI showing extent of image degradation due to clip artefact

Analysis of CT and MRI

a. Preoperative studies.

Studies were performed preoperatively on 30 patients. The CT scans (21 CT 1010, 9 Tomoscan) were reviewed by a consultant radiologist without reference to the MR findings, and the performance and diagnostic yield of both CT and MRI were analysed using eight criteria. The findings are summarised in table 10.

Feature demonstrated	**CT**	**MRI**
Subarachnoid blood	24	25
Intracerebral blood	10	12
Intraventricular blood	11	10
Shift/space-occupying effect	9	8
Hydrocephalus	11	8
Ischaemia	-	-
Localisation of bleed	11	16
Visualisation of aneurysm	0	14

table 10.

unenhanced CT and MRI findings in 30 unoperated patients with acute subarachnoid haemorrhage.

These findings are summarised in fig. 14.

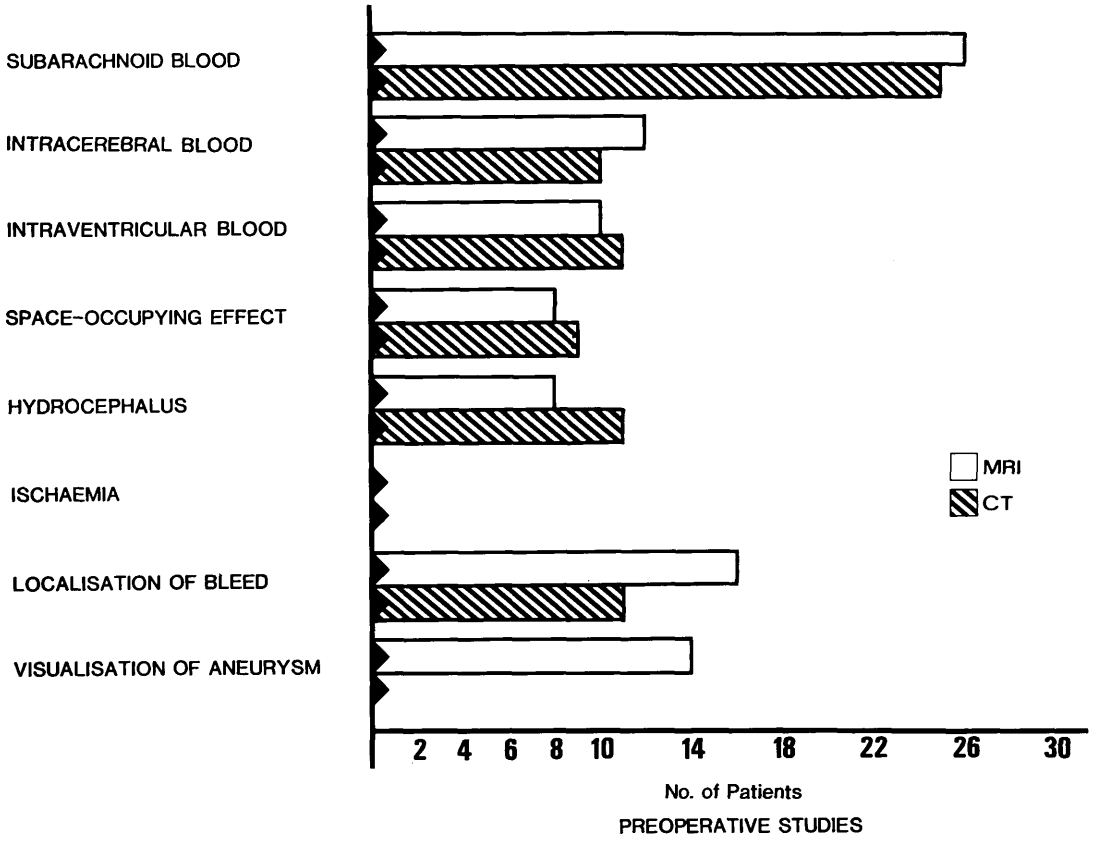

fig. 14

bar graph summarising preoperative CT and MRI findings in 30 patients

MRI was very similar to CT in the detection of intracranial bleeding in the subarachnoid space (χ^2=0.11, p=NS) and ventricles (χ^2=0.07, p=NS), and also in the identification of intracerebral clots (χ^2=0.29, p=NS). Midline shift or local space-occupying effects were seen with both techniques. Hydrocephalus was reported slightly more often with CT than MRI (χ^2=0.69, p=NS), but this difference represents a subjective variance in radiological interpretation rather than a conflict in the results of the two techniques.

MRI showed local abnormalities indicating the area likely to

have been the site of origin of the bleed in more patients than did CT (X^2 = 1.68; p = NS). These abnormalities included small haematomas and areas of local oedema at the site of aneurysm rupture.

The most striking difference between MRI and CT was in the number of patients in whom the actual lesion responsible for the bleed could be seen. Thus, in 14 (47%) of the patients the MRI showed a signal void indicative of an aneurysm. In none of the patients did CT identify directly the likely source of the bleed (χ^2=18.2, p<0.001).

There was no difference in the CT diagnostic yield between CT1010 and Tomoscan in any of the categories. Of the six scans failing to demonstrate subarachnoid blood, five were CT1010 and one was Tomoscan. When related to eventual diagnosis, however, three of the patients with negative CT1010 studies had negative LP and/or angiography findings and one had also a normal MRI investigation. One patient with negative CT1010 findings had positive MRI. The patient with negative Tomoscan findings was the one whose MRI was aborted due to restlessness.

b. Postoperative studies.

Four patients had both CT and MRI after operation to clip an aneurysm. The findings are seen in Table 11.

Feature demonstrated	CT	MRI
Metallic artefact > $2cm^2$	4	0
Extracerebral collection	1	3
Local oedema/contusion	2	4
Ischaemia	-	-
Hydrocephalus	1	1
Space-occupying effect	1	1

table 11

CT and MRI findings in 4 patients following aneurysm surgery.

Artefacts due to the metal of the aneurysm clip were seen with both CT and MRI. The extent of the artefact was consistently less with MRI ($\chi^2=8$, $p<0.01$): all four CT scans showed extensive streak artefact covering the whole image on at least two slices, but no MR image showed a defect of $>2cm^2$.

An extracerebral collection was shown in 3 patients with MRI and in 1 with CT; none of these had to be evacuated.

Each of the 4 patients showed evidence on T2 weighted sequences of a focal increase in signal at the operative site; corresponding changes could be seen in 2 patients with CT. MRI and CT were similar in the detection of hydrocephalus and space-occupying effect. As in the preoperative studies, neither showed definite evidence of ischaemia. Evidence of bleeding from an unclipped aneurysm was seen with both techniques in one patient who had multiple aneurysms, one of which had been left unclipped.

Intracranial Haematoma

1. Patient studies

20 patients with intracerebral haematomas measuring 1.5cm or more in diameter were studied retrospectively. Twelve patients were male and eight female. Haematomas known or subsequently found to be associated with intracranial tumours were excluded, as were cases where the onset of the bleed and the time of MRI were separated by more than 48 hours. All cases had CT scans which confirmed the presence of an acute haematoma. The site, aetiology and MR characteristics of the haematoma are shown for each patient in table 12, and summarised in tables 13 and 14.

case no.	site	aetiology	MR characteristics
1	post fossa	AVM	hypo; hyper rim
2	rt. fr-par	trauma	all hyper
3	rt. frontal	spont.	mixed
4	lt. bas gang	trauma	hypo; hyper rim
5	rt. occipital	trauma	hypo; hyper rim
6	rt. fr-temp	aneurysm	all hyper
7	rt. frontal	trauma	hypo; hyper rim
8	post fossa	trauma	all hyper
9	bifrontal	trauma	hypo; hyper rim
10	rt. occipital	trauma	hypo; hyper rim
11	rt. bas gang	spont.	iso; hyper rim
12	rt. bas gang	spont.	hypo; hyper rim
13	rt. bas gang	spont.	hypo; hyper rim
14	rt. temporal	trauma	all hyper
15	rt. par-temp	aneurysm	hypo; hyper rim
16	rt. temporal	trauma	hypo; hyper rim
17	pons	spont.	hypo; hyper rim
18	lt. temporal	aneurysm	all hyper
19	lt. bas gang	trauma	all hyper
20	lt. fr-temp	trauma	hypo; hyper rim

table 12

site, aetiology and MR characteristics

in 20 cases of intracerebral haematoma

(rt. = right; lt. = left; fr = frontal; temp = temporal;

par = parietal; occ = occipital; bas gang = basal ganglia.

hypo, iso, hyper = intensity on SE 2200/40 sequence)

The cause of the bleed is summarised in table 13.

cause	trauma	aneurysm	AVM	spont (other)
no.	11	3	1	5

table 13

cause of bleeding in 20 cases of ICH

as seen on MRI

The main site of the bleed is shown in table 14.

site	frontal	temporal	occipital	BG/IC	post. fossa
no.	6	4	2	5	3

table 14

site of ICH in 20 patients examined by MRI

(BG = basal ganglia; IC = internal capsule)

A variety of appearances were seen in recent intracerebral haemorrhage. The most frequent finding (in 13 patients) was of a hypo- or isointense area (the haematoma) surrounded by a hyperintense area of local oedema. Three such cases are illustrated in figs. 15, 16, & 17.

Fig. 15 shows the MR and CT appearances in a 15 year old girl who was admitted following a fall from a horse. Having been initially comatose, she was conscious but disorientated at the time of imaging. Both images were obtained within six hours of injury, and show bifrontal intracerebral haematomas; associated oedema is well demonstrated by MR.

The MR and CT images in fig. 16 were obtained within 24 hours in a 21 year old scaffolding erector who fell about 20 feet and suffered a head injury. He was in coma from the time of the injury and had a left sided weakness. Appearances are again similar, with oedema being highlighted on MR. Anatomical detail in the brain stem, and incipient uncal herniation, are demonstrated well by MR.

The patient whose CT and MR are shown in fig. 17 had a spontaneous intracerebral haemorrhage, subsequently proved to be due to rupture of a middle cerebral artery aneurysm. There are no features to distinguish spontaneous from traumatic bleeding, and again extensive signal change due to oedema is shown by MR.

fig. 15

(a) axial MR image (SE2200/80) showing traumatic bifrontal haematomas in a 15 year old female 6 hours after injury. (b) CT scan same day

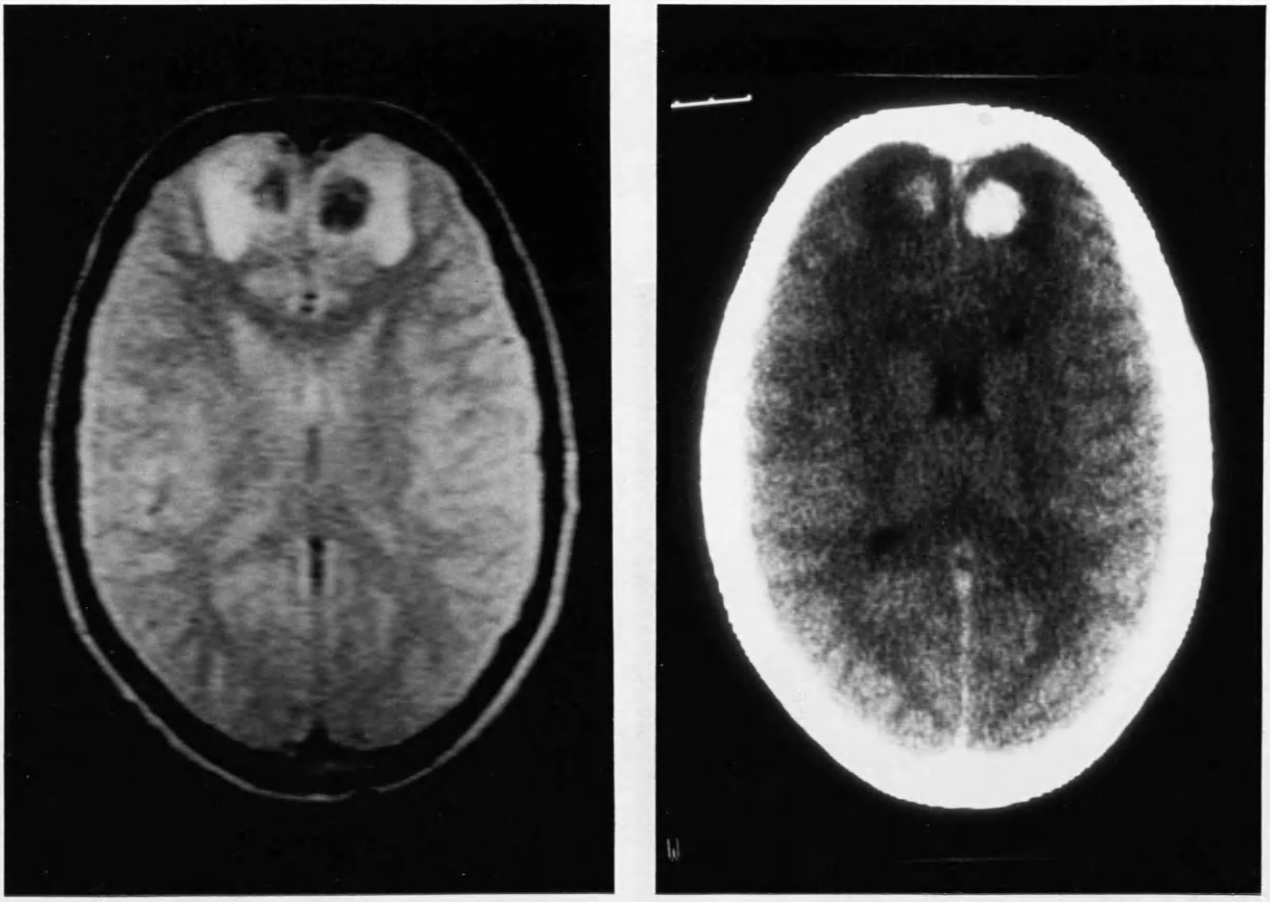

a b

fig. 16

(a) axial MR image (SE2200/80) showing traumatic right occipital intracerebral haematoma in a 21 year old male 24 hours following a fall. Note area of high signal around contralateral uncus, and deformation of brain stem. (b) CT scan on arrival

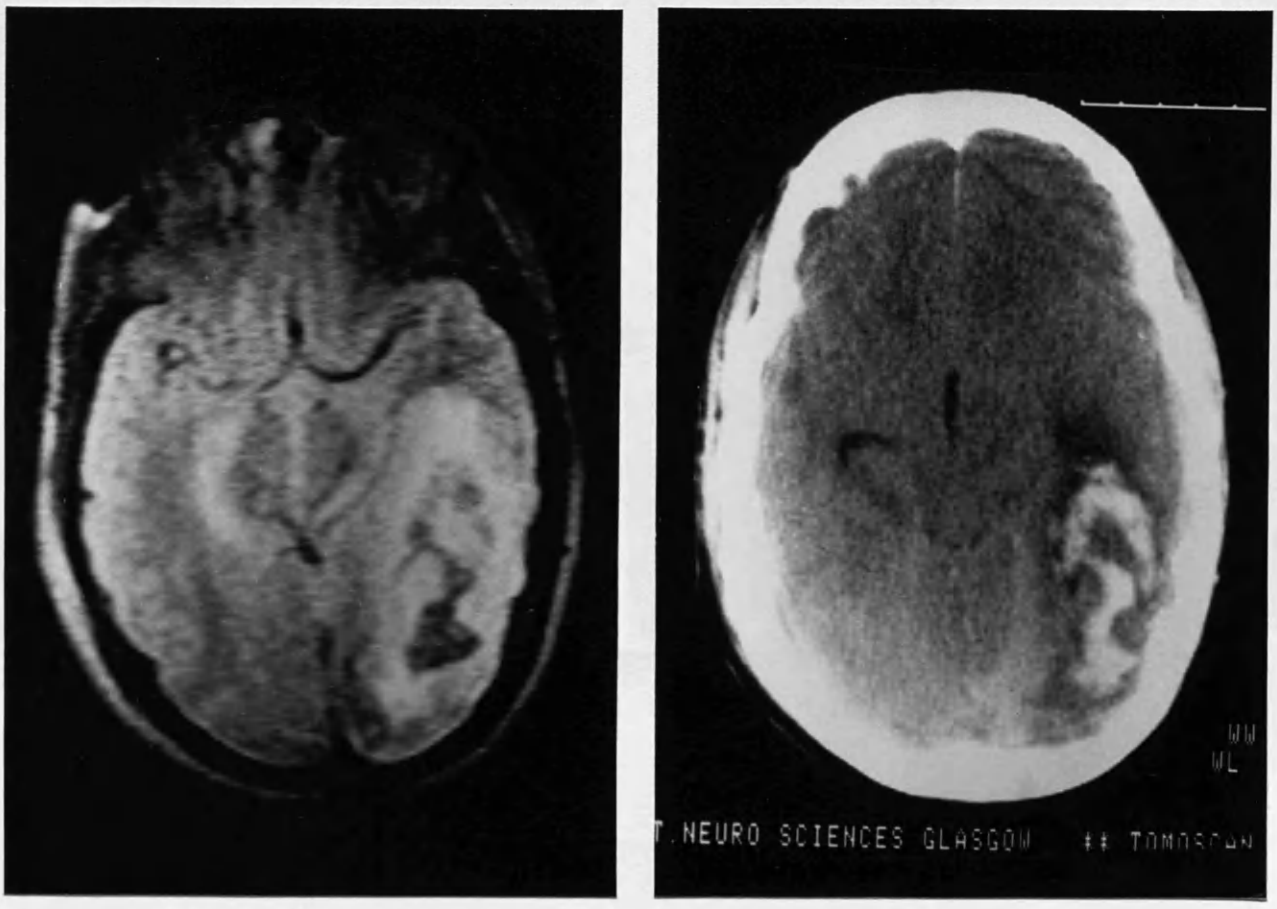

a b

fig. 17

(a) axial MR image (SE2200/80) showing spontaneous intracerebral haematoma in a 40 year old patient following right middle cerebral artery aneurysm rupture. ((b) CT Scan

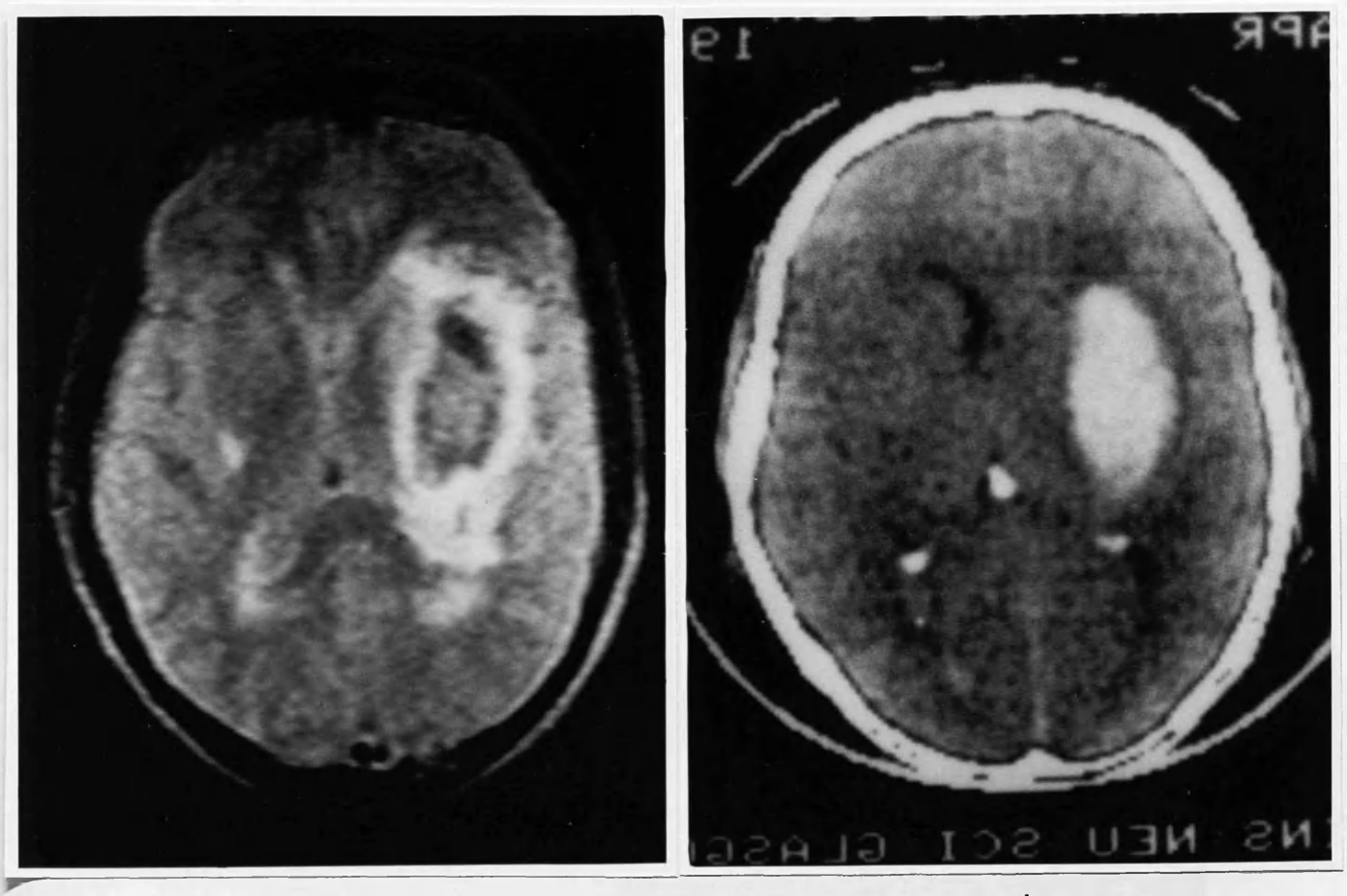

a b

Even using the same imaging criteria, haematomas were seen in 6 patients as entirely hyperintense areas with no apparent central area of hypointensity (fig 12, 18).

Fig. 12 (b) shows the MR appearances at 18 hours in a patient with subarachnoid haemorrhage from rupture of an aneurysm of the anterior communicating artery. A uniformly hyperintense interfrontal haematoma is demonstrated.

Fig. 18 shows similar appearances in a patient following rupture of a middle cerebral artery aneurysm.

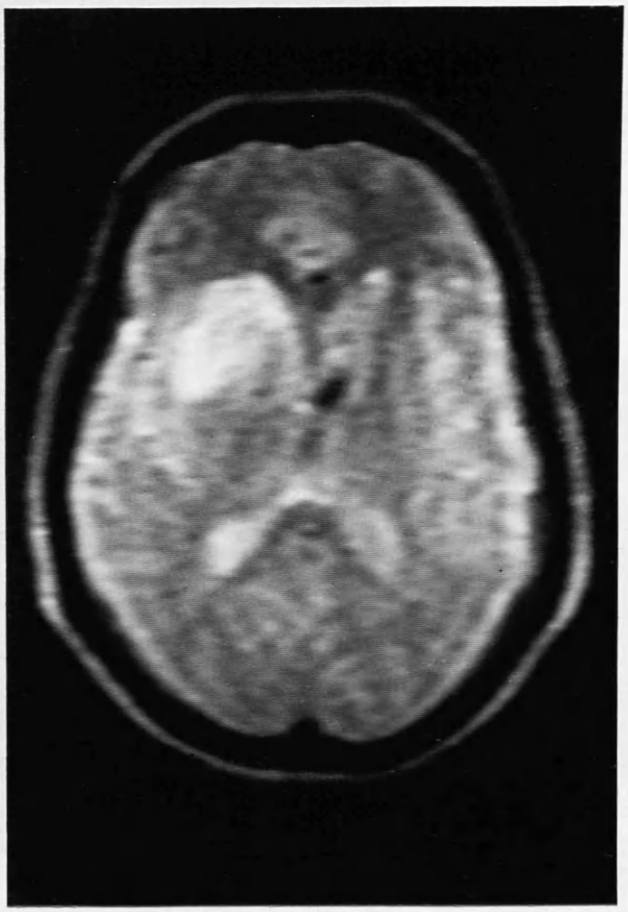

fig. 18
small left frontotemporal haematoma follwing MCAA rupture. SE2200/80

Patients on anticoagulant therapy have 8-11 times the risk of developing spontaneous intracerebral haemorrhage (Kase 1986), and bleeding may persist or recur over a period of days. Fig. 19 shows

the MRI of such a patient, showing different degrees of intensity within a giant haematoma. This appearance presumably corresponds with such a process.

fig. 19

giant frontal haematoma in an anticoagulated patient

2 days after commencement of symptoms. SE2200/80

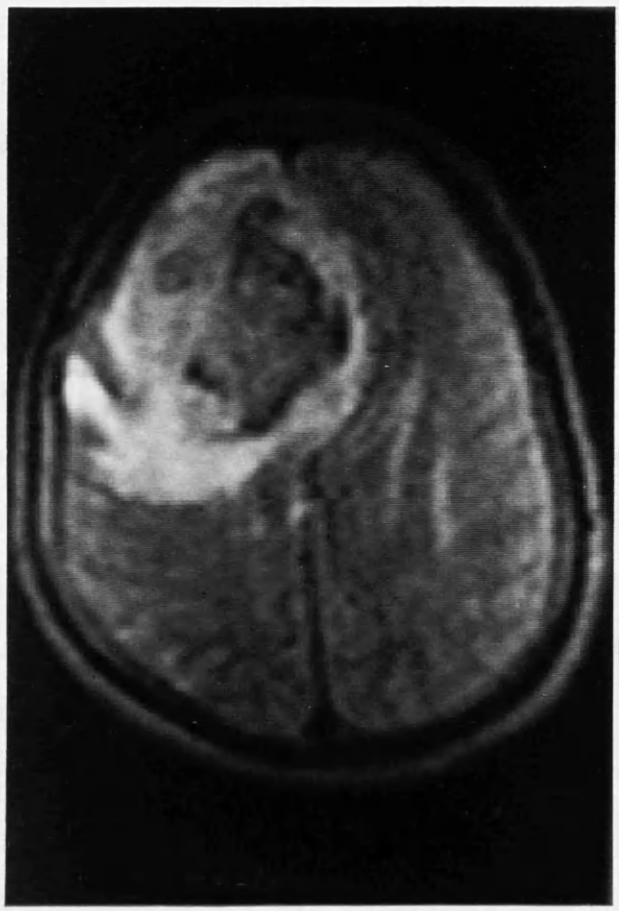

With the exception of this single patient, there was no relationship found between the aetiology of a haematoma and its MR

appearances. Similarly the site of the haematoma did not affect the signal intensity.

In the majority of patients, the haematoma itself was of lower signal intensity, relative to brain in regions remote from the bleed, than would have been predicted from the *in vitro* studies and computer-modelled signal intensities of normal brain and of blood of varying ages. The signal intensity of "normal" areas of brain in the haematoma patients did not differ from that in volunteers, using similar pulse sequences and window settings. This implies that the signal intensities of haematomas were genuinely lower in the studies than would have been predicted, and that their relaxation times - in these T2 weighted studies, principally T2 - are therefore lower. Possible explanations for this will be discussed.

Due to the poor clinical state of patients with ICH, it did not prove possible during the period of the study to obtain sufficient patients for inclusion in a formal prospective study using a variety of pulse sequences predicted on the basis of the *in vitro* and computer studies, or to carry out follow-up scans on patients to assess the evolution of the MR appearances.

In one patient with traumatic bifrontal haematomas, in whom serial imaging was carried out, the hyperintense rim of the haematoma expanded over the first seven days with a concomitant reduction in T1 of the haematoma itself. Over the next week, the surrounding oedema subsided while the T1 of the haematoma continued to fall. The patient was re-examined at 15 weeks when cerebromalacia was well-established at the site of both haematomas.

2. Animal studies

Because of the logistical difficulties in imaging patients with haematoma, an animal model was set up. Three adult rabbits were anaesthetised with intramuscular barbiturate and an incision made over the calvarium. With reference to a stereotactic atlas of brain anatomy, a 1mm burrhole was made over the left frontal lobe. 2ml of autologous blood were obtained and injected into the left frontal lobe. The anaesthetised animal was then imaged using the computer-predicted pulse sequences. The intention was to repeat the imaging at time intervals up to ten days to obtain information about changes in the appearance of the haematoma and the surrounding brain.

Unfortunately, although the lesion could be accurately placed (fig. 20), the limits imposed by slice width, signal-to-noise ratio and the small size of the rabbit brain meant that the haematoma could not be detected on the MR images obtained on any of the three animals used. As it would not be feasible to image larger animals in this way the model had to be abandoned.

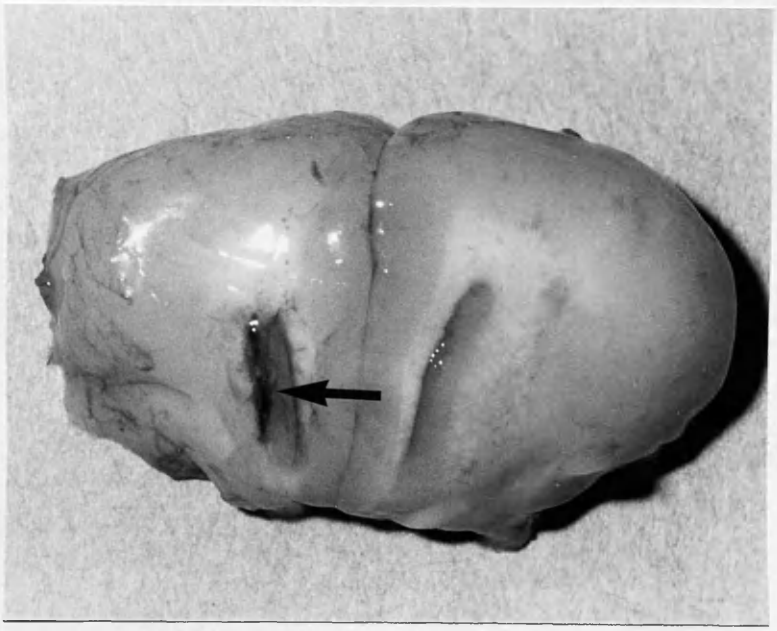

fig. 20
coronal section through frontal lobes showing intracerebral haematoma

Head Injury

50 patients were examined by both MRI and CT within 7 days of a head injury, 34 being studied within 48 hours. They were as far as possible consecutive unit admissions, except where transfer of the patient to another hospital, necessity for immediate operation, processing during a weekend, or imager breakdown and maintenance prevented inclusion. Ages ranged from 4 to 72 years, with a mean of 31. The causes of injury are shown in table 15.

cause	RTA-occ	RTA-ped	fall	assault	other
no.	10	11	17	6	6

table 15

causes of head injury in 50 patients examined by MRI.

RTA-occ = vehicle occupant; RTA-ped = pedestrian

All severities of injury were included. On admission to hospital, 14 patients were in coma (Glasgow Coma Score <8), 28 had impaired consciousness (GCS 9-14), and eight were fully conscious, of whom four had never lost consciousness. 29 patients had a skull fracture. The duration of loss of consciousness is shown in table 16.

duration (min)	nil	<5	5-30	30-60	>60	not known
no.	4	8	6	4	21	7

table 16

duration of loss of consciousness after head injury

in 50 patients examined by MRI

MRI was performed as the first investigation in 5 patients, the remainder being imaged by CT first. A SE200/40 pilot scan was followed in all cases by a 16 slice SE2200/80 sequence and when the patient's condition permitted by an 8 slice IR 2000/600/40 sequence. 27 CT examinations were carried out on a CT1010 scanner and 23 on a Tomoscan.

The analysis of the images assessed the ability of MRI to fulfil two main criteria:

1. Can it demonstrate macroscopic intracranial haematomas reliably in the acute phase, thus enabling it to be used as an emergency screening procedure to detect "surgical" lesions?

2. Can it furnish evidence of microscopic cerebral disruption and bleeding not visible on CT scan, thus giving potential for early prognostic assessment in both operated and unoperated patients?

Because of the difference in image quality between the two CT scanners used, an retrospective internal comparison was made. Although anatomical clarity was greater on the Tomoscans, an equal proportion of scans taken on each machine demonstrated the

abnormalities sought. This is presumably because the abnormalities are fairly gross: where there was dubiety over the presence of a lesion on either CT or MRI examinations, the lesion was discounted. Because of the lack of a standard CT machine, however, no statistical comparisons were made between CT and MRI.

Of seven patients who required surgery for an intracranial haematoma, four were imaged preoperatively by MRI. All four haematomas were easily identified by MR without reference to the CT images. MRI successfully demonstrated all 20 haematomas measured on CT as >1cm diameter (fig 15, 16). In 8 patients, areas defined on CT as small haematomas were defined on MRI reports as contusions. In no patient was extra- or intracerebral bleeding identified on CT and missed on MRI.

The CT and MR images were examined for focal changes in signal indicating the presence of cortical contusions, subcortical white matter lesions, deep white matter lesions and basal ganglia lesions. Table 17 shows the incidence of each of these as found by CT and MRI.

Site of Abnormality	CT	MRI
Cortex	23	44
Subcortical white matter	23	29
Deep white matter	1	15
Basal ganglia	2	10

table 17

incidence and site of abnormality on CT and MRI images of 50 head-injured patients.

All these abnormalities were seen as regions of hyperintense signal on T2 weighted Spin-echo MR images. Fig. 21 shows such appearances in the MR study of a 50 year old man who was admitted in coma following an assault. CT showed only a small frontotemporal haematoma, while MR showed widespread areas of abnormal signal.

fig. 21

(a) MRI and (b) CT of a 50 year old man following an assault. In addition to the right frontotemporal haematoma seen on CT, MRI shows lesions in the cortex, subcortical white matter, deep white matter and corpus callosum. (SE2200/80)

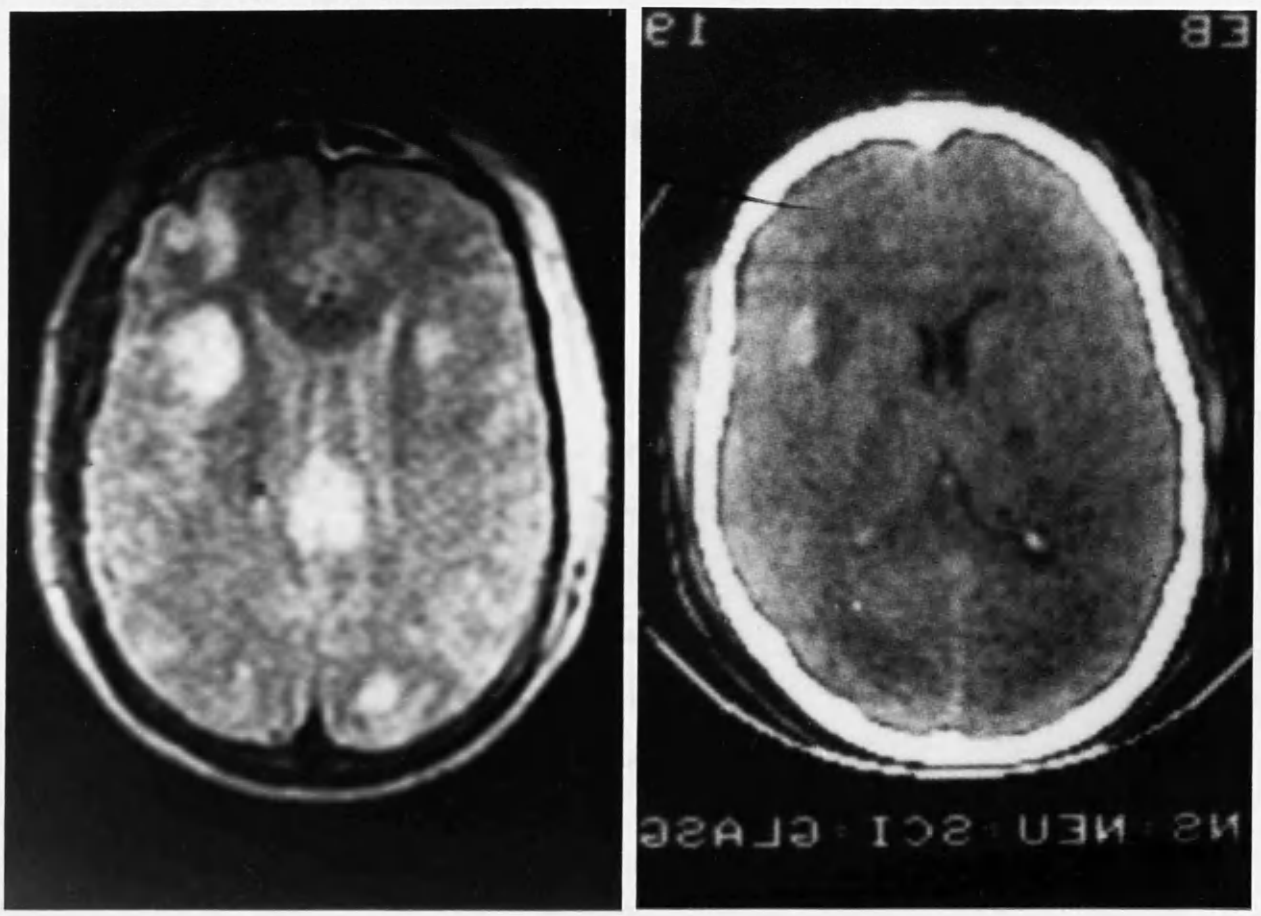

The sites of these lesions correlated well with the level of consciousness of the patients on admission to hospital (table 18).

site of lesions	**level of consciousness**		
seen on MR	**full**	**impaired**	**coma**
	(n = 8)	**(n = 28)**	**(n = 14)**
none	2	1	1
cortex	6	28	13
subcortical w. m.	-	19	10
deep w. m.	-	7	8
basal ganglia	-	5	5

table 18

level of consciousness and lesions seen on MRI

in 50 patients after head injury

In the eight patients who had recovered consciousness fully, only cortical lesions were identified. Lesions in the deep white matter or basal ganglia were seen only in patients with continuing conscious level impairment; more than half of the patients still in coma had such lesions. The relationship of the level of consciousness to the presence of deep intracerebral lesions was highly significant ($\chi^2 = 15.05$; $p < 0.001$).

SUMMARY

The performance of Magnetic Resonance Imaging was assessed in patients with subarachnoid haemorrhage, intracerebral haematoma and head injury. Where possible, RF pulse sequences were used which were selected on the basis of computer analysis of *in vitro* tissue studies.

In subarachnoid haemorrhage, MRI showed subarachnoid blood to have a higher signal than surrounding brain or CSF at all stages from 0 - 5 days. This enabled the diagnosis of SAH to be made on almost all patients subsequently proven to have had a bleed. Aneurysms were seen in almost half of the patients examined preoperatively, and MRI was an effective screening technique for complications of SAH such as intracerebral haemorrhage and hydrocephalus. Studies were not carried out on patients with established signs of delayed ischaemia, but one post-operative study showed appearances in keeping with ischaemic oedema associated with a clinical deterioration.

Intracranial haematoma was clearly and consistently identified, usually as a hypo- or isointense area surrounded by a rim of hyperintensity. Acute haematoma had a lower signal intensity than would have been predicted by *in vitro* analysis. Some smaller haematomas were uniformly hyperintense. The intensity did not correlate with anatomical site or aetiology.

Areas of abnormality, perhaps indicative of neural and/or vascular damage, were identified on the majority of MR images of head injured patients. The presence of such areas in the deeper parts of the brain correlated well with the severity of the injury as assessed

by depth and duration of unconsciousness. Lesions requiring surgery were readily identified.

Chapter 6

METHODS AND RESULTS: 4

Experimental Intracerebral Haematoma

Experimental Intracerebral Haematoma

To study the effects of an intracerebral haematoma produced under experimental conditions, an animal model was set up based on that of Bullock et al (1984) with the modifications of Nath et al (1986). In this model, autologous blood can be injected at arterial pressure into the basal ganglia of a rat to a constant predetermined site. Although the small size of the rat brain precluded concurrent MR studies, it is ideal for quantitative autoradiography; the numbers of subjects required for the study prevented the use of larger animals. The animals survived a haemorrhagic insult with no apparent neurological deficit or behavioural change, enabling survival experiments to be performed.

The intention of the study was to elucidate some of the pathophysiological mechanisms subsequent on the production of a small haematoma in both the short and the long term, and to compare these in the short term with those following the production of a comparable but inert mass lesion.

Experiments performed by FP Nath and the author (1986, 1987) showed that the injection of blood into the rat caudate nucleus produced a local fall in blood flow which depended on the size of the haematoma. In addition, flow throughout the hemisphere was reduced, at least transiently, on the side of the lesion. It was intended to replicate these experiments in part, this time comparing the effects of a haematoma with those of an inert mass lesion of comparable size.

Review of the previous haematoma experiments, in which

injections of 25, 50 and 100 µl were used, suggested that the 25µl haematoma was the largest which could be reliably expected to confine itself to the caudate nucleus without overflow to the convexity subarachnoid and subdural spaces. Indeed, the pressure differential between the caudate nucleus with haematoma in situ and the outside meant that the larger haematoma frequently tracked around the injecting needle to the exterior. A 25µl injection volume was therefore chosen; further steps taken in this experiment to eliminate the pressure differential will be referred to.

A previous experiment (Jenkins & Nath, 1984, unpublished observations) had used systemically administered Evans' blue dye to compare the effect on local blood-brain barrier permeability of a lesion of 25µl of blood and 25µl of mock cerebrospinal fluid. Blood-brain barrier disruption at 4 hours after production, as assessed by visual comparison of the extent of Evans' blue extravasation, was less with the CSF lesion.

This suggested that there were likely to be differences between a haematoma and an pure mass lesion. With the CSF lesion, however, the mass might diminish during the time course of the experiment, due either to absorption in the parenchyma, diffusion, or flow along the outside of the injecting needle. It was therefore necessary to find in addition a material which had the same viscosity as blood but which was physiologically inert.

Blood viscometers require for their calibration a series of inert silicone oils of known viscosities. The flow rate of each of these was compared to the measured flow rate of rat blood through the injection apparatus; the viscosity of blood and other colloidal

suspensions varies with the speed of flow and the diameter of the vessel. Oil with a viscosity of 5 centiPoise was found to have the same flow rate as blood in the experimental circumstances. The effect of the oil on local vasculature was assessed in a separate experiment by injecting small quantities around the exposed pial vessels of a cat and measuring vasoconstriction or dilatation by microscopy. There was no measurable vasomotor response.

Regional and hemispheric blood flow was assessed on animals sacrificed 60-90 seconds following placement of the lesion. Neuropathological analysis of irreversible ischaemia was performed on a separate group of animals sacrificed at 4 hours.

Four groups of animals were studied. One group (n=4) had a sham operation; the remaining three groups had a 25μl injection of autogenous blood (n=5), inert silicone oil (n=5) or mock CSF (n=4).

Fasting adult male Sprague-Dawley rats weighing between 370 and 480g were anaesthetised with a 5% Halothane-air mixture and then maintained via a tracheostomy with 0.5-0.75% Halothane in a 70:30% vol mixture of nitrous oxide and oxygen, delivered using a small animal ventilator. Femoral arterial and venous lines were inserted bilaterally. One arterial line was used for the continuous monitoring of arterial blood pressure; samples for blood gas analysis were taken from the other. PaO_2 and $PaCO_2$ were measured intermittently and maintained at physiological levels (PaO_2 > 100mmHg, $PaCO_2$ = 35-40mmHg). One venous line was used for isotope administration and the other for fluid replacement. Body temperature was maintained at 37°C with heating lamps.

The anaesthetised animal was placed in a stereotaxic frame. A

1cm midsagittal incision was made in the scalp and the positions of the right mid-caudate nucleus and the left lateral ventricle were marked on the skull using co-ordinates derived from the stereotaxic atlas of König and Klippel (1963). The co-ordinates used for the ventricle, with reference to the bregma, were 1mm posterior, 1.5mm lateral; and for the Caudate nucleus, 1mm anterior, 2.8mm lateral. Using a Zeiss operating microscope and a dental drill, a 1mm burrhole was made over the ventricle and a 0.7mm burrhole drilled above the caudate nucleus. The dura was opened with a sharp hook. An 18G polythene catheter, connected via a pressure transducer to a chart recorder, was advanced 2.5mm into the ventricle until oscillation of the trace with cardiac and respiratory cycles confirmed its position. Intracranial pressure was measured continuously throughout the experiment. A 25G needle connected to a graduated catheter was introduced into the caudate nucleus to a depth of 5mm and cemented in place using dental cement. The catheter, prefilled with whole unheparinised blood, mock CSF or silicone oil as appropriate, was connected via a 3-way tap to a mercury manometer primed to generate an injection pressure of 100mmHg through an underwater reservoir system. The lesion was made by opening the 3-way tap and allowing 25µl of the test substance, as measured on the graduated catheter, to flow into the caudate nucleus. The needle was kept in place until the end of the experiment. The control group of animals underwent an identical procedure but no injection was made.

Blood Flow Studies

Regional blood flow was measured 60-90 seconds after placement of the lesion in all test groups. A ramped infusion of ^{14}C iodoantipyrine was injected by infusion pump into a femoral venous line, giving a dose of 50mCi in 30 seconds. During the infusion, blood from a femoral arterial catheter was sampled at recorded time intervals onto pre-weighed filter discs. At 30 seconds cardiac asystole was produced by rapid intravenous injection of concentrated KCl; the brain was removed immediately and snap-frozen in isopentane at -45°C for cryostat sectioning. Coronal sections (20μm) were cut and heat fixed on glass coverslips. Together with methyl acrylate isotope impregnated standards, these were exposed against industrial X-ray film for 7 days, and the resulting autoradiographs analysed by microdensitometry (Quantimet 720, Cambridge inst.). The filter discs were re-weighed and the volume of blood on each was calculated. The isotope concentration of each sample was measured by scintillation counting after the discs had been immersed in the counting medium for 24 hours. The cerebral isotope concentration measured densitometrically was converted into regional blood flow measurements using a computer-derived curve of blood isotope concentration against time, together with the blood-brain partition coefficient of the isotope (Sakurada et al 1978).

Neuropathology

A further four groups of animals underwent an identical operative procedure and were maintained lightly anaesthetised for 4 hours. At the end of this period the brain was fixed by intracardiac perfusion fixation with a formaldehyde, acetic acid and methanol mixture (FAM) (Brown & Brierley 1968). The brain was removed and placed in FAM for a further 12 hours. The forebrain was cut into 4 equal sized blocks which were embedded in paraffin wax; 8μm sections were then cut and stained with haematoxylin and eosin and with a stain combining cresol violet and Luxol fast blue. Signs of irreversible ischaemic damage were identified by light microscopy without the nature of the lesion being revealed to the microscopist (Professor D I Graham, INS); and recorded on line diagrams drawn from the atlas of König and Klippel (1963).

Statistics

The standard paired t-test was used for the comparison of blood flow in the cerebral hemispheres within each group of animals, with the unpaired t-test being used to compare results between groups. The Wilcoxson rank sum test was used to compare the size of the ischaemic area between groups in the Neuropathology series.

Survival Experiments

The pathophysiological consequences of a haematoma have not been systematically followed in the laboratory animal. In parallel with the above experiments, therefore, a model was set up which allowed survival of a group of animals following the production of a 25µl haematoma. The operative details were similar to the above experiment except for the following:

A tracheostomy was not established, and the animals breathed spontaneously throughout. Anaesthetic gases and oxygen were supplied via a specially-designed mask.

Access for blood withdrawal and blood pressure monitoring was obtained by catheterisation of the tail vessels. Arterial blood pressure and $p_{a}O_{2}$ were maintained at the same levels as in the previous experiments, but it proved impossible to ensure that $p_{a}CO_{2}$ was in the 35-40mmHg range. Values of 35-45mmHg were therefore accepted.

Intracranial pressure was not measured. In each group, the contralateral hemisphere was used as a control.

At the conclusion of the experiment, the cranial and caudal wounds were irrigated with 1% lignocaine and sutured. Sutures were removed at 7-10 days in animals with longer survival times.

The animal was allowed to breathe 100% oxygen until awake. All animals were observed closely for signs of distress or neurological disturbance, but these were not a feature.

Two animals were studied at each of these survival times: 2 hours, 6 hours, 15 hours, 24 hours, 48 hours, 4 days, 8 days, 14 days and three months. At the end of the survival period the animal was

re-anaesthetised and underwent intracardiac perfusion fixation as for the earlier Neuropathology series. The fixative used in this case was 2.5% buffered glutaraldehyde, pH 7.2, as it is intended to examine the brains by electron microscopy at a future date. After perfusion, the brain was left *in situ* for at least 4 hours. It was then removed and placed in the same fixative for 24 hours. After detatching the hindbrain, the cerebral hemispheres were cut into 1-2mm thick coronal slices. The slices containing the haematoma were post fixed in osmium, processed and embedded in Araldite. Semi-thin sections were cut and stained with Toluidine Blue, and were examined by light microscopy.

RESULTS

Physiological data

There were no significant differences between the mean values for the blood gases, mean blood pressure (BP) or body weight of the four groups in the blood flow experiments, all values except weight being obtained at the time of lesion production. (table 19)

In the Neuropathology series, physiological variables (except weight) were sampled at 1, 10, 30 and 120 minutes, and just before termination of the experiment. The mean of the 5 measurements in each animal was used to obtain the means and standard errors shown in table 20.

table 19

PHYSIOLOGICAL VARIABLES (blood flow series)

(mean ± SEM; pa in mmHg, weight in g)

	control (n=4)	CSF (n=4)	oil (n=5)	blood (n=5)
pHa	7.46 ± 0.02	7.44 ± 0.01	7.49 ± 0.01	7.47 ± 0.01
$paCO_2$	37.5 ± 0.7	37.8 ± 0.6	37.5 ± 0.5	38.8 ± 0.3
paO_2	120 ± 2	112 ± 11	131 ± 4	123 ± 3
mean BP	91 ± 4	82 ± 2	95 ± 5	88 ± 5
weight	433 ± 15	422 ± 32	457 ± 26	385 ± 8

table 20

PHYSIOLOGICAL VARIABLES (neuropathology series)

(mean ± SEM)

	control (n=5)	CSF (n=5)	oil (n=5)	blood (n=5)
pHa	7.47 ± 0.01	7.44 ± 0.01	7.40 ± 0.03	7.45 ± 0.02
$paCO_2$	37.6 ± 0.3	36.5 ± 0.4	37.5 ± 0.9	36.3 ± 0.6
paO_2	130 ± 8	127 ± 13	123 ± 11	115 ± 9
mean BP	81 ± 3	85 ± 5	88 ± 4	91 ± 3
weight	362 ± 16	348 ± 6	354 ± 5	478 ± 17

There was a trend, which reached significance only for blood group vs. control ($p<0.05$), for mean arterial pressure to be higher in animals receiving a space-occupying lesion.

Intracranial Pressure

Intracranial pressure was measured in each experiment. Immediately following injection, ICP rose to a peak in the lesioned animals. In animals receiving artificial CSF this peak was reached 2-3 seconds earlier and was significantly higher than in the oil and CSF groups; however the ICP then fell abruptly so that at 10s post peak there was not a significant difference between groups, and ICP stabilised at a similar level in all groups. Mean arterial blood pressure did not change in any animal during this time, and so the change in cerebral perfusion pressure (CPP) was equal to the change in ICP. Initial ICP, ICP at 10 seconds and ΔICP (ΔCPP) are shown in

table 21.

table 21

Intracranial Pressure (ICP; mmHg, mean ± SEM)

(blood flow & neuropath. series)

	control	**CSF**	**oil**	**blood**
	(n=9)	(n=9)	(n=10)	(n=10)
initial	6.4 ± 0.7	7.5 ± 1.1	5.5 ± 0.5	4.4 ± 0.3
10 secs	6.1 ± 0.6	9.0 ± 1.2	7.1 ± 0.8	6.9 ± 0.7
ΔICP	-0.3 ± 0.2	+1.5 ± 0.5	+1.6 ± 0.4	+2.5 ± 0.5

These increases in ICP were small and did not reduce cerebral perfusion pressure. In the four hour experiments, ICP fell by one hour to the pre-injection value or below.

Lesion Topography

As silicone oil and CSF are both colourless, the lesion was visible on frozen section only in the haematoma group. Lesions were well contained within the caudate nucleus, with some dissection into the white matter tracts of the corpus callosum. Prior assessment of the distribution of the CSF injection using CSF stained with Evans Blue showed that it was distributed in the same way as the blood injected. In only one animal (Neuropathology series, figure 23) was there a small surface collection.

Blood Flow Studies

A typical autoradiograph at mid caudate level for each of the groups of animals is shown in fig 22.

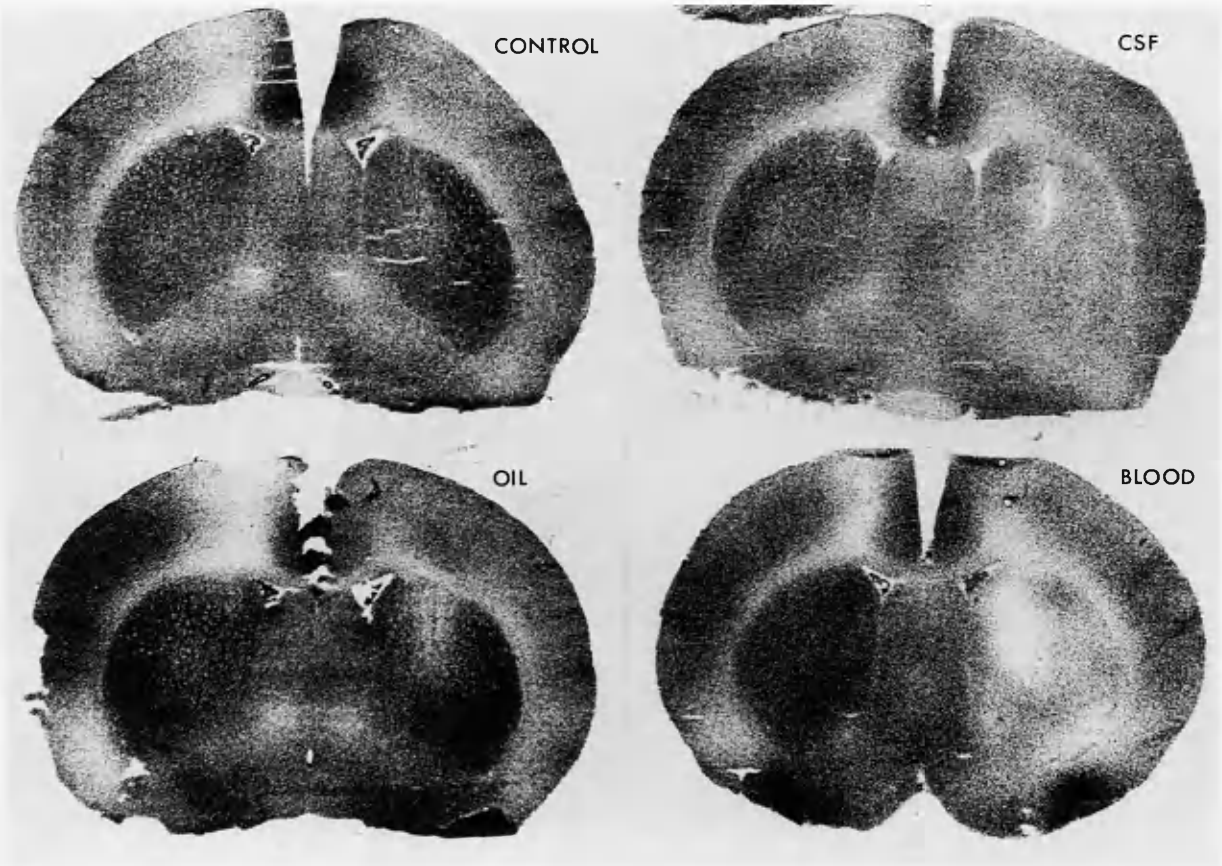

fig. 22

^{14}C autoradiographs of coronal sections at mid-caudate level one minute after lesion production

1. REGIONAL BLOOD FLOW

Areas of interest 3x3mm were selected in both hemispheres as shown in table 21. At anterior, mid and posterior levels in the caudate nucleus, blood flow measurements were performed on a standard area of cortex and on the areas of highest (H) and lowest (L) blood flows in the caudate nucleus itself. A standard area of the Corpus Callosum, and highest and lowest levels in the Globus Pallidus, were also measured. Table 22 shows blood flow in right and left hemispheres in the animals of each group.

table 22

REGIONAL CEREBRAL BLOOD FLOW (ml/100g/min, ± SEM)

in the left (L) (control) and right (R) (lesioned) hemispheres of each group.

(H = highest and L = lowest flow.)

	control		**CSF (25µl)**		**oil (25µl)**		**blood (25µl)**	
REGION	L	R	L	R	L	R	L	R
Fr. Cx	81±4	91±6	108±10	87±6	96±7	91±3	108±8	66±9*
Ant Caud H	117±16	112±14	154±13	139±9	118±18	91±11	131±4	86±5**
Ant Caud L	80±10	91±13	119±6	113±14	85±15	69±14	113±5	61±10*
Cx(Midcaud)	91±4	86±2	133±13	89±10	102±9	106±10	114±5	79±4**
Mid Caud H	120±16	123±9	170±11	164±13	107±12	95±11	140±8	86±9*
Mid Caud L	83±14	95±12	121±5	46±6**	80±11	50±7§	112±8	41±9**
Post Caud H	99±12	98±11	137±5	149±10	90±8	82±6	128±5	78±4**
Post Caud L	65±13	64±10	86±10	67±16	59±11	48±4	83±6	53±4*
Glob Pall H	66±7	74±13	90±8	85±6	64±6	74±8	87±11	78±3
Glob Pall L	52±7	57±8	60±7	48±6	40±7	51±4	66±8	54±7
Corp Callos	39±6	38±5	42±1	36±5	34±2	38±5	48±4	32±4§

p values for R vs L, paired t-test: §=0.05; *=0.01, **=0.001

Fr. Cx = frontal cortex, Caud = Caudate nucleus, Cx (Midcaud) = cortex at that level, Glob Pall = Globus Pallidus, Corp Callos = Corpus Callosum

When flow values in the lesioned (R) side were compared with those of the (L) side in each group, reduction in flow was seen at the midcaudate level in all lesioned groups (for p values, see table 21). Significant reduction in blood flow at other sites, however, was seen only in animals injected with blood.

When regional flow levels in the lesioned (R) hemisphere of the sham operated group were compared with the (R) hemisphere of each of the injection groups, a highly significant reduction in flow was seen in the mid-caudate nucleus of all lesioned groups ($p<0.001$ in each case). In both the oil and haematoma groups, a significant reduction was also seen at the posterior caudate level ($p<0.01$). In the haematoma group alone, reduced flow was also seen in the cortex at caudate level ($p<0.01$), in the anterior caudate ($p<0.01$), and in the frontal cortex ($p<0.001$), when compared to the sham operated group.

When compared with the group given a CSF injection, a significantly greater reduction in blood flow was seen in both the oil and blood injection groups in anterior, middle and posterior caudate nucleus regions ($p<0.001$ in each case for the highest flows in each area).

Comparison between the groups given oil and blood injections showed a highly significant difference in blood flow to the cortex at frontal and midcaudate levels ($p<0.001$). Flows in all other areas were reduced in the blood injection group, but the differences did not reach statistical significance.

2. HEMISPHERIC CEREBRAL BLOOD FLOW

The autoradiographs were analysed by outlining each hemisphere at midcaudate level and measuring optical density at flow thresholds set by reference to isotope standards. Blood flow from 25-300ml/100g/min was measured in increments of 25ml/100g/min and the results were expressed as the percentage of each hemisphere with blood flow ≤25, ≤50, ≤75ml/100g/min etc. (cumulative percentage). From these, the percentage area of the hemisphere with a flow of <25, 26-50, 51-75 etc. (differential percentage) was calculated. These results are shown in table 23. The percentage area at each flow level in the right and the left hemisphere of each group was compared, and comparison of right (lesioned) hemisphere flow was made between groups.

There was an increase in the proportion of the (R) hemisphere with blood flow levels indicative of ischaemia (less than 25ml/100g/min) compared to the (L) in all lesioned animals. This was statistically significant at midcaudate level (the site of the maximum lesion) only in the haematoma group ($p<0.01$). In the other 2 injection groups, the area of 'lowest flow' was also greater in the injected hemisphere, but the difference was not significant.

A significant difference was found between blood flow to the right hemisphere at low flow levels (<25; 26-50 ml/100g/min) in sham and oil groups ($p<0.05$) and sham and blood groups ($p<0.01$), but not between sham and CSF groups. Comparison of right hemisphere flow between the CSF, oil and blood injection groups showed no consistent difference.

table 23

HEMISPHERIC CEREBRAL BLOOD FLOW, MIDCAUDATE LEVEL

(Lesion in Right (R) side)

(cumulative area percentage, ± SEM)

	control		CSF		oil		blood	
BLOOD FLOW (ml/100g/min)	**L**	**R**	**L**	**R**	**L**	**R**	**L**	**R**
<25	1.1±0.3	0.4±0.1	0.6±0.2	1.8±1.7	1.3±0.9	2.6±1.7	0.5±0.2	2.2±0.8
<50	5.1±0.8	4.6±1.5	4.0±1.8	7.4±4.6	7.1±2.5	13.3±5.8	3.7±0.6	11.8±2.8
<75	33.0±3.9	33.1±7.4	8.6±3.7	25.0±8.3	41.1±8.6	50.3±13	16.2±3.2	46.2±5.5

(differential area percentage, ± SEM)

	control		CSF		oil		blood	
BLOOD FLOW (ml/100g/min)	**L**	**R**	**L**	**R**	**L**	**R**	**L**	**R**
<25	1.1±0.3	0.4±0.1	0.6±0.2	1.8±1.7	1.3±0.9	2.6±1.7	0.5±0.2	2.2±0.8*
26-50	7.0±3.2	4.2±1.4	3.4±1.4	5.6±2.5	5.7±1.6	10.7±3.8	3.2±0.5	9.7±2.0§
51-75	32.3±5.8	28.6±5.1	7.9±2.4	17.6±3.6	27.7±7.5	37.0±6.6	12.6±2.5	34.4±3**
>75	59.6±20	66.9±15	88.1±9	75.0±17	65.2±23	49.7±29	83.8±7	53.8±12**

§, $p<0.02$; *, $p<0.01$; **, $p<0.001$

p values for R vs. L, paired t-test

NEUROPATHOLOGY

Line diagrams of brain showing the distribution of irreversible ischaemic damage at 4 hours after lesion production are shown in fig 23. The midcaudate level of each of five animals in the four groups is shown.

In the sham operated group, a small ischaemic lesion was seen at the site of the needle track in all animals. In no case was ischaemic damage seen outwith this site. In some animals a small amount of blood was also shown along the needle track.

As it is not possible using this method to measure the actual area or volume of ischaemia, the Wilcoxson Rank Sum Test was used for comparison (table 24).

In the animals with a mock CSF injection, the size of the ischaemic lesion was not significantly different from that of the sham operated group.

In animals injected with either oil or blood, the cavity of the lesion in the caudate nucleus was seen to be surrounded by a larger area of ischaemia. There was no significant difference in the size of the ischaemic lesion between the two groups, but in both, after subtracting the lesion cavity, the ischaemic lesion was significantly larger than in the control or CSF groups.

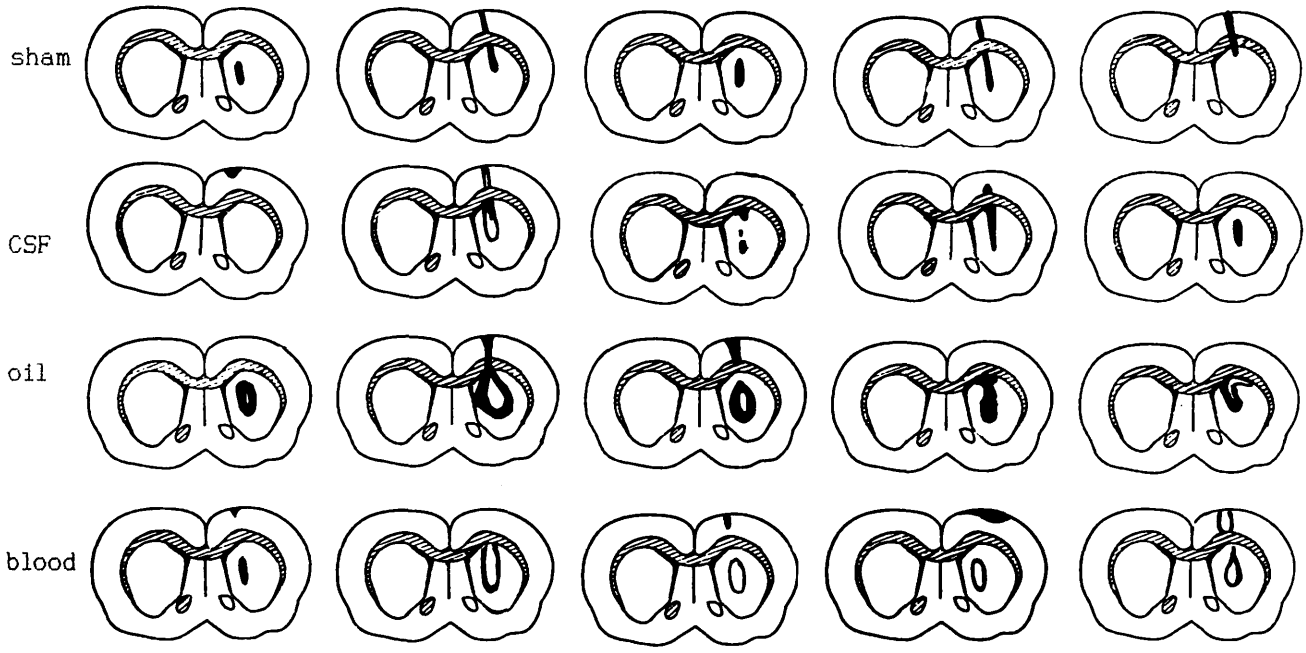

fig. 23

distribution of irreversible ischaemia as seen on light microscopy at four hours

table 24

ISCHAEMIC LESION, RIGHT HEMISPHERE, SEEN BY LIGHT MICROSCOPY IN LESIONED ANIMALS COMPARED WITH CONTROLS.

p values by Wilcoxson rank sum test.

		cortex	caudate
control group vs.	CSF	NS	NS
	oil	NS	p=0.005
	blood	NS	p<0.05

Survival Experiment

Pairs of animals were sacrificed at serial time intervals (2, 6, 15, 24, 48, and 96 hours; 8, 14 and 90 days) following the injection of a 25ul haematoma into the right caudate nucleus. Photomicrographs of representative coronal sections through the caudate nucleus are shown and described in fig. 24 (a - o).

2 hours (24a, 24b).

24a: A track (T) passes into the caudate nucleus, where it expands to form the haematoma cavity. Most of the haematoma has fallen out during processing. At the edge of the haematoma there is perivascular cuffing where red cells have tracked from the haematoma along the outside of parenchymal vessels (arrows). Immediately medial to the haematoma is an area of pallor (P) and spongiform change with a well-defined margin, affecting both the grey and white matter of the caudate.

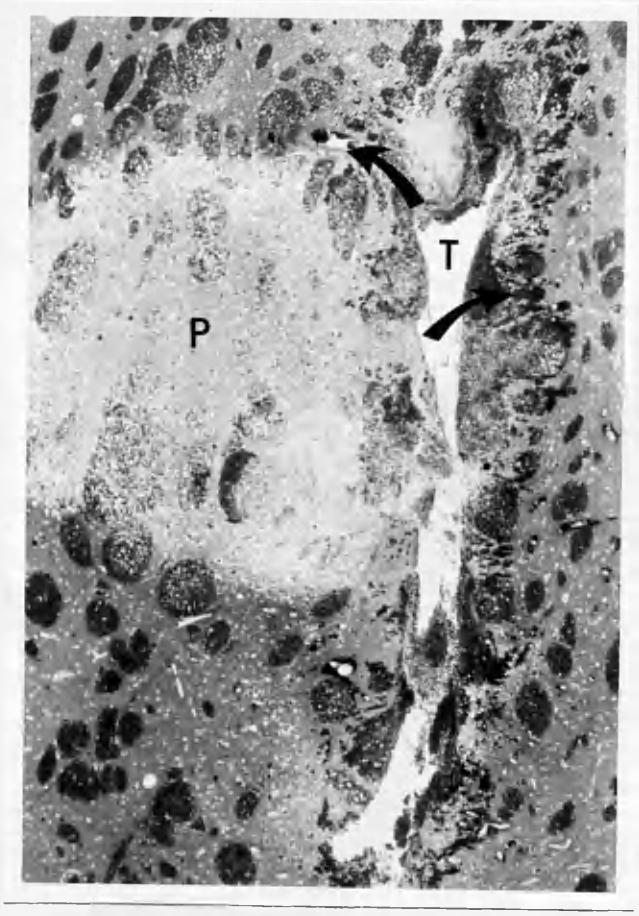

x54

24b: Some darkly-staining, ischaemic neurones are seen (arrows). This area has the appearance of ischaemia and oedema.

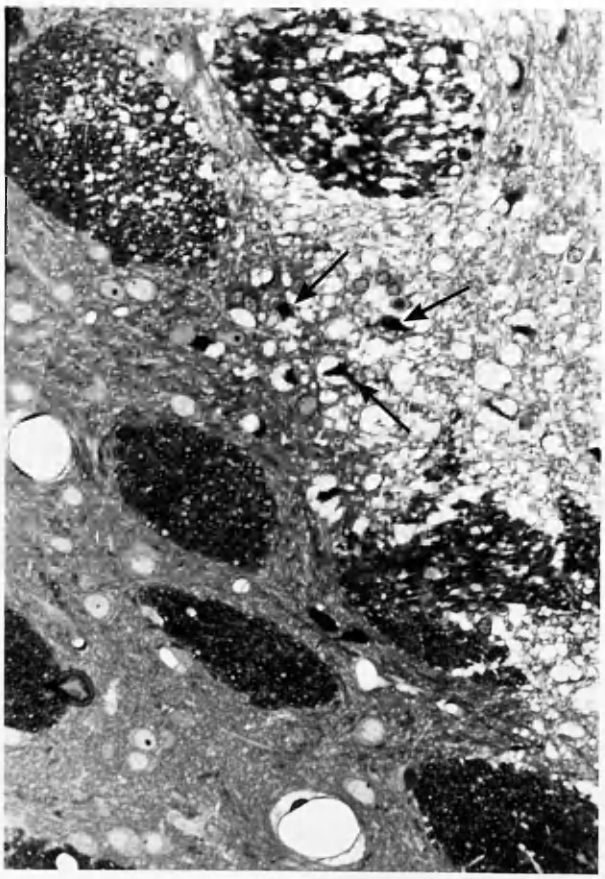

×335

6 hours (24c).

24c: In addition to the haematoma within the caudate (A), some blood was seen to track into the corona radiata. The spongy, vacuolated neuropil seen in the 2 hour histological slides was again apparent, but evidence of axonal damage can now be seen at the margin of the haematoma - black arrows indicate enlarged, swollen axons. Swollen astrocytes were also seen in this situation. There was as yet no cellular infiltrate, but increased prominence of the endothelial cells was noted.

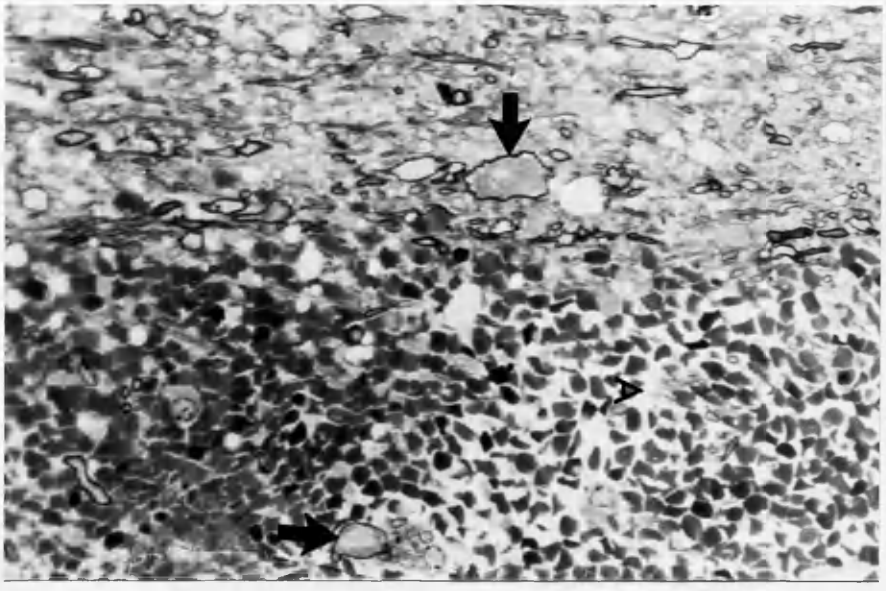

x535

15 hours (24d).

24d: The section is cut just anterior to the haematoma. There is by now considerable swelling of the corona radiata (CR). At the margin of the lesion ischaemic necrosis of the caudate was shown, with evidence of axotomy and early breakdown of myelin.

x54

24 hours (24e, 24f, 24g).

24e: The area of pallor and oedema was more extensive at this stage than earlier, and considerable swelling of the white matter was seen (P).

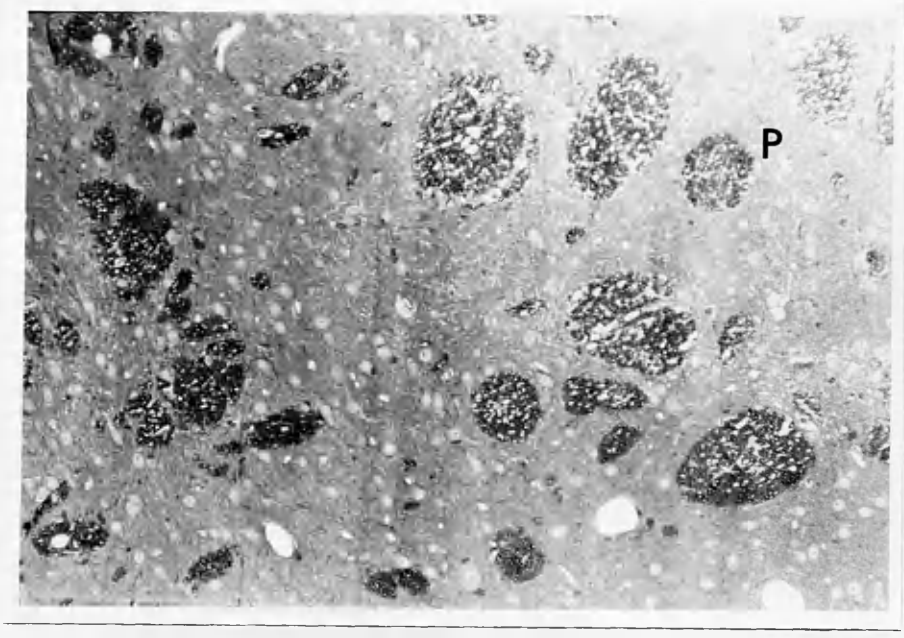

x335

24f: Most neurones (NC) in the oedematous area are normal or swollen; only adjacent to the haematoma were they seen to be darkly staining, indicating irreversible ischaemic damage.

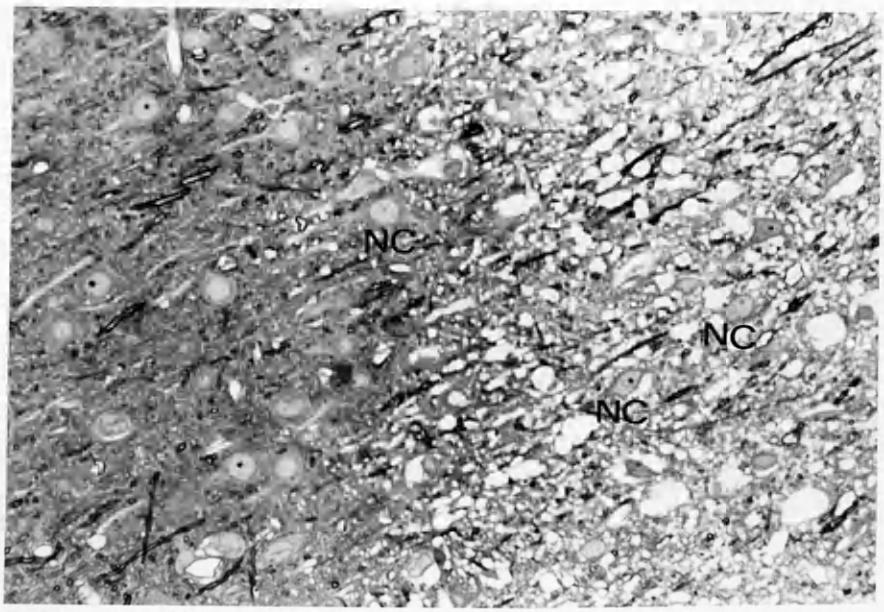

x535

24g: Retraction bulbs of axotomised neurones are seen (arrows). Astrocytic swelling is apparent both at the haematoma margin and at more distant sites. Cell debris is now seen within the haematoma. There is still no cellular infiltrate.

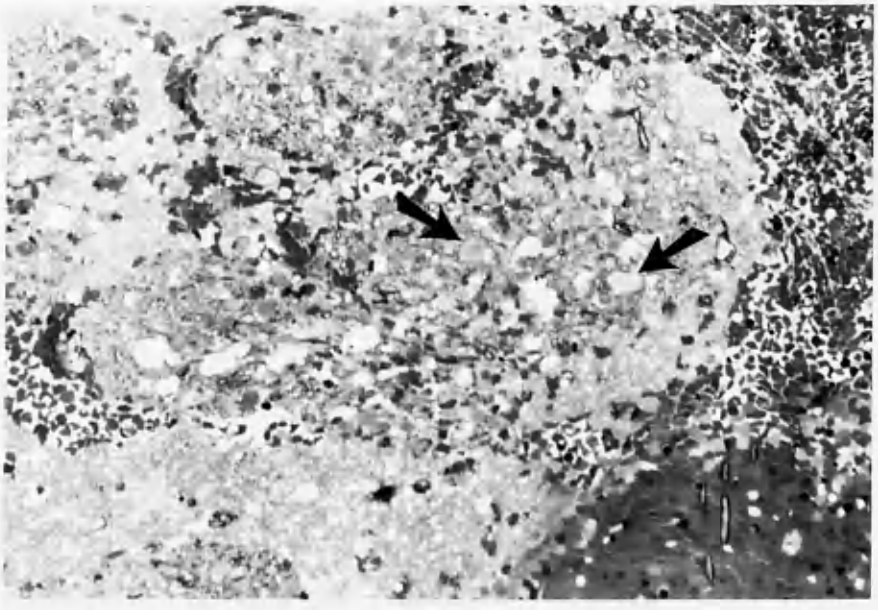

x535

48 hours (24h).

24h: The haematoma appears more compacted. It is surrounded by an irregular collar of oedema and vacuolation, which is no larger than at 24 hours. Axonal damage is again seen (black arrow), and the retraction bulbs appear larger. There is now evidence of a cellular response, with monocytes (white arrows) and polymorphs moving into the vacuolated area. The irregular nuclei of the former indicate a phagocytic response. Astrocytes are larger, and the breakdown of myelin is more advanced.

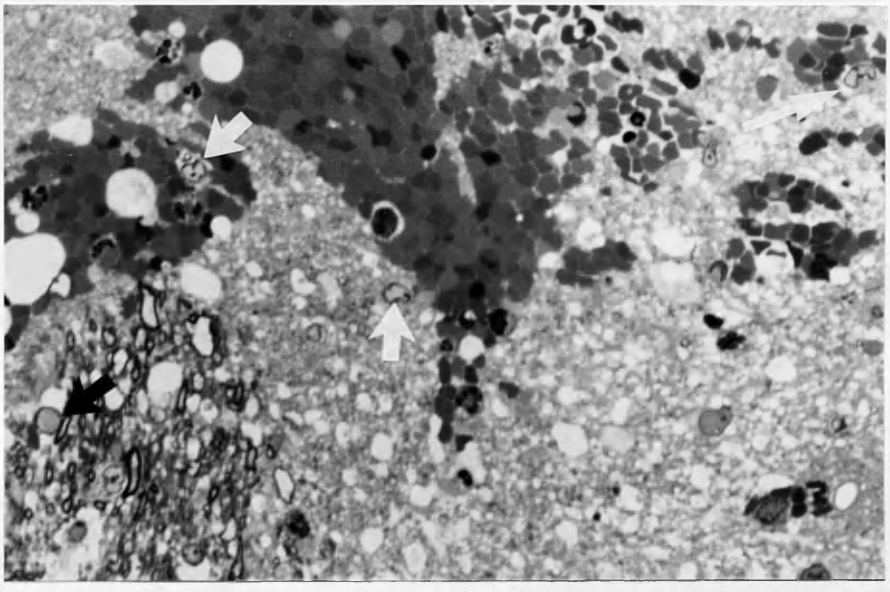

x535

4 days (24i, 24j).

24i: Oedema and vacuolation (P) are much less extensive, and are seen only at the margin of the haematoma (H).

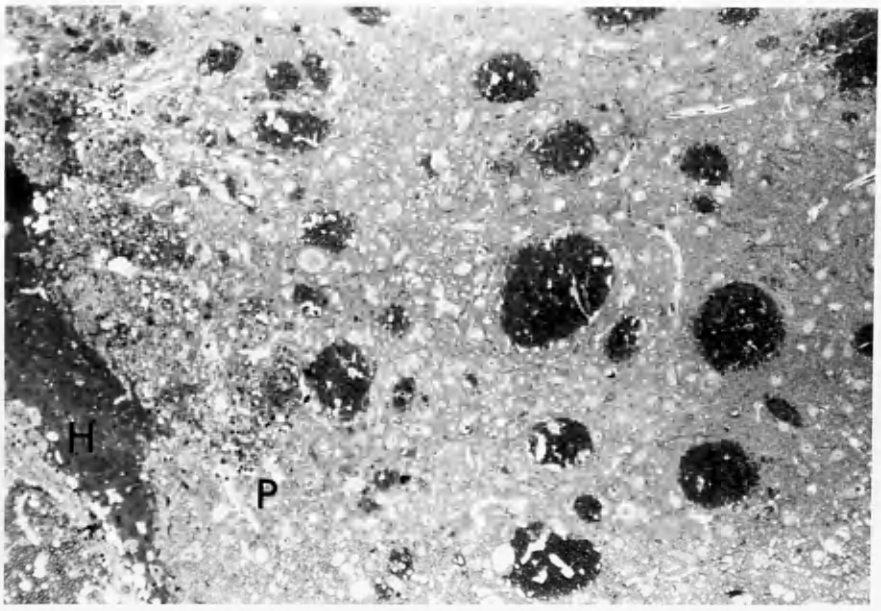

x54

24j: Blood vessels were by now covered by a sheet of cells, the source of the considerable macrophage (M) influx seen in and around the haematoma cavity (H). Mitotic figures (MIT) are apparent in many of the macrophages and in the enlarged astrocytes (arrow) as they respond to the presence of the haematoma.

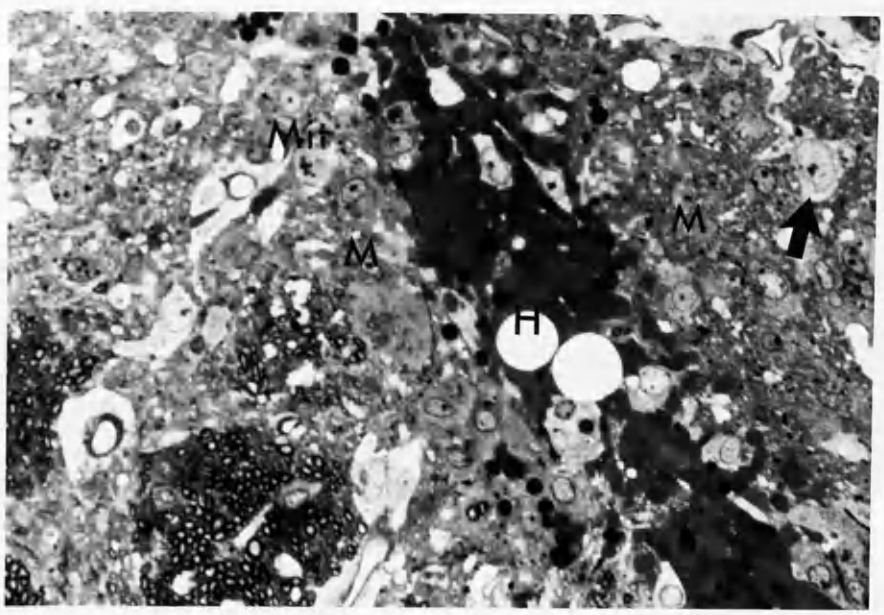

x535

8 days (24k, 241).

24k: The haematoma cavity (H) contains some residual blood and large numbers of macrophages (M).

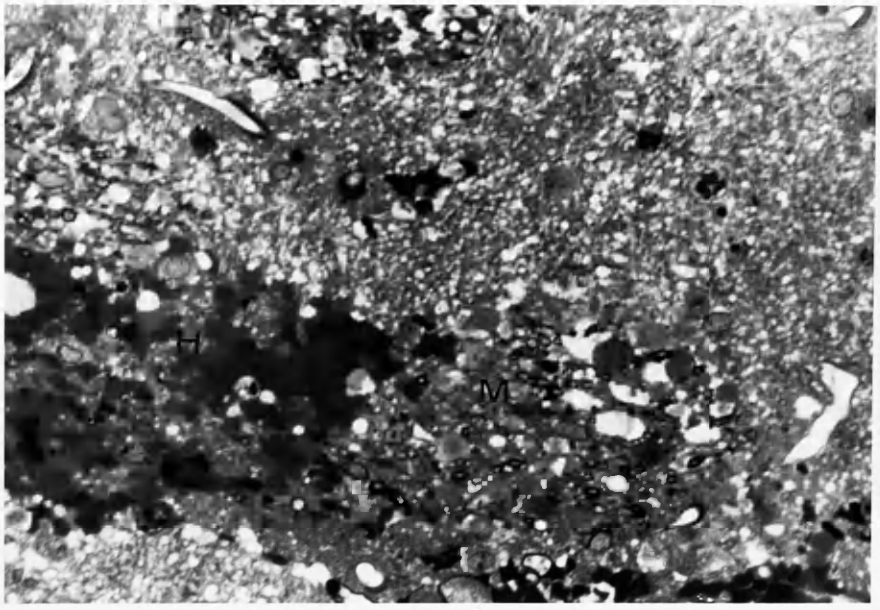

x535

241: The band of macrophages (M) and astrocytes (black arrows) at its margin is now more orientated, the cells being arranged parallel to the lesion edge. Mitotic figures are seen in the astrocytes as they hypertrophy and proliferate to form a glial scar. Vacuolation of the white matter was still apparent, but its extent was less and it had a clearer margin.

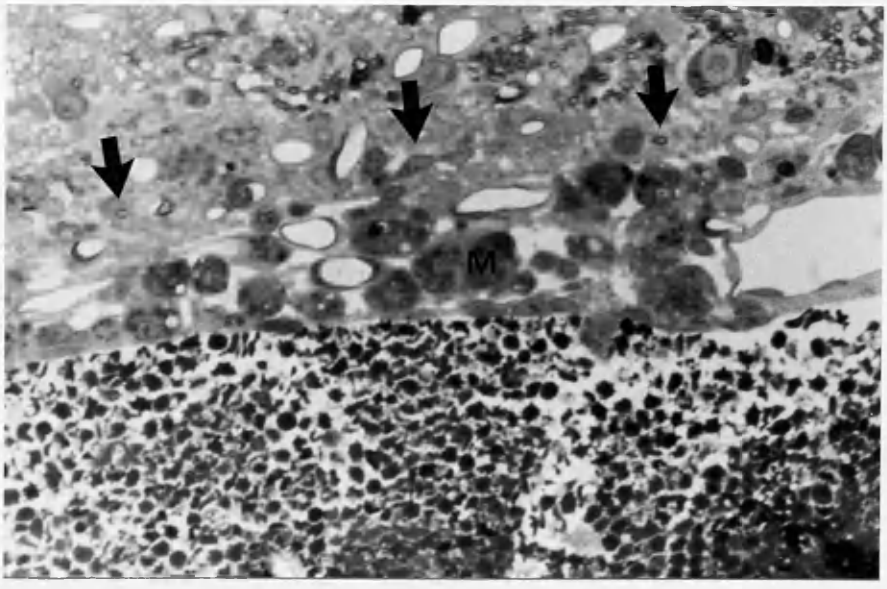

x535

14 days (24m, 24n).

24m: In only two areas is there residual blood, surrounded and invaded by macrophages (M) and astrocytes (arrows).

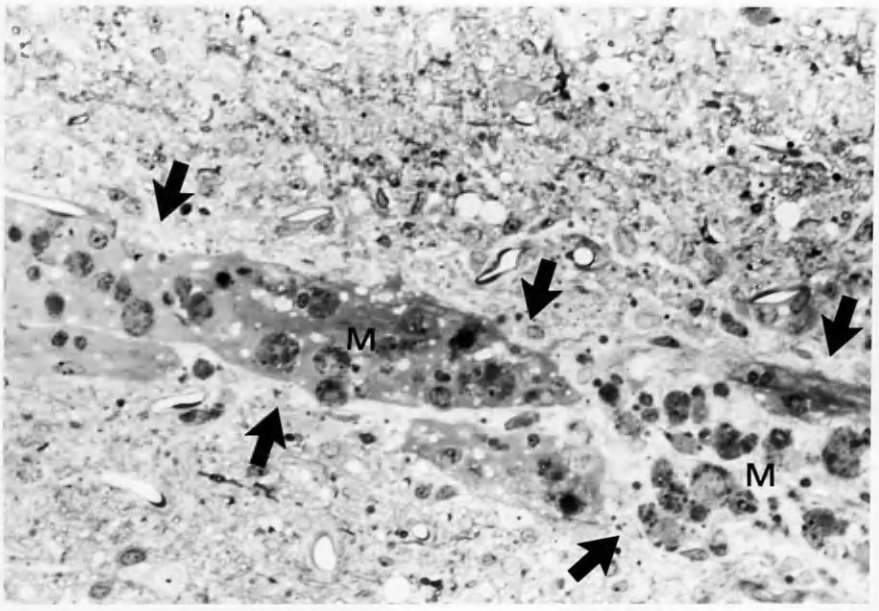

X335

24n: In the residual track of the haematoma (T) there are pigmented macrophages (siderophages) and glial cells.

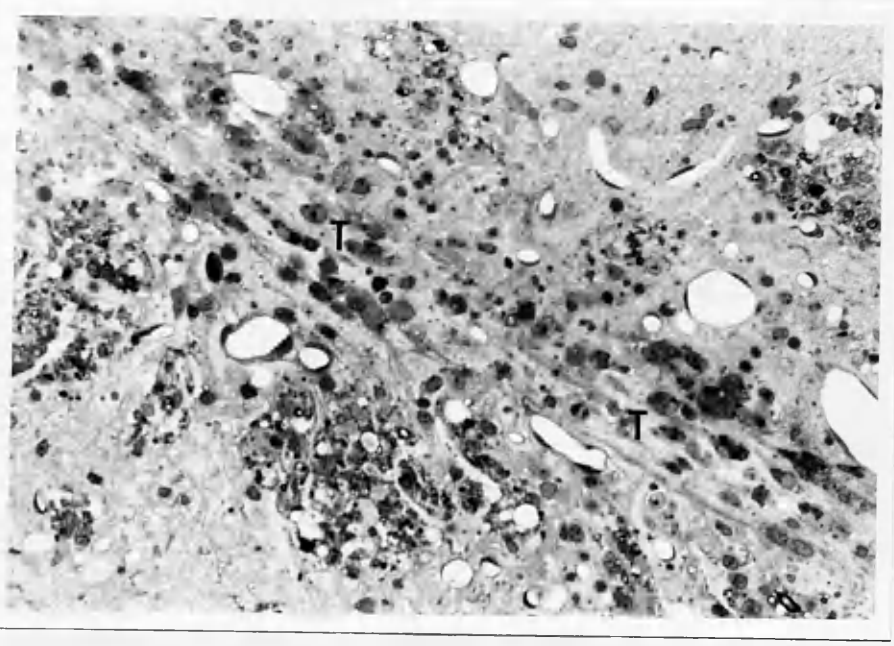

x335

3 months (24o).

24o: The haematoma and the subsequent phagocytic and astrocytic response are no longer present. The only evidence of the lesion is a thin glial scar (black arrows). Wallerian degeneration is still apparent (white arrows).

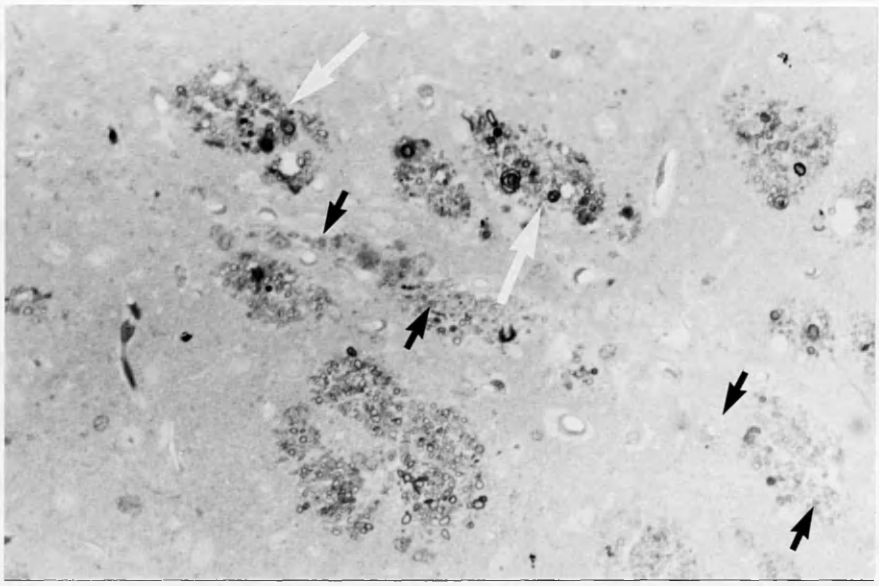

x335

SUMMARY

In a small animal model of an intracerebral space-occupying lesion, intracranial pressure, early cerebral blood flow and sequential neuropathological change were studied.

25μl lesions of mock CSF, inert silicone oil and autologous blood all caused significant perifocal reductions in blood flow, as measured by ^{14}C IAP autoradiography. Only with a blood lesion was significant reduction in flow seen in sites distant from the lesion and in the ipsilateral cerebral hemisphere as a whole. Reductions in flow were sufficient to produce irreversible ischaemic neuronal damage, as assessed by light microscopy at 4 hours, only in the area immediately adjacent to the lesion, and there was no significant difference in the amount of ischaemic damage produced by the blood and the inert oil lesions. Rises in intracranial pressure on production of the lesion were small and short-lived, being insufficient to cause significant changes in cerebral perfusion pressure.

The sequence of events following the experimental production of a small haematoma in the basal ganglia of the rat, as revealed by serial light microscopy, can be summarised as follows.

On production of the lesion, a variable amount of blood tracks along the less compact and resistant white matter tracts, and also along the local blood vessels. An area of oedema and ischaemia appears early; the variable shape of this implies that chemically and/or physically mediated distortion of the local vasculature is partially responsible. Over the first 24-48 hours the oedema becomes

more widespread, affecting both grey and white matter. Swollen astrocytes and severed axons become apparent. From 2 days onwards, there is a considerable cellular response; monocytes and polymorphs migrate via local capillaries to remove the haematoma by phagocytosis, while proliferation and hypertrophy of astrocytes lead to the production of the *glia limitans* and then a glial scar. By 14 days, the absorption of the haematoma is almost complete, and by three months the area is again quiescent with a residual glial scar and persistent Wallerian degeneration.

Chapter 7

DISCUSSION

MAGNETIC RESONANCE

The possibility that intracranial lesions might be characterised by their relaxation times was one of the strong initial attractions of MRI. Results, particularly for tumours, have so far been disappointing: it has not proved easy to separate the relaxation times of different tumours sufficiently to enable definitive diagnosis (Araki et al 1984). This finding was confirmed for the CNS tumours examined here. There is, however, a degree of concurrence between centres in the measurements derived from analysis of normal tissues at appropriate field strengths (Beall et al 1984). Thus it is consistently possible to separate most normal tissues from each other on MR images if appropriate imaging strategies are used.

This study used measurements only of brain, blood and CSF. The technique of *in vitro* measurement used is a refinement of that of Beall (1983) and is designed to minimise tissue degradation due to the effects of evaporation, temperature variation and time. This ensures that the MR parameters obtained from *in vitro* studies mimic as closely as possible those which would be obtained from *in vivo* measurements of the same tissues, and provides accurate, reproducible results. Errors due to individual sample variation have been reduced by the pooling of numbers of samples from different subjects. A vital factor was the ability of the Brüker analyser to measure accurately substances with long relaxation times; thus CSF T1 and T2 measurements in this study are substantially higher than many previously quoted (Bradley 1987, Beall et al 1984) which are essentially the default highest values for the equipment used. Because the relaxation times of CSF are so long, few commonly used

sequences have a repetition time sufficiently long for a major part of its signal to be detected. This explains the approximate isointensity of brain and CSF on the SE2200/80 sequence used for most of the succeeding study. Values obtained for the relaxation times of grey and white matter and of fresh blood are similar to those obtained at other centres (Beall et al 1984); grey and white matter, fresh blood and CSF have relaxation times differing substantially from each other and should therefore be eaily distinguishable on appropriately chosen MRI sequences. The data on the changes in the relaxation times of blood of increasing age are in accord with the reports of other authors (Bradley 1987, Brooks et al 1985).

The changes in relaxation times of blood *in vitro* are reflected by the changing appearance of intracranial haematomas in the sequential *in vitro* and clinical imaging studies, implying that the changes are not artefactual or due to contamination. Similarly, the changes occur in both clotted and defibrinated blood, and are therefore not due to fibrinolysis and liquefaction. The most convincing explanation to date for the progressive fall in T1 and T2 observed over several days is that initially proposed by Brooks et al (1975), and refined by other researchers (Bradley 1987, Gomori et al 1985). The gradual absorption of serum from a clot, and the appearance of deoxyhaemoglobin in the red cells, both produce a shortening of T2 which is responsible for the central hypointensity seen in high-field imaging studies of haematoma (Gomori et al 1985). The conversion of haemoglobin to methaemoglobin and finally haemosiderin leads to a shortening of T1 and T2, and then a

lengthening of T2. *In vitro* no such lengthening of T2 was noted, presumably because methaemoglobin was not formed in sufficient quantities.

Recently published information about blood in CSF (Bradley & Schmidt 1985) suggests that significant signal change does not appear for a matter of days and that this is similarly a result of the degradation of oxyhaemoglobin to deoxyhaemoglobin and then to methaemoglobin. Although deoxyhaemoglobin only exerts its paramagnetic effect when the red cell is intact, lysis was found not to affect the relaxation times. The *in vitro* studies reported here, however, both show that a substantial change in the signal intensity of CSF is present from the time of haemorrhage; and the patient studies confirm that it is apparent on images taken within four hours of haemorrhage. It is possible that the use of a low-field system may influence the appearances. Bradley found a 10% decrease in T1 and T2 as the concentration of blood in the CSF rose from 0% to 10%, but felt that this reduction could not be responsible for the increased signal intensity seen in SAH. It should be noted that the relaxation times of CSF quoted in his paper (T1 ≃ 2s, T2 ≃ 1s) are much lower than those reported here, and that measurements were made at 20MHz. The results of the computer modelling experiment show that it is precisely this small reduction which makes bloodstaining visible if appropriate pulse sequences are chosen.

Recent work in the Glasgow MR unit (Grant et al 1987) has shown that there is a 14-16% decrease in the relaxation times of CSF if equilibration of pO_2 and pCO_2 is allowed to occur after withdrawal from the body. In the first series reported here, measurements were

made after such equilibration had been allowed to occur; similarly, measurements on bloodstained CSF were made after reoxygenation of the venous blood samples used by equilibration with CSF and air. In the second series, anaerobic conditions were maintained throughout. Although relaxation times differed between the two series, there was no material difference in the predicted signal intensity values of bloodstained CSF. Changes in gas partial pressures and in temperature are thus unlikely to be responsible for the changes in relaxation times.

The similarity between relaxation time measurements of bloodstained CSF, its acellular component, and plasma protein/CSF solutions suggests that although the immediate and substantial alteration of the relaxation times of CSF by the addition of even small amounts of blood may due in part to paramagnetic effects, it is mainly due to the presence of protein, both in the plasma and in the red cell membrane and cytoplasm. Protein is known to reduce the T1 and T2 of CSF substantially (Brant-Zawadski 1987). Subsequent changes are likely to be due to the continuing denaturation of haemoglobin, and serve to increase the difference from normal CSF.

These results give credence to the suggestion that haemorrhage, whether into brain or CSF, has imaging characteristics which differ sufficiently from those of surrounding brain or normal CSF to enable it to be diagnosed with confidence by MRI. The results of *in vitro* studies were found to be reproducible on the apparatus used, but would have to be repeated at appropriate field strengths if the use of other types of imager were to be contemplated. There is

not sufficient data in the literature to suggest whether the tissue differentiation observed here would be maintained at other field strengths. The application of the results in the development of imaging strategies will be discussed in the next section.

Sequence Prediction

Using *in vitro* data to dictate *in vivo* imaging strategies is only possible if both MR analyser and imager run at similar frequencies: although the relaxation times of free water are fixed, those of living tissues are not absolute and depend on field strength (Fullerton et al 1984). The analyser and imager used in this study are of similar frequencies and made such comparison valid.

Computer modelling of relaxation times enabled the calculation of signal intensities for the whole spectrum of possible combinations of MR imaging parameters available on the Picker imager. Using a graph plot of these results, it proved possible to select pulse sequences which separated the calculated intensities of brain, blood, CSF and bloodstained CSF sufficiently to suggest that they could be differentiated on *in vivo* images.

Inversion recovery sequences, as predicted, were generally poor at separating the signal intensities of acute blood and brain; CSF is very easily distinguishable in most sequences as a negative signal intensity, but this is altered little by the presence of small amounts of blood. Because of its excellent tissue delineation, resolution and grey-white matter contrast, the IR mode is used in many centres as standard. In these circumstances, acute intracranial haemorrhage may be missed.

Spin-Echo sequences were therefore used for diagnostic purposes, with the addition of other SE or IR sequences for extra anatomical information. After clinical assessment of the alternative sequences offered by the computer analysis, a SE2200/80 16 slice axial sequence was used if SAH was suspected; this also showed mass

haemorrhagic lesions well, particularly at an early stage, and proved exquisitely sensitive to oedema. It was also fast: the investigation of acute neurosurgical problems has to be quick and reliable. This sequence was therefore used for the imaging of patients with head injury or intracranial haemorrhage, and became a standard screening sequence. Refinement of images by increasing numbers of averages taken or decreasing slice width was found to improve resolution, but did not increase contrast or diagnostic specificity.

This method gave a logical rationale for the choice of MRI pulse sequences in imaging both subarachnoid and intracerebral haemorrhage. It proved to be easy to use; entering tissue relaxation times and basic sequence information (SE40, IR600 etc) into the computer programme gave a full intensity profile for each tissue in less than five minutes. Once plotted graphically, the information was easy to use, maximum tissue contrast being ensured simply by finding sequences which gave the tissues the greatest intensity difference. The two or three sequences thus chosen could then be tested clinically to ascertain which was most appropriate.

In vitro analysis can thus be useful in predicting the potential of Magnetic Resonance Imaging in particular disease processes: imaging time can be reduced and the information yield of the modality increased by the selection of appropriate pulse sequence protocols on the basis of such investigations. However, measurements and predictions made for one imager field strength will not be valid for another. Other pathologies may prove more difficult to investigate by this method: whereas fairly large samples of blood,

brain and CSF are reasonably easy to acquire and give consistent and reproducible relaxation values, many tumours are noted for the heterogeneity of their MR characteristics and also for the scarcity of available tissue.

The computer-based system of pulse sequence prediction proved to be both quick and valid. Long and often fruitless systematic studies of patients were avoided; this is particularly important in the conditions studied here, where patients are often ill or unstable and where the difference between an informative fifteen-minute scan and a semi-informative scan lasting an hour can be vital. If reproducible T1 and T2 measurements can be made on tissues involved in other pathologies, this method could prove to have a wide application.

IMAGING STUDIES

Safety

MRI was shown to be safe for routine use in patients with acute intracranial haemorrhage. Time spent in the imager is comparable to that of CT for a multislice spin-echo sequence, although in this study most patients underwent more than one sequence. In the experience of most MR users, about 1% of orientated patients experience claustrophobia; with either CT or MRI, disorientated patients may require sedation. MR compatible monitoring and support equipment is necessary for patients who have impaired consciousness or are unstable, but many commercially-available units are suitable - indeed it often proved to be easiest to continue ventilation on the small portable ventilator used for patient transfer. Access to the patient is restricted; this proved to be more of a problem in the prevention of movement producing artefact than in the assessment of the patient's needs. The patients included in the studies were of necessity selected; most metabolic and haemodynamic problems had been stabilised by the time of their imaging, and in most cases imaging was avoided if acute neurological deterioration was thought likely. Nevertheless a proportion of patients examined were in an unstable condition, and in a few MR was the first emergency investigation due to non-functioning of the CT scanners. In these circumstances no problems were encountered.

Low field (0.15T) MRI also proved safe for postoperative studies on patients with aneurysm clips if the clips used had minimal ferromagnetic content. This confirmed the work of New et al (1983).

The Sugita range of clips fulfils the requirements of MRI and has proved generally acceptable with operators; using these clips, artefact is little larger than the clip itself, and there is no danger of clip movement or distortion of vessels. Similar studies should be carried out on high field imagers: even if movement of the clip does not occur, it is possible that a larger signal defect may be produced at the site of the clip by a larger field.

Imaging

Tissue signal intensity values computed from *in vitro* studies suggested that intracranial haemorrhage could be shown on MRI if appropriate imaging pulse sequences were selected. On this basis a SE2000/80 sequence was chosen as the standard first investigation. This sequence optimised the contrast between the shortened T2 signal from blood or bloodstained CSF and the signal from normal CSF and brain; in addition it was sensitive to oedema and gave good anatomical resolution within the constraints of a practical imaging time.

1. Subarachnoid haemorrhage

The findings in these patients, in whom MRI and CT were performed when a provisional clinical diagnosis of SAH had been made, show that MRI is at least as useful as CT in the demonstration of subarachnoid blood. Chakeres and Bryan (1986) debated whether changes in signal in the narrow subarachnoid spaces might be obscured either by partial volume averaging or by flow effects. This study shows that even on a low-field system, with a slice width of

8mm., obvious signal changes are seen if an appropriate sequence is used; the changes are most marked in the prepontine cistern. The present study extended up to six days after the initial bleed. The sequential *in vitro* experiments suggest that the distinction between bloodstained and normal CSF will become more marked with time as the relaxation times decrease further, probably as a result of the appearance of deoxyhaemoglobin and finally methaemoglobin (Bradley & Schmidt 1985), before being washed out of the CSF spaces.

Studies in other central nervous system conditions showed that a high CSF signal can be seen in conditions where CSF protein is substantially raised: one patient with meningeal metastases and one with severe purulent meningitis showed similar appearances on MR imaging. In neither case was there any clinical confusion with SAH. This does however raise the possibility that MRI may have an as yet undefined "false-positive" rate when protein levels are of the same order as those found in SAH; the *in vitro* measurements suggest a level of 5g/l or more. These levels are rarely found in meningitis, and it is highly unlikely that the clinical history in infective or neoplastic conditions would mimic that of SAH so closely that a lumbar puncture would not be performed in any case.

Complications of subarachnoid haemorrhage such as intracerebral haemorrhage and hydrocephalus were readily demonstrated with MRI. Overall, MRI identified more haematomas in preoperative patients than did CT; however the use of the lower-definition CT1010 scanner in the earlier studies may account for some of the difference. All haematomas of surgical significance were identified by both methods. Hydrocephalus was only reported on MR images if the ventricles were

unequivocally enlarged; all such patients had CT reports of hydrocephalus. In the remaining patients reported to have enlarged ventricles on CT, the ventricular enlargement was minimal. Increased familiarity with MR appearances should enable the identification of the milder increases in ventricle size; in addition, the method of differential intracranial and intraventricular volume measurement described by Grant et al (1986) will enable more positive diagnosis and serial measurements of ventricular volume.

The signal void produced by swiftly flowing blood leads to vessels being imaged directly with MRI without the use of contrast agents (Singer & Crooks, 1983). The potential for visualising aneurysms or AVMs is thus much greater with MRI than with non-contrast CT. MRI can be used to demonstrate aneurysms or arteriovenous malformations in most of the patients in whom a cause of SAH is found. While it is unlikely that MRI will replace angiography in this field, it can be helpful to have a working diagnosis in patients in the lower clinical grades before embarking on this potentially hazardous investigation. MRI can provide this in a significant number of patients without the use of contrast media and in a total scan time similar to CT. In patients with multiple aneurysms, its sensitivity in the detection of small areas of oedema means that operation can be directed with more certainty to treatment of the aneurysm which has bled. In general, CT only provides this information by inference from the area showing the highest concentration of blood, and this is often inaccurate.

MRI is very sensitive to oedema: each of the ten patients imaged by MRI postoperatively showed local increase in signal levels

on the T2 weighted images at the site of operation, presumably as a result of operative trauma from retraction. These changes were not apparent on the CT scans. To what extent these appearances correlate with dysfunction or with blood flow disturbances has yet to be established, and no clinically useful information was gained from such observations in this study.

Apart from local hyperintensity on the T2 weighted images, convincing evidence of delayed ischaemia was not detected. Even though the patients studied did not have clinical evidence of ischaemia, the reported sensitivity of MRI to small changes in tissue water would suggest that it could show signs of unsuspected minor ischaemic change. Studies of patients with clinical evidence of ischaemia, and of the MRI changes in response to treatment, will be of interest.

In the investigation and follow-up of patients following aneurysm clipping, the use of MRI has advantages over CT in that parenchymal changes or haematomas adjacent to aneurysm clips are not masked by artefact to the same extent. It is, however, of paramount importance that investigations are only carried out on patients in whom MR-compatible clips are used; as a result of this study, this information is now recorded on the front page of each patient's case notes prior to leaving theatre.

2. Intracerebral haematoma

The appearance of intracerebral haematoma in this study was not entirely uniform. Inversion-recovery images were in general not diagnostic but showed the lesion as a distortion of the normal

anatomy. Other investigators (DeLaPaz et al 1984) have confirmed the lack of sensitivity of IR sequences at moderate to high field strengths, but in many units they are still used as the primary imaging sequence due to their superb anatomical definition. The finding on spin-echo sequences - specifically the SE 2200/80 sequence, but also others investigated - of a hypo- or isointense area surrounded by a variable region of hyperintensity is in accordance with the findings of Sipponen et al (1985) who studied intracerebral haemorrhage at 0.02 and 0.17T. They found that a SE 2000/160 sequence showed a hyperintense rim with both field strengths, with the lower field showing an isointense and the higher field a hypointense centre.

Exceptions to this pattern, however, have been illustrated. Specifically, several acute haematomas appeared uniformly hyperintense. These were all smaller haematomas, and it is possible that the 8mm slice width led to a swamping of a central hypo- or isointense signal by partial volume averaging effects. Interestingly, Swensen et al (1985) found similar appearances in acute experimental haematoma using an SE 2100/80 sequence on identical MR equipment, and highlighted in their paper the confusion surrounding the variable appearances reported in the literature. Once again, the clinical histories of the patients examined in the present series made a mistaken diagnosis unlikely, but it is conceivable that the variable appearance of malignant intracranial tumours could lead to problems in image interpretation, particularly if haemorrhage into a tumour was a possiblility.

The common finding of a hypo- or isointense centre is at

variance with the signal intensities predicted for recent bleeding by computer analysis of its *in vitro* relaxation times. This implies that the MR characteristics of the haematoma change in the first few hours after formation by mechanisms not active in the *in vitro* model. Temperature, viscosity, pH, haemoglobin and methaemoglobin levels are all known to affect the relaxation times of blood: T1 and T2 rise with increasing pH and fall with increasing haemoglobin concentration, methaemoglobin concentration, viscosity and osmolality. The inevitable conclusion is that the haematoma interacts with its surroundings soon after formation, resulting in changes in relaxation times which may well be reciprocal. The work of Tsubokawa et al (1983) looking at the spread of Evans' Blue dye from experimental haematoma led them to conclude that the early "vasogenic" oedema noted around a haematoma was initially derived by diffusion of fluid from the haematoma itself. This theory would explain not only the lower-than-expected signal intensities of acute haematomas, but also the rapid appearance of the surrounding area of hyperintensity: the diffusion of part of the fluid component from the haematoma leads to increased osmolality, viscosity and haemoglobin concentration, all of which reduce relaxation times and consequently signal intensity. Subsequent fall in pH with the inflammatory response will lead to further attenuation of T1 and T2 in the acute phase, with the gradual conversion of haemoglobin to methaemoglobin being responsible for further changes as shown in the clinical and *in vitro* studies. Subsequent spread of oedema would be by the accepted mechanisms of vasogenic and cytotoxic oedema (Baethmann et al 1980).

3. Head Injury

Large haematomas in head injured patients did not differ in their MR characteristics from spontaneous haematomas. A greater area of signal change due to oedema was seen around haematomas with MRI than with CT, particularly in the first 24 hours following injury. Further studies may reveal the association of this appearance with intracranial pressure and neurological dysfunction.

The performance of MRI was similar to that of CT in the detection of such mass lesions; the availability of coronal plane imaging proved useful in delineating the extent of clots, particularly in the temporal and subtemporal regions. This supports the work of Han et al (1984) who found that multiplanar MR imaging was better than CT in assessing the entire extent of extracerebral lesions, particularly when small. On the basis of these studies, there would be little hesitation in recommending MRI as a valid alternative to CT in head injury. Clinicians interviewed were in agreement, particularly after the breakdown of CT equipment on a number of occasions forced their hand! The sensitivity of MRI in haematoma detection may, however, be in part field-related: Snow et al (1986), in a study at 0.5T, agreed that extracerebral lesions were equally well seen but felt that "because of the potential failure of MRI to diagnose acute subarachnoid or acute parenchymal haemorrhage, CT remains the procedure of choice in diagnosing head injuries less than 72 hours old". No such limitation was found in the present study.

The mechanism of production of the many parenchymal abnormalities seen on MRI is not clear. Close comparison with post-mortem microscopic appearances in those patients imaged who

subsequently die will be necessary to establish pathologic correlates; similarly, serial imaging of patients with such lesions is currently in progress and will show the evolution of the changes seen acutely. Nevertheless, it seems likely that many of the areas of abnormality seen reflect oedematous change around micro-haematomas not visible on CT, and give *in vivo* corroboration of the pathological processes involved in primary brain injury but normally only seen post-mortem.

Magnetic Resonance Imaging has already demonstrated exciting possibilities in Neurosurgery, and has become the accepted method of investigating a few disease processes. Its performance in spinal work makes it likely that myelography and contrast CT studies will be used considerably less extensively in the future, and raises the possibility of units functioning without a CT scanner. This would only be feasible if MRI were found to perform at least as well as CT in both the emergency and the routine situations. These studies confirm that MRI can function as an adequate screening tool in subarachnoid haemorrhage, intracerebral haematoma and head injury, and that it may in addition have an important contribution to make to understanding of their pathophysiology.

EXPERIMENTAL INTRACRANIAL HAEMATOMA

This study was set up to examine the pathophysiological processes occurring after an intracerebral haematoma, specifically in the area around the clot where high intensity was seen on MR images in the patient studies.

The comparative study of acute space-occupying lesions showed that the effects on cerebral blood flow of an intracerebral injection of blood are not solely due either to its space-occupying effect or to the vasomotor effects of blood. Each type of lesion led to a significant decrease in flow in the brain immediately adjacent to the site of the injection; space-occupying effect alone can therefore produce ischaemia. Blood did not differ greatly from oil or CSF in the intensity of this local effect, but blood flow in regions not immediately adjacent to the lesion was reduced significantly only in the blood injection group. Regional blood flow was reduced by up to 50% even in areas remote from the site of injection of blood, and there was a four-fold increase in the percentage area of the hemisphere with flow below ischaemic levels. Significant ischaemic brain damage was observed at the site of the injection in animals with oil or blood injections, but not with CSF injection.

The ICP changes were modest, and the local drop in regional CBF around the injection site was not due to a global reduction in cerebral perfusion pressure (CPP). It is more likely that the mechanical lesion produced a rise in local tissue pressure, with a consequent fall in local CPP. Since Cushing's description in 1902, Langfitt (1964) and Mizukami (1983) have produced further evidence that 'squeezing of the microcirculation' around a space-occupying

lesion is responsible for the surrounding ischaemia and its propagation. In this experiment, however, a difference was found between the effect of blood and other inert fluids on cerebral blood flow outside the immediate area of the injection. It is therefore necessary to postulate an additional mechanism to explain the widespread ischaemia seen immediately in the haematoma group.

The consistent and significant differences between the animals injected with blood and the other groups may reflect the effect of vasoactive substances. Blood contains many substances which are potentially vasoconstrictor in effect. Fresh blood applied directly to the adventitia of the exposed basilar artery causes immediate and marked vasospasm (Echlin 1965); serotonin, contained in blood and also formed by platelet breakdown during clotting, causes a similar effect. The Kallikrein-kinin system causes increased blood-brain barrier permeability and direct cell injury, but also causes vasoconstriction (Baethmann et al 1980). Histamine is a potent vasoconstrictor. Thromboxane A_2, also produced by platelets, antagonises the vasodilator action of prostacyclin and may be responsible for later vasoconstriction. These and many other plasma components, if released into the surrounding tissues, could affect the smooth muscle of arterial and arteriolar walls, and it may prove difficult to separate their actions experimentally.

Previous studies have demonstrated a profound and extensive area of ischaemia around an intracerebral haemorrhage (Mendelow et al 1984, Nath et al 1987), in proportion to the volume of blood injected (Nath et al 1987 (2)). Despite the initial reduction in CBF seen in the present series, there was not a significant difference

in the microscopic extent of the ischaemic lesions seen at 4 hours in the haematoma and oil injection groups. This may reflect the small size of the lesion: 25μl was chosen because preparatory work showed that larger injections could not be reliably contained within the caudate nucleus without tracking to the cortical surface. The early changes in regional CBF may not correspond with the pattern of flow 4 hours later, the time of the neuropathological study. Further experiments using autoradiographic blood flow measurement at four hours in similar experimental groups might demonstrate areas of ischaemia comparable to those seen by light microscopy. There is experimental evidence suggesting that local blood flow may even be increased at this time (Nath et al 1987 (2)) in the same way that haemorrhagic and ischaemic strokes in humans may show areas of luxury perfusion at a late stage. It must be stressed that blood pressure was strictly maintained in all animals throughout the experiment and that they were anaesthetised; the brain was therefore to some degree protected from the effects of temporary reductions in local blood flow. After spontaneous haemorrhagic stroke in humans there is unlikely to be such protection.

The experimental data suggest that vasoactive substances in blood may contribute to ischaemia after intracerebral haemorrhage. This raises the possibility that the sequelae of intracranial haemorrhage might be reduced by pharmacological means, as well as by the evacuation of the blood. This could be achieved by the systemic administration of agents which antagonise vasoconstrictor effect, either by acting on vascular smooth muscle directly or on its membrane receptors. It is unlikely that only one of the many

potentially vasoactive blood constituents is responsible for the reduced cerebral blood flow. The effect of surgical removal of the mass component has yet to be determined, but it would seem to hold little promise of reversal of the local ischaemia. Initial experimental data support this view (Kingman 1988). Clinically, operation is only likely to help if high intracranial pressure is present, but the benefits of such an operation are in doubt (McKissock et al 1961, Volpin et al 1984). The possibilty that ischaemia produced by intracerebral haematoma might be minimised by pharmacological methods deserves further study.

The serial study of intracerebral haematoma shows that oedema appears soon after the bleed and becomes maximal at around 48 hours. The small size of the haematoma in this model, together with the small and transient rise in ICP measured in the acute series, make it likely that this oedema, which is extensive and irregular, is not caused entirely by the effect of transmitted pressure rises on small arteries in the region. Blood is seen to track along these local vessels, sometimes for some distance, and swelling of the endothelium is noted at 6 hours. It is probable that the vasoconstrictive and cytotoxic actions of blood constituents, reaching local vessels by diffusion and perivascular permeation, is responsible at least in part for the propagation of oedema and reduced regional blood flow.

Chapter 8

CONCLUSIONS

Conclusions

Magnetic resonance imaging is safe and effective for use in patients with head injury, subarachnoid and intracerebral haemorrhage. Its performance as a screening method is good, although imaging times are longer than with CT scanning and specialised monitoring and support apparatus is required. Potential advantages lie in its sensitivity to early tissue changes, its ability to demonstrate normal and abnormal vasculature without intravenous contrast, and the small extent of signal degradation when appropriate non-ferromagnetic aneurysm clips are used.

The differentiation of signal intensity values derived from *in vitro* MR tissue analysis is a valid and swift way of predicting appropriate RF pulse sequences for use in MR imaging.

The relaxation times of CSF are much longer than those previously published, which accounts both for its appearance in images of normal patients and for the dramatic changes in signal seen in subarachnoid haemorrhage. There is evidence from these studies that such changes are present from the time of the bleed and are largely due to the presence of plasma and red cell protein in the CSF, and not in the early stages due to the paramagnetic effects of haemoglobin breakdown products.

Spin-echo Magnetic resonance studies in acute intracerebral haematoma have good diagnostic specificity. Most studies showed signal intensities in haematomas which, when compared with the relative intensities predicted by computer analysis of *in vitro* relaxation times, suggested early changes in haematoma composition.

High signal was found in the surrounding brain parenchyma. These two findings might be explained by diffusion of fluid from the clot. Studies in subacute and chronic haematoma show progressive signal changes in the clot, indicative of the appearance of haemoglobin breakdown products.

There is only a small rise in intracranial pressure on the introduction of a small intracerebral haematoma in the experimental model. This is in accordance with clinical findings. Although this rise is not sufficient to compromise cerebral perfusion pressure, there is a transient fall in perfusion throughout much of the ipsilateral cerebral hemisphere which is maximal around the haematoma. It is likely that the main component of this effect is due to the action of vasoactive substances released at the time of haematoma production; reduction in blood flow is less extensive when inert substances are used to form a similar mass lesion. Vasoactive substances may reach regional vessels by diffusion from the haematoma and by blood tracking from the haematoma along the outside of vessels.

BIBLIOGRAPHY

Adams JH, Doyle D, Graham DI, Lawrence AE, McLellan DR. Gliding contusions in non-missile head injury in humans. Arch Pathol Lab Med. 1986; 110:485-8

Adams JH, Graham DI, Murray LS, Scott G. Diffuse Axonal Injury due to non-missile head injury in humans. An analysis of 45 cases. Annals of Neurology 1982; 12:557-63

Araki T, Inouye T, Suzuki H, Machida T, Iio M. Magnetic Resonance Imaging of brain tumours: measurement of T1. Radiology 1984; 150(1):95-98

Arana-Iniguez R, Wilson E, Bastarrica E, Medici M. Cerebral Haematomas. Surgical Neurology 1976; 6:45-52

Arseni C, Ionescu S, Maretsis M, Ghitescu M. Primary Intraparenchymatous Haematomas. J Neurosurg 1967; 27:207-15

Asano T, Sano K. Pathogenetic rôle of no-reflow phenomenon in experimental subarachnoid haemorrhage in dogs. J Neurosurg 1977; 46:454-66

Axel L. Surface coil Magnetic Resonance Imaging. J Comput Assist Tomogr. 1984; 8(3):381-4

Backlund E-O, von Holst H. . Controlled subtotal evacuation of intracerebral haematomas by stereotactic technique. Surg Neurol 1978; 9:99-101

Baethmann A, Oettinger W, Rothenfulsser W, Kempski O, Unterberg A, Geiger R. Brain oedema factors: current state with particular reference to plasma constituents and glutamate. Adv Neurol 1980; 28:171-95

Bagley C Jr. Spontaneous Cerebral Haematoma: discussion of 4 types, with surgical considerations. Arch Neurol Psychiatr 1932; 27:1133-1174

Bailes DR, Young IR, Thomas DJ, Straughan K, Bydder GM, Steiner RE. NMR Imaging of the brain using Spin-Echo Sequences. Clin Radiol. 1982; 33:395-414

Beall PT. Practical Methods for Biological NMR Sample Handling. Mag Res Imaging 1983; 1(3):165-80

Beall PT, Amtey SR, Kasturi SR. NMR Data Handbook for Biomedical Applications. 1984, Pergamon Press, New York.

Beischer J, Knepton P. Influence of strong magnetic fields on the ECG of squirrel monkeys. Aerospace Med 1964; 35:939-44

Besson JAO, Corrigan FM, Iljon Foreman EL et al. Proton NMR Observations in Dementia. Proc. SMRM, San Francisco 1983, p43-4

Bilaniuk LT, Zimmerman RA, Grossman RI et al. Cerebral NMR of pediatric brain tumors. Radiology 1983; 149(P):178

Bloch F, Hansen WW, Packard M. Nuclear Induction. Phys Rev 1946; 69:127

Bolander HG, Kourtopoulos H, Liliequist B, Wittboldt S. Treatment of spontaneous intracerebral haematoma. A retrospective analysis of 74 consecutive cases with special reference to computertomographic data. Acta Neurochir 1983; 67:19-28

Bosch DA. Successful stereotactic evacuation of an acute pontomedullary haematoma. Case report. J Neurosurg 1985; 62:153-6

Bostrom K, Helander CG. Aspects on pathology and Neuropathology in head injury. Acta Neurochir Supplement 1980; 36:51-5

Bradley WG. Pathophysiologic correlates of signal alterations. In: Magnetic Resonance Imaging of the Central Nervous System. eds. Brant-Zawadski M, Norman D. New York 1987: Raven Press, pp 23-42

Bradley WG, Schmidt PG. Effect of Methaemoglobin Formation on the MR Appearance of Subarachnoid Haemorrhage. Radiology 1985; 156:99-103

Bradley WG, Waluch V, Yadley RA, Wycoff RR. Comparison of CT and MR in 100 patients with suspected disease of the brain and spinal cord. Radiology 1984; 152:695-702

Brant-Zawadski M. In: Magnetic Resonance Imaging of the central nervous system. eds. Brant-Zawadski M, Norman D. New York 1987: Raven Press, p 9

Brant-Zawadski M, Norman D, Newton TH et al. Magnetic Resonance of the Brain: the Optimal Screening Technique. Radiology 1984; 152(1):71-77

Brant-Zawadski M, Davis PL, Crooks LE et al. NMR demonstration of cerebral abnormalities: comparison with CT. AJR 1983; 140: 847-854

Bratton CB, Hopkins AL, Weinberg JW. NMR studies of living muscle. Science 1965; 147:738-9

Brooks RA, Battocletti JH, Sances AJR, Larson SJ, Bowman RL, Kudravcev V. Nuclear magnetic relaxation in blood. IEEE Trans Biomed Eng 1975; 22:12-18

Brooks RA, Di Chiro G, Girton M et al. The changing appearance of blood: an *in vivo* and *in vitro* study. Proc. SMRM, London 1985, pp325-6

Brown AW, Brierley JB. The nature and distribution and earliest stages of anoxic-ischaemic nerve cell damage in the rat brain as defined by the light microscope. Br J Exp Pathol 1968; 49:87-106

Brown FD, Hanlon K Mullan S. Treatment of aneurysmal hemiplegia with dopamine and mannitol. J Neurosurg 1978; 49:525-9

Bryant DJ, Payne JA, Firmin DN, Longmore DB. Measurement of flow with NMR Imaging using a Gradient Pulse and phase difference technique. J Comput Assist Tomogr. 1984; 8(4):588-93

Budinger TF. Indirect electrical stimulation of the visual apparatus. Lawrence Radiation Lab Report UCRL-18347, 1968

Budinger TF. Thresholds for physiological effects due to RF and magnetic fields used in NMR imaging. IEEE Trans Nuc Sci 1979; NS26(2):2821-5

Budinger TF. Nuclear Magnetic Resonance (NMR) *in vivo* studies. Known Thresholds for Health Effects. J Comput Assist Tomogr 1981; 5:800-811

Budinger TF. Potential medical effects and hazards with NMR human studies. In: Kaufman L, Crooks LE, Margulis AR, eds. Nuclear Magnetic Resonance Imaging in medicine. Tokyo: Igaku-Shoin, 1981: 207-231

Bullock R, Mendelow AD, Teasdale GM, Graham DI. Intracerebral Haemorrhage induced at arterial blood pressure in the rat. Part 1: Description of technique, ICP changes and Neuropathological findings. Neurol Res (1984) 6:184-188.

Bydder GM. NMR Imaging of the brain. British Medical Bulletin 1984; 40(2):170-4

Bydder GM, Pennock JM, Young IR. Magnetic Resonance Imaging of Intracerebral Haematoma at low field (0.15T). In: Proceedings of the European Society of Magnetic Resonance in Medicine and Biology, 1986; 3:30-1

Bydder GM, Steiner RE, Thomas DJ et al. NMR imaging of the posterior fossa: 50 cases. Clin Radiol 1983; 34: 173-88

Bydder GM, Steiner RE, Young IR et al. Clinical NMR imaging of the brain: 140 cases. AJR 1982; 139: 215-236

Carr DH, Brown J, Leung AW-L, Pennock JM. Iron and gadolinium chelates as contrast agents in NMR imaging: preliminary studies. J Comput Assist Tomogr. 1984; 8(3):385-9

Chakeres DW, Bryan RN. Acute Subarachnoid Haemorrhage: *in vitro* comparison of Magnetic Resonance and Computed Tomography. AJNR 1986; 7: 223-8

Chan K, Mann K. Intraventricular haemorrhage: management of comatose patients by valve-regulated external ventricular drainage. BJNS 1988; 2:465-9

Chilton HM, Ekstrand KE. Principles and applications of nuclear Magnetic Resonance Imaging. Am J Hospital Pharmacy 1984; 41:763-8

Cohen MD, McGuire WDA, Smith JA. MR appearance of blood and blood products: an *in vitro* study. Am J Radiol 1987; 148:1215-8

Condon BR, Patterson J, Jenkins A, Wyper DJ, Hadley MDM, Grant R, Rowan JO, Teasdale GM. MR Relaxation times of Cerebrospinal Fluid. J Comput Assist Tomogr 1987; 11(2):203-7

Condon BR, Patterson J, Wyper DJ, Hadley MDM, Jenkins A, Grant R, Teasdale GM, Rowan JO. Use of Magnetic Resonance Imaging to measure Intracranial Cerebrospinal Fluid Volumes. Lancet 1986 I:1355-1356

Condon BR, Patterson J, Wyper DJ, Jenkins A, Hadley MDM. Image Non-uniformity in Magnetic Resonance Imaging: its Magnitude and methods for its correction. Br J Radiol 1987; 60:83-7

Condon BR, Patterson J, Wyper DJ, Hadley MDM, Teasdale GM, Grant R, Jenkins A, McPherson P, Rowan JO. A quantitative index of ventricular and extraventricular Cerebrospinal Fluid volumes using MRI. J Comput Assist Tomogr 1986; 10:784-92

Condon BR, Patterson J, Wyper DJ, Lawrence A, Hadley MDM, Jenkins A, Rowan JO. Digital Mapping of multi-parameter contrast functions in MRI using a standard MR computer and image display. Computerized Radiology 1986; 10(6):269-77

Condon B, Patterson J, Wyper D, Hadley DM, Jenkins A, Lawrence A, Rowan J. Comparison of Calculated Relaxation Parameters between an MR Imager and Spectrometer operating at similar frequencies. Magn. Reson. Imaging 1986; 4:449-454

Crompton MR. Cerebral infarction following the rupture of cerebral berry aneurysms. Brain 1964; 87:263-80

Crooks LE, Arakawa M, Hoenninger J et al. Nuclear Magnetic Resonance Whole Body Images operating at 3.5 KGauss. Radiology 1982; 143:169-174

Crooks LE, Arakawa M, Hoenninger J, McCarten B, Watts J, Kaufman L. Magnetic Resonance Imaging: Effects of Magnetic Field Strength. Radiology 1984; 151:127-33

Crooks LE, Hoenninger J, Arakawa M et al. High-resolution Magnetic Resonance Imaging. Technical concepts and their implementation. Radiology 1984; 150:163-71

Cuatico W, Adib S, Gaston P. Spontaneous Intracerebral Haematomas. A Surgical appraisal. J Neurosurg 1965; 22:569-575

Cushing H. Some experimental and clinical observations concerning states of increased intracranial tension. Am J Med Sci 1902; 124:375-400.

Damadian R. Tumor detection by Nuclear Magnetic Resonance. Science 1971; 171:1151-3

Damadian R, Goldsmith M, Minkoff L. NMR in Cancer: XVI. FONAR Image of the Live Human Body. Physiol Chem Phys. 1977; 9:97-100

Damadian R, Minkoff L, Goldsmith M, Stanford M, Koutcher J. Field Focusing Nuclear Magnetic Resonance (FONAR) image of a Tumor in a live Animal. Science 1976; 194:1430-2

Davis PL, Crooks L, Arakawa M, McRee R, Kaufman L, Margulis AR. Potential hazards in NMR imaging: heating effects of changing magnetic fields and RF fields on small metallic implants. AJR 1981; 137:860

Delapaz RL, New PFJ, Buonanno FS et al. NMR imaging of Intracranial Haemorrhage. J Comput Assist Tomogr 1984; 8(4):599-607

Doyle FH, Gore JC, Pennock JM et al. Imaging of the brain by Nuclear Magnetic Resonance. Lancet 1981; ii:53-7

Droege RT, Wiener SN, Rzeszotarski MS. A Strategy for MRI of the head: Results of a semi-empirical model. Radiology 1984; 153:419-433

Duff TA, Ayeni S, Levin AB, Javid M. Non-surgical management of Spontaneous Intracerebral Haematoma. Neurosurgery 1981; 9:378-92

Echlin FA. Spasm of basilar and vertebral arteries caused by experimental subarachnoid haemorrhage. J Neurosurg 1965; 23:1-11

Edelman RR, Johnston K, Buxton R et al. MR of Haemorrhage: a new approach. American Journal of Radiology 1986; 7:751-6

Enzmann DR, Britt RH, Lyons BE, Buxton JL, Wilson DA. Natural history of experimental intracranial haemorrhage: Sonography, computed tomography and neuropathology. AJNR 1981; 2:517-26

Evens RJ. Economic costs of Nuclear Magnetic Resonance Imaging. J Comput Assist Tomogr 1984; 8(2):200-3

Fisher CM. Pathological observations in hypertensive cerebral haemorrhage. J Neuropath Exper Neurol 1971; 30:536-50

Franken EA, Berbaum KS, Dunn V et al. Impact of MR Imaging on clinical diagnosis and management: a prospective study. Radiology 1986; 161(2):377-80

Fujita S. Computed tomographic grading with Hounsfield number related to delayed vasospasm in cases of ruptured cerebral aneurysm. Neurosurgery 1985; 17:609-12

Fullerton GD, Cameron IL, Ord VA. Frequency dependence of Magnetic Resonance spin-lattice relaxation of protons in biological materials. Radiology 1984; 151:135-8

Gabillard R. Measurement of relaxation time T1 in the presence of an inhomogeneous magnetic field. C R Acad Sci (Paris) 1951; 232:1551-3

Gaetani P. y Baena RR, Silvani V, Rainoldi F, Paoletti P. Prostacyclin and vasospasm in subarachnoid haemorrhage from ruptured intracranial aneurysm. A preliminary clinical study. Acta Neurol Scand 1986; 73:33-8

Gaffney CT, Tenforde TS. Electrical properties of conducting frog sciatic nerves exposed to high DC magnetic fields. Bioelectromagnetics 1980; 1:208

Gandy SE, Snow RB, Zimmerman RD, Deck MDF. Cranial Nuclear Magnetic Resonance Imaging in head trauma. Ann Neurol 1984; 16:254-7

Gomori JM, Grossman RI, Goldberg HI, Zimmerman RA, Bilaniuk LT. Intracranial Haematomas: Imaging by High-field MR. Radiology 1985; 157:87-93

Hackney DB, Lesnick JE, Zimmerman RA et al. MR Identification of Bleeding Site in subarachnoid haemorrhage with multiple intracranial Aneurysms. J Comput Assist Tomogr 1986; 10(5):878-880

Hadley MDM, Jenkins A, McPherson P, Patterson J, Wyper DJ, Condon BR, Lawrence A, Rowan JO, Teasdale GM. Magnetic Resonance in Subarachnoid Haemorrhage: an *in vitro* and *in vivo* study. In: Proceedings of the 2nd Congress of the European Society of Magnetic Resonance in Medicine and Biology, Montreux 1985, pp 306-317

Hadley MDM, McPherson P, Jenkins A, Patterson J, Wyper DJ, Condon BR, Mendelow AD, Lawrence A, Rowan JO, Teasdale GM. Magnetic Resonance Imaging in acute Subarachnoid Haemorrhage. In: 4th annual meeting of the Society of Magnetic Resonance in Medicine (London 1985) Vol. 1 pp357-358

Han JS, Kaufman B, Alfidi RJ et al. Head Trauma evaluated by Magnetic Resonance and Computed Tomography: a comparison. Radiology 1984; 150:71-7

Haughton VM, Ho KC, Williams AL, Elderik OP. CT detection of demyelinated plaques in multiple sclerosis. Am J Radiol 1979; 132:213-5

Hawkes RC, Holland GN, Moore WS, Worthington BS. Nuclear Magnetic Resonance (NMR) tomography of the brain: a preliminary clinical assessment with demonstration of pathology. J Comput Assist Tomogr 1980; 4:577-86

Ho C, Russu IM. Proton Nuclear Magnetic Resonance investigation of haemoglobins. Methods Enzymol 1981; 76:275-312

Høedt-Rasmussen K, Skinhøj E, Paulson O et al. Regional cerebral blood flow in acute apoplexy. The "luxury perfusion syndrome" of brain tissue. Arch Neurol 1967; 17:271-81

Holland GN, Hawkes RC, Moore WS. Nuclear Magnetic Resonance (NMR) Tomography of the Brain: Coronal and Sagittal Sections. J. Comput Assist. Tomogr. 1980; 4:429-433

House W. Introduction to the principles of NMR. IEEE Trans Nucl Sci 1980; NS27(3):1220-6

Hutchison JMS, Edelstein WA, Johnson G. A whole-body NMR imaging machine. J Phys E: Sci Instrum 1980; 13:947-55

Hutchison JMS, Mallard JR, Goll CC. *In vivo* imaging of body structures using proton resonance. In: Allen PS, Andrew ER, Bates CA, eds. Proceedings of the 18th Ampere congress. University of Nottingham, Nottingham, England, 1974, p 283

Hutchison JMS, Smith FW. NMR Clinical Results: Aberdeen. In: Partain CL, James AE, Rollo FD, Price RR, eds. Nuclear Magnetic Resonance (NMR) Imaging. Philadelphia: WB Saunders, 1983:231-49

Ishii R. Regional cerebral blood flow in patients with ruptured intracranial aneurysms. J Neurosurg 1979; 50:587-94

Jackson JA. Whole body spectrometer. Rev Sci Instrum 1968; 39:510-3

Jenkins A, Teasdale GM, Hadley MDM. Magnetic Resonance Imaging in Traumatic Brain Damage. Proceedings of the Society of British Neurological Surgeons, Cambridge, April 1986. J Neurol Neurosurg Psychiatr 1986; 49:1332

Jenkins A, Teasdale GM, Hadley MDM. Primary Traumatic Brain Damage: Magnetic Resonance Imaging and Clinical Features. Surgical Research Society, Manchester 1986. Abstract in Br. J. Surg. 73(6):490, June 1986

Jenkins A, Condon BR, Patterson J, Hadley MDM, Teasdale GM. Intracranial Haematoma: Use of *in vitro* measurements to guide clinical imaging. In: Proceedings of the 2nd Congress of the European Society of Magnetic Resonance in Medicine and Biology, Montreux 1985, pp278-282

Jenkins A, Teasdale GM, Hadley MDM, McPherson P, Rowan JO. Brain lesions detected by Magnetic Resonance Imaging in mild and severe head injuries. Lancet 1986; 2: 445-446

Johnson MA, Pennock JM, Bydder GM et al. Clinical NMR Imaging of the brain in children: Normal and Neurologic Disease. AJNR 1983; 4:1013-1026

Kanako M, Koba T, Yokoyama T. Early surgical treatment for hypertensive intracerebral haematoma. J Neurosurg 1977; 46:579-83

Kase CS. Intracerebral Haematoma: non-hypertensive causes. Stroke 1986; 17:590-5

Kido DK, Morris TW, Erickson JL, Plewes DB, Simon JH. Physiologic changes during high field strength MR imaging. AJR 1987; 148:1215-8

Kingman TA, Mendelow AD, Graham DI, Teasdale GM. Experimental intracranial mass: description of model, intracranial pressure changes and early neuropathological consequences. J Neurosurg 1988 (in press)

Kingman TA, Mendelow AD, Graham DI, Teasdale GM. Experimental intracranial mass: effects on local cerebral blood flow determined by ^{14}C iodoantipyrine autoradiography. J Neurosurg 1988 (in press)

Komiyama M, Yagura H, Baba M et al. MR Imaging: Possibility of Tissue Characterisation of Brain Tumours using T1 and T2 Values. AJNR 1987; 8:65-70

König JFR, Klippel RA. The Rat Brain: a Stereotactic Atlas. New York: Krieger, 1963

Lai CM, Lauterbur P. True three-dimensional image construction by by Nuclear Magnetic Resonance Zeugmatography. Phys Med Biol 1981; 26:851-6

Langfitt TW, Weinstein JD, Kassel NF et al. Transmission of increased Intracranial Pressure within the supratentorial space. J. Neurosurg. 1964; 21:998-1005.

Lauterbur P. Image formation by induced local interactions: examples employing Nuclear Magnetic Resonance. Nature 1973; 242:190-1

Leussenhop AJ, Shevlin WA, Ferrero AA, McCullough DC, Barone BM. Surgical management of Primary Intracerebral Haemorrhage. J Neurosurg 1967; 27:419-27

Levin HS, Handel SF, Goldman AM, Eisenberg HM, Guinto FC Jr. Magnetic Resonance Imaging after "diffuse" non-missile head injury. A neurobehavioural study. Arch Neurol 1985; 42:963-8

Little JR, Dial B, Bellanger G, Carpenter S. Brain Haemorrhage from intracranial tumour. Stroke 1979; 10:283-8

Lukes SA, Norman D, Mills C. Acute disseminated encephalomyelitis: CT and NMR findings. J Comput Assist Tomogr 1983; 7:182

Mallard J, Hutchison JMS, Edelstein W, Ling R, Foster M. Imaging by nuclear magnetic resonance and its bio-medical implications. J Biomed Eng 1979; 1:153-60

Mansfield P, Maudsley AA. Medical imaging by NMR. Br J Radiol 1977; 50:188-94

McGinnis BD, Brady TJ, New PFJ. Nuclear Magnetic Resonance (NMR) imaging of tumors in the posterior fossa. J Comput Assist Tomogr 1983; 7:575-84

McKissock W, Richardson A, Taylor J. Primary Intracerebral Haemorrhage: a controlled trial of surgical and conservative treatment in 180 unselected cases. Lancet 1961; 2:221-6

MacPherson P, Teasdale E, Dhaker S, Allerdyce G, Galbraith S. The significance of traumatic haematoma in the region of the basal ganglia. J Neurol Neurosurg Psychiatr 1986; 49:29-34

Mendelow AD, Bullock R, Nath FP, Jenkins A, Kingman T, Teasdale GM. Intracranial Pressure Changes and Cerebral Blood Flow. In: Intracranial Pressure VI. eds: Miller JD, Teasdale GM, Rowan JO, Galbraith SL, Mendelow AD. Berlin, Heidelberg: Springer-Verlag, 1986:515-520.

Mendelow AD, Bullock R, Teasdale GM, Graham DI, McCulloch J. Intracerebral Haemorrhage induced at arterial blood pressure in the rat. Part 2: Short term changes in local cerebral blood flow measured by autoradiography. Neurol Res 1984; 6:189-192

Mendelow AD, Karmi MZ, Paul KS, Fuller GAG, Gillingham FJ. Extradural haematoma: effect of delayed treatment. Br Med J 1979; i:1240-2

Mitsuno T, Kanaya H, Shirakata S, Ohsawa K, Ishikawa Y. Surgical treatment of hypertensive intracerebral haemorrhage. J Neurosurg 1966; 24:70-6

Mitzukami M, Kawase T, Usami T, Tazawa T. Prevention of vasospasm by early operation with removal of subarachnoid blood. Neurosurgery 1982; 10:301-7

Mizukami M, Tazawa T. in: Theoretical background for surgical treatment in hypertensive intracerebral haematoma. eds. M Mizukami. H Kamaya and K Kogure. New York: Raven Press, 1983, pp239-247.

Modesti LM, Binet EF. Value of Computed Tomography in the diagnosis and management of Subarachnoid Haemorrhage. Neurosurgery 1978; 3:151-6

Mohr JP, Caplan LR, Melski JW et al. The Harvard co-operative stroke registry: a prospective registry. Neurology 1978; 28:754-62

Mohr JP, Kase CS, Adams RD. Cerebrovascular disorders. In: Harrison's Principles of Internal Medicine, 10th ed. RG Petersdorf et al (eds), ch. 356, pp2028-2060

Mohr JP, Lorenz R. The effect of experimentally produced Intracranial Haematoma upon ICP. In: Intracranial Pressure IV. eds. Shulman K, Marmarou A. Miller JD, Becker DP, Hochwald GM, Brock M. Berlin, Heidelberg, New York: Springer-Verlag 1980

Mohsen F, Pomonis S, Illingworth R. Prediction of delayed ischamia after subarachnoid haemorrhage by computed tomography. J Neurol Neurosurg Psychiatr 1984; 47:1197-202

Moon KL Jr, Brant-Zawadski M, Pitts LH et al. Nuclear Magnetic Resonance Imaging of CT isodense subdural haematomas. AJNR 1984; 5:319-22

Muizelaar JP, Becker DP. Induced hypertension for the treatment of cerebral ischaemia after subarachnoid haemorrhage. Direct effect on cerebral blood flow. Surg Neurol 1986; 25:317-25

Nath FP, Jenkins A, Mendelow AD, Graham DI, Teasdale GM. Experimental Intracerebral Haematoma: early haemodynamic changes.
J Neurosurg 1987 (in press)

Nath FP, Jenkins A, Mendelow AD et al. Experimental Intracerebral Haematoma: Effects on Blood Flow, capillary permeability and histochemistry. J. Neurosurg. 1987; 66:555-62

Nath FP, Nichols D, Fraser RJA. Prognosis in Intracerebral haemorrhage. Acta Neurochir 1983; 67:29-35.

National Radiological Protection Board. Revised guidance on acceptable limits of exposure during nuclear magnetic resonance clinical imaging. Br J Radiol 1983; 56: 947-77

Nehls DG, Flom RA, Carter LP, Spetzler RF. Multiple intracranial Aneurysms: Determining the site of rupture. J Neurosurg 1985; 63:342-8

New PFJ, Rosen BR, Brady TJ et al. Potential hazards and artifacts of ferromagnetic and non-ferromagnetic surgical and dental materials and devices in Nuclear Magnetic Resonance Imaging. Radiology 1983; 147: 139-148

Ngo FQH, Glassner BJ, Bay JW, Dudley AW, Neaney TF. T1 and T2 Relaxation Measurements of Human Brain Tissues and NMR Imaging Optimisations. Proc SMRM, San Francisco 1983, p264-5

Odeblad E, Lindstrom G. Some preliminary observations on the PMR in biological samples. Acta Radiol 1955; 43:469-76

Ojemann RG, Mohr JP. Hypertensive brain haemorrhage. Clin Neurosurg 1975; 23:220-44

Oppenheimer DR. Microscopic lesions in the brain following head injury. J Neurol Neurosurg Psychiatr 1968; 31:299-306

Paillas JE, Alliez B. Surgical treatment of Spontaneous Intracerebral Haemorrhage: immediate and long-term results in 250 cases. J Neurosurg 1973; 39:145-51

Pasqualin A. Intracerebral Haematomas following aneurysm rupture: Experience with 309 cases. Surgical Neurology 1986; 25:6-17

Pavlicek W, Geisinger M, Castle L, Borokowski GP, Meaney TF, Bream BL, Gallagher JH. The effects of Nuclear Magnetic Resonance on patients with cardiac pacemakers. Radiology 1983; 147:149-53

Pilz P. Axonal injury in head injury. Acta Neurochirugica Supplement 1983; 32:119-23

Purcell EE, Torrey HC, Pound RV. Resonance absorption by nuclear magnetic moments in a solid. Phys Rev 1946; 69:37

Ravinovitch P. Enzyme substrate reactions in very high magnetic fields: I. Biophys J 1967; 7:187-204

Rowan JO, Johnston HI, Harper AM, Jennett WB. Perfusion Pressure in Intracranial Hypertension. In: Intracranial Pressure. eds. Brock M, Dietz H. Berlin: Springer-Verlag, 1972: 165-70

Rubin JI, Gomori JM, Grossman RI, Gefter WB, Kressel HY. High-field MR imaging of extracranial haematomas. Am J Radiol 1987; 148:813-7

Sakurada O, Kennedy C, Jehle J, Brown JD, Carbin GL, Sokoloff L. Measurement of local cerebral blood flow with iodo(^{14}C)antipyrine. Am J Physiol 1978; 234:H59-H66

Sasaki T, Asano T, Takakura K, Sano K, Kassell NF. Nature of the vasoactive substance in CSF from patients with subarachnoid haemorrhage. J Neurosurg 1984; 60:1186-91

Schwartz JL. Influence of a constant magnetic field on nervous tissue I: nerve conduction velocity studies. IEEE Trans Biomed Eng 1978; BME25(5):467-73

Scott M, Werthan M. The fate of hypertensive patients with clinically proven intracerebral haematomas treated without intracranial surgery. Stroke 1970; 1:286-300

Seelig JM, Becker DP, Miller JD et al. Traumatic acute subdural haematoma. Major mortality reduction in patients treated within four hours. N Engl J Med 1981; 304:1511-8

Shaw TM, Elsken RH, Kunsman CH. Proton magnetic resonance absorption and water content of biological materials. Physiol Review 1956; 69:37-43

Singer JR. Blood flow rates by Nuclear Magnetic Resonance measurements. Science 1959; 130:1652-3

Singer JR, Crooks LE. Nuclear Magnetic Resonance blood flow measurements in the human brain. Science 1983; 221:654-6

Sipponen JT. Visualisation of Brain Infarction with Nuclear Magnetic Resonance Imaging. Neuroradiology 1984; 26(5):387-91

Sipponen JT, Kaste M, Ketonen L et al. Serial Nuclear Magnetic Resonance (NMR) Imaging in patients with Cerebral Infarction. J Comput Assist Tomogr 1983; 7(4):585-9

Sipponen JT, Sepponen RE, Sivula A. Chronic Subdural Haematoma: Demonstration by Magnetic Resonance. Radiology 1984; 150:79-85

Sipponen JT, Sepponen RE, Sivula A. Nuclear Magnetic Resonance (NMR) Imaging of Intracerebral Haemorrhage in the acute and resolving phases. J Comput. Assist. Tomogr. 1983; 7:954-9

Sipponen JT, Sepponen RE, Tanttu JI, Sivula A. Intracranial haematomas studied by MR imaging at 0.17 and 0.02T. J Comput Assist Tomogr 1985; 9(4):698-704

Smith AS, Weinstein MA, Modic MT et al. Magnetic Resonance with marked T2 weighted images: improved demonstration of brain lesions, tumor, and edema. AJR 1985; 145(5):949-55

Snow RB, Zimmerman RD, Gandy SE, Deck DF. Comparison of Magnetic Resonance Imaging and Computed Tomography in the evaluation of head injury. Neurosurgery 1986; 18(1):45-52

Sussman BJ, Barber JB, Goald H. Experimental Intracerebral Haematoma. Reduction of Oxygen tension in Brain and Cerebrospinal Fluid. J Neurosurg 1974; 41:177-86

Swensen SJ, Keller PL, Bernquist TH, McLeod RA, Stephens DH. Magnetic Resonance Imaging of haemorrhage. Am J Radiol 1985; 145:921-7

Teasdale E, Cardoso E, Galbraith S, Teasdale G. CT scan in severe diffuse head injury: physiological and clinical correlations. J Neurol Neurosurg Psychiatr 1984; 47:600-3

Teasdale G, Galbraith S. Acute traumatic intracranial haematomas. In: Krayenbuhl H, Maspes PE, Sweet WH, eds. Progress in neurological surgery. Vol 10. Basle: Karger, 1981:252-90

Teasdale G, Galbraith S, Murray L, Ward P, Gentleman D, McKean M. Management of traumatic intracranial haematoma. Brit Med J 1982; 285:1695-7

Teasdale GM, Hadley MDM, Jenkins A, McPherson P, Patterson J, Condon BR, Rowan JO, Wyper DJ, Lawrence A. MRI in Acute Head Injury: an Alternative to CT? In: Proceedings of the 2nd Congress of the European Society of Magnetic Resonance in Medicine and Biology, Montreux 1985, pp291-305

Teasdale GM, Hadley MDM, Jenkins A, McPherson P, Patterson J, Condon BR, Rowan JO, Wyper DJ, Lawrence A. MRI in Acute Head Injury: an

Alternative to CT? In: 4th annual meeting of the Society of Magnetic Resonance in Medicine (London 1985) Vol. 1 pp406-407

Thulborn KR, Waterton JC, Matthews PM, Radda GK. Oxygen dependence of the transverse relaxation time of water protons in whole blood at high field. Biochim Biophys Acta 1982; 714:265-70

Tsubokawa T, Doi N, Ohata H, Kondo T. The effects of brain edema fluid on cerebral blood flow in the tissue infusion model. in: Ishii S, Nagai H, Brock M (eds). Intracranial pressure V. Berlin, Heidelberg: Springer-Verlag, 1983:419-423

Vermuelen M, Lindsay KW, Murray GD et al. Antifibrinolytic treatment in subarachnoid haemorrhage. N Engl J Med 1984; 31:432-7

Vinters HV, Gilbert JJ. Cerebral amyloid angiopathy: incidence and complications in the aging brain II. The distribution of amyloid vascular changes. Stroke 1983; 14:924-8

Volpin L, Cervellini P, Colombo F et al. Spontaneous Intracerebral Haematomas: a new proposal about the usefulness and limits of surgical treatment. Neurosurgery 1984; 15:663-6

Wehrli FW, MacFall JR, Shutts D, Breger R, Herfkens RJ. Mechanisms of contrast in NMR imaging. J Comput Assist Tomogr 1984; 8(3):369-80

Weisberg L. CT in Intracerebral Haemorrhage. Arch Neurol 1979; 36:422-6

Weisman ID, Bennett LH, Maxwell LR, Woods MW. Recognition of cancer *in vivo* by nuclear magnetic resonance. Science 1972; 178:1288-90

White RP. Vasospam. I: Experimental findings. in: Fox JL (ed). Intracranial aneurysms. Heidelberg, New York, Tokyo: Springer-Verlag, 1983:218-49

Wikswo JP, Barach JP. An estimate of the steady magnetic field strength required to influence nerve conduction. IEEE Trans Biomed Eng 1980; BME27(12):722-3

Wilberger JE Jr, Ziad D, Rothfus W. Magnetic Resonance Imaging in cases of severe head injury. Neurosurgery 1987; 20:571-6

Wilkins RH. Attempted prevention or treatment of intracranial arterial spasm: a survey. Neurosurgery 1980; 6:198-210

Wyper DJ, Turner JW, Patterson J, Condon BR, Grossart KWM, Jenkins A, Hadley MDM, Rowan JO. Accuracy of Stereotactic localisation using MRI and CT. J Neurol Neurosurg Psychiatr 1986; 49:1445-8

Young IR, Burl M, Clarke GJ et al. Posterior Fossa: Magnetic Resonance Properties. AJR 1981; 137:895-901

Young IR, Bydder GM, Hall AS et al. The rôle of NMR imaging in the diagnosis and management of acoustic neuroma. AJNR 1983; 4:223-4

Young IR, Bydder GM, Hall AS et al. Extracerebral Collections: Recognition by NMR Imaging. AJNR 1983 4(3): 833-4

Young IR, Hall AS, Pallis CA, Legg NJ, Bydder GM, Steiner RE. Nuclear Magnetic Resonance Imaging of the brain in multiple sclerosis. Lancet 1981; ii:1063-6

Young IR, Khenia S, Thomas DGT, Davis CH, Gadian DG, Cox IJ, Ross BD, Bydder GM. Clinical susceptibility mapping of the brain. J Comput Assist Tomogr 1987; 11(1):2-6

Young SW. Nuclear Magnetic Resonance Imaging. Basic principles. New York: Raven Press, 1984. Chapter 1, p1

Zimmerman RA, Bilaniuk LT, Grossman RI et al. Resistive NMR of intracranial haematomas. Neuroradiology 1985; 27:16-20

Zimmerman RA, Bilaniuk LT, Hackney DB et al. Head injury: Early results comparing CT and high-field MR. AJR 1986; 147(6):1215-22

Zingesser LH, Schechter MM, Dexter J et al. On the significance of spasm associated with rupture of a cerebral aneurysm. The relationship between spasm as noted angiographically and regional blood flow determinations. Arch Neurol 1968; 520-528, 1968